UiT The Arctic University of Norway

Department of Medical Biology

A study of TRIM32 self-ubiquitination

Waqas Khan

Master's thesis in Biomedicine…MBI-3911…May 2020

Acknowledgements

This research thesis was prepared to fulfill the requirement of Master of Science degree in the Department of Medical Biology at the University of Tromsø, Norway and performed at the Molecular Cancer Research Group.

I would like to express my deepest gratitude to my supervisors Eva Sjøttem and Juncal Garcia Garcia for good support, encouragement and excellent guidance, which enabled me to understand this research work. I am very thankful to my supervisor Eva Sjøttem for her guidance in writing and laboratory work. I am also thankful to my co-supervisor Juncal Garcia Garcia for her support in better understanding of the different lab techniques. I would also like to thank all members of Molecular Cancer Research Group for providing full support during my research.

My sincere thanks to all scientists, phd fellows, Post Docs and technicians especially Gry Evjen, Hanne Britt Brenne, Aud, Abudu Yakubu, Anthimi, Katrine Overå, Mireia, Trond, Nikoline who worked with me and assisted in the laboratory. I am also thankful to Terje Johansen who provide me the opportunity to work in his research group.

Finally, I would like to greatest thanks to my parents and other family members for their support and care.

Abbreviations

BafA1: Bafilomycin A1

BBS11: Bardet-Biedl syndrome 11

Cas9: CRISPR-associated protein 9

CRISPR: Clustered Regularly Interspaced Short Palindromic Repeats

CC: coiled-coil domain

DMEM: Dulbecco's Modified Eagle Medium

DNA: Deoxyribonucleic acid

ddNTPs: dideoxynucleotides

dNTP: deoxynucleotide

EGFP: Enhanced Green Fluorescent Protein

gRNA: Guide RNAs

kDa: kilodalton

LGMD2H: Limb-girdle muscular dystrophy 2H

MEM: Minimum Essential Media

NHL: NCL1, HT2A and LIN41 domain

PBS: Phosphate Buffered Saline

PCR: Polymerase chain reaction

PEST: Proteolytic signal sequences

p62/SQSTM1: Sequestosome-1

RT: Room temperature

R-domain: RING finger domain

TRIM: Tripartite motif (TRIM) proteins

Ub/Ubi: Ubiquitin

wt: wild type

Abstract

TRIMs (tripartite motif proteins) constitute a family of ubiquitin E3 ligases that are involved in a variety of cellular processes including autophagy and carcinogenesis. TRIM32 contains an N-terminal RING finger domain, B-box region, a coiled-coil domain and six NHL repeats in the C-terminal region, which are involved in protein dimerization and substrate recognitions. Various mutations in the NHL domains are associated with limb-girdle muscular dystrophy 2H (LGMD2H). TRIM32 is shown to have the capability to ubiquitinate actin and thus possibly participates in myofibrillar protein turnover, especially during the period of muscle transformation and adaptation. TRIM32 is activated by self-ubiquitination induced upon dimerization. Mass spectrometry analysis of EGFP-TRIM32 expressed in HEK293 FlpIn cells suggested three lysine residues, K50, K247 and K401, as putative target sites for the self-ubiquitination activity. The aim of this work was to investigate the importance of these lysine residues for TRIM32 mediated self-ubiquitination. Expression plasmids of EGFP-TRIM32 single, double and triple mutants were established by site–directed mutagenesis. These mutants were transfected into various cell lines and TRIM32 self-ubiquitination analyzed by Western blotting. Introduction of single or double K to R mutations did not seem to abolish self-ubiquitination. However, the double mutant EGFP-TRIM32-K247R/K401R and the triple mutant EGFP-TRIM32-K49R/K247R/K401 displayed a faster migration band on the blot, suggesting that these proteins were cleaved. Inhibition of the lysosome or the proteasome did not inhibit cleavage of EGFP-TRIM32 K49R/K247R/K401R. Localization studies using confocal microscopy showed that both EGFP-TRIM32 WT and the K to R double and triple mutants had a tendency to aggregate in cells, clustering with the Golgi protein GM130 and the autophagy receptor p62/SQSTM1. Since mutations in TRIM32 leads to muscle dystrophy, the second aim of this project was to establish myoblast TRIM32 KO cell lines. These cells would represent good model systems for functional analysis of TRIM32 mutations. Guide RNAs (gRNA) sequences for mouse and rat TRIM32 were selected by bioinformatics tools and cloned into the CRISPR/Cas9 pX458 plasmid. Successfully cloned plasmids were transfected into the mouse myoblast cell line C2C12 and the rat myoblast cell line H9c2. Transfected cells were selected by cell sorting, and expanded clones analyzed by Western blotting. Two promising myoblast C2C12 TRIM32 KO cell lines were successfully established.

Table of Contents

List of Tables

List of Figures

1. Introduction

The protein quality control system is essential for cellular health, especially in case of muscles and nervous system tissues, which contain long living cells. Dysregulation of protein quality control results in protein aggregation and progression of diseases with growing prevalence related to age. The two most important biological processes for controlling protein degradation are autophagy and the ubiquitin-proteasome system (UPS) (Overa et al., 2019). The mechanism of autophagy is considered as a survival pathway, which is utilized by both the normal as well as tumor cells to survive during starvation and stress (White and DiPaola, 2009). Human cells express more than 10,000 various proteins at any given time. The majority of these proteins must fold (and usually gather) to precise, three-dimensional structures to allow a multiple of cellular functions. Strongly folded proteins may unfold and perhaps accumulate under various stress conditions such as elevated temperatures. When proteins become misfolded as well as are no longer functionally needed, they must be degraded to prevent the harmful effects caused by their continued existence. This not only requires tough regulation of the initial production and folding of a protein, but it also requires conformational maintenance, regulation of abundance and subcellular localization and most importantly removal of these proteins by degradation (Klaips, Jayaraj, and Hartl, 2018; Balch et al., 2008).

To maintain protein homeostasis (proteostasis), the cells have developed a broad range of molecular chaperones as well as protein quality-control factors, which are functionally connected with protein degradation machineries and this system is known as proteostasis network. This proteostasis network can be divided into three parts; firstly, protein synthesis, secondly folding, trafficking and conformational maintenance, and thirdly protein degradation mechanism; the ubiquitin–proteasome system (UPS) and autophagy–lysosome system (Klaips, Jayaraj, and Hartl, 2018; Balch et al., 2008).

1.1. Ubiquitin Proteasome system (UPS)

The process of releasing amino acids from a protein can be differentiated into two parts, which are based on the usage of metabolic energy such as ATP followed by ATP-independent events (Figure 1). This key model of protein unfolding, which is further followed by degradation is conserved and involves various steps. First, in eukaryotes the proteins directed for degradation

are generally polyubiquitinated and restrained to regulators for ATP-dependent proteases. Second, these proteins are unfolded through regulators by using the way of conformation changes directed by ATP hydrolysis. Third, these unfolded proteins are firmly translocated into the proteolytic compartments. Finally, polypeptides are degraded by endopeptidases, aminopeptidases and carboxypeptidases in an ATP-independent manner (Nandi et al., 2006).

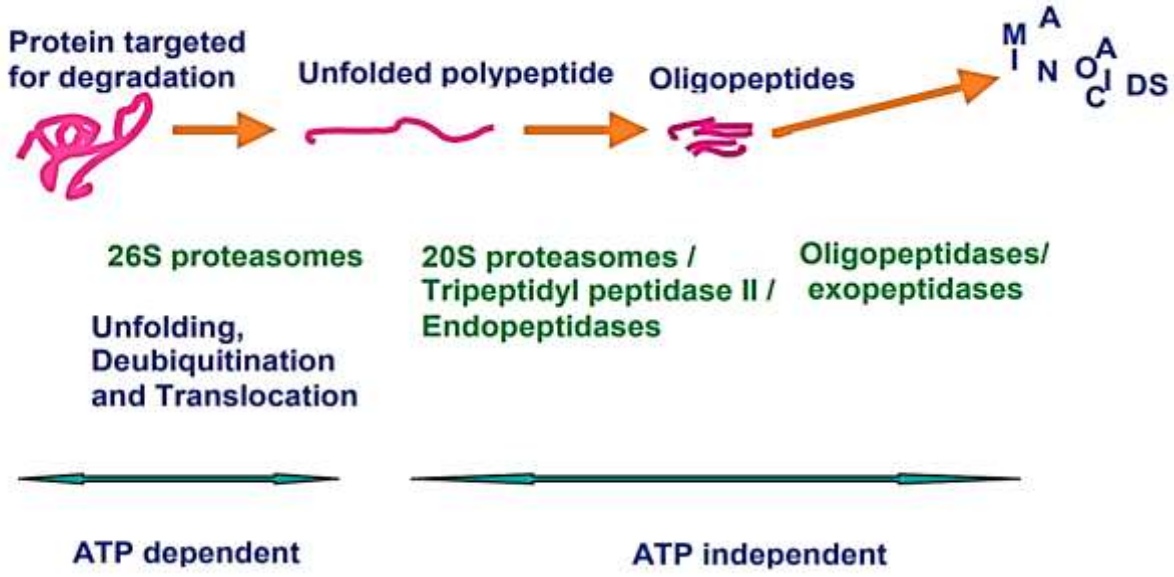

Figure 1: **The overall view of the protein degradation pathway in eukaryotes.** The whole mechanism is followed by the protein degradation, which is leading to free amino acids. The proximal steps in this pathway is operated by enzyme of 26S proteasomes, while the latter steps are performed by ATP- independent proteases and peptidases (Obtained and modified from Nandi et al., 2006).

Various catabolic conditions have been recognized by activation of a short protein of 76-amino acids called ubiquitin (Ub). It is present in all tissues of eukaryotes. The cellular proteins are changed and modified by covalent attachment to Ub proteins by a cellular regulatory mechanism, which is known as ubiquitination. This ubiquitination mechanism can mark proteins for degradation due to the ability of the 26S proteasome complex to identify ubiquitin chains, which are connected to proteins. This protein degradation system through the proteasome complex is known as ubiquitin-proteasome system (UPS) (Khalil, 2018; Bilodeau, Coyne, and Wing, 2016). It plays a significant role in controlling protein turnover and coordinating a number of signaling pathways and other central cellular processes (Ito et al., 2017) such as, cell cycle control, metabolic regulation, apoptosis, development, protein quality

control and antigen presentation. Faults in this system drive to serious diseases such as inflammation, cancer and neurodegeneration (Sommer and Wolf, 2014).

The discovery as well as the identification of both the ubiquitin conjugation pathway and the 26S proteasome opened a new way into an entirely new world of cellular regulation, which is due to their powerful role as the machine degrading polyubiquitinated proteins (Sommer and Wolf, 2014). Proteasomes are commonly found in eukaryotes, archaea and some bacteria. The 26S proteasome found in eukaryotes is a big multi-subunit complex that is used to degrade most of the proteins in the cell under normal conditions. This 26S proteasome structure can be further divided into two sub-units, the 19S regulatory particle cap and the 20S core particle (Figure 2) (Nandi et al., 2006; Budenholzer et al., 2017).

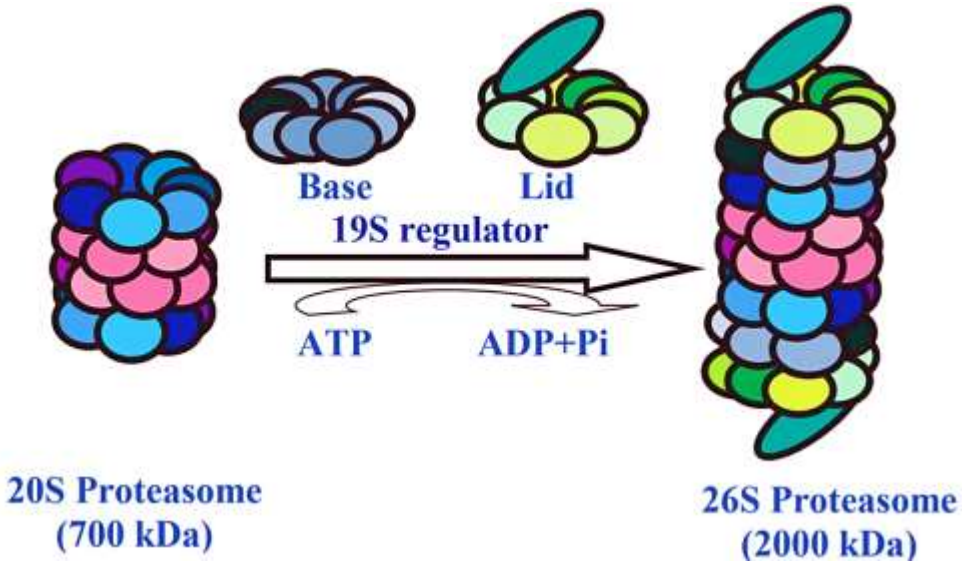

Figure 2: The development of the 26S proteasome by combination of the catalytic 20S proteasome with the 19S regulators by using energy in form of ATP (Obtained from Nandi et al., 2006).

1.2. Ubiquitination

Ubiquitin is a highly conserved protein, which consists of 76-amino acid residues, and is normally found in all eukaryotes (Hatakeyama, 2017). Ubiquitination is a post-translational modifications process, that results in covalent attachment of the ubiquitin peptide to a target protein either in the form of a single unit or chain formats. The ubiquitination regulates various intracellular events such as signal transduction, protein stability by protein quality control, trafficking and progression of cell cycle, transcription, apoptosis and differentiation (Brigant et

al., 2018; Lazzari and Meroni, 2016; Meroni, 2012; Watanabe and Hatakeyama, 2017; van Tol et al., 2017; Borlepawar, Frey, and Rangrez, 2019). The complex process of ubiquitination is accomplished by various kind of enzymes, the ubiquitin-activating enzyme (E1), the ubiquitin-conjugating enzyme (E2) and the ubiquitin ligase (E3). The E3 ubiquitin ligases play main roles as receptors for identifying target proteins. The complete pathway of ubiquitination is initiated by ubiquitin activation through enzyme E1 that binds to the C-terminal part of a glycine of the ubiquitin molecule to its active-site cysteine by using ATP. This creates a high-energy thioester bond. The interaction of the E1 enzyme with ubiquitin clear a site to admit the entry of the next enzyme. By using a trans-thiolation reaction, the ubiquitin is transported from the E1 to the E2 conjugating enzyme active-site cysteine, which is known as ubiquitin conjugation by E2 enzyme. Once the ubiquitin is bound, ubiquitin ligation by an E3 ligase is initiated. The E3 ubiquitin ligase merges with an E2-ubiquitin conjugate and supports in the transport of the ubiquitin from the E2 onto a target protein (Figure 3) (Brigant et al., 2018; Watanabe and Hatakeyama, 2017; van Tol et al., 2017; Borlepawar, Frey, and Rangrez, 2019; Meroni, 2012). Beside the role of ubiquitination in the protein degradation pathways it is involved in various basic cellular approaches, which includes the cell cycle progression, DNA repair, gene transcription, virus budding, receptor endocytosis and apoptosis (Khalil, 2018).

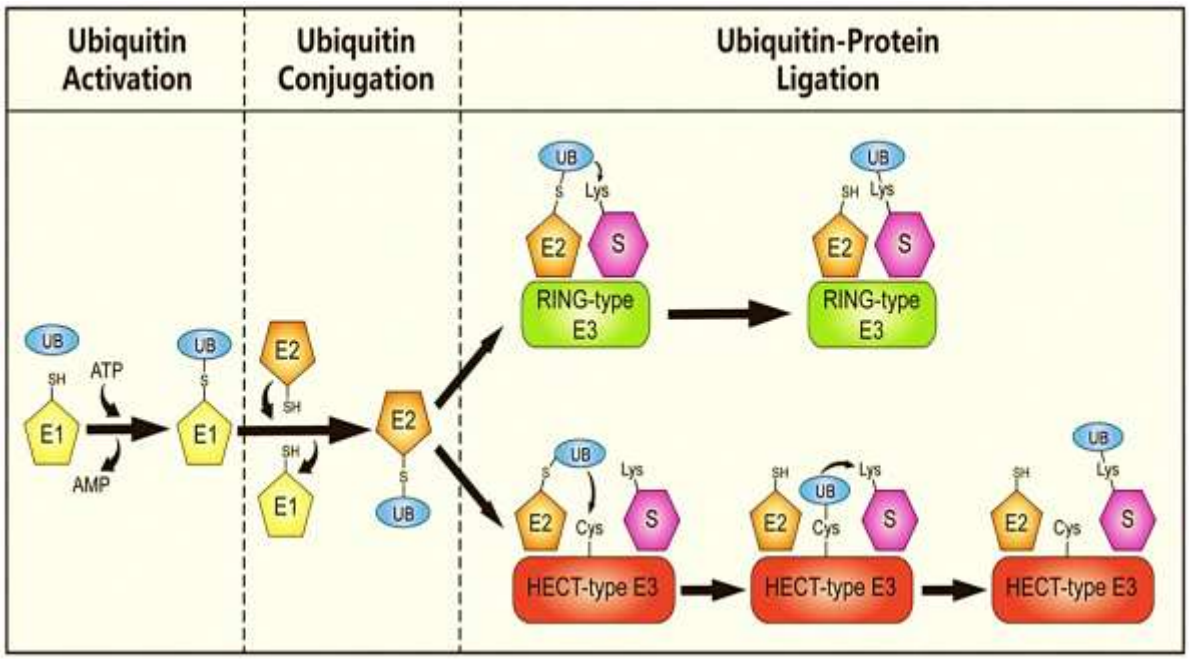

Figure 3: The complete mechanism of ubiquitination is relied upon three enzymatic steps. Firstly, it initiates when an E1 ubiquitin-activating enzyme binds to and activates ubiquitin. This activated ubiquitin is further used to trans-thiolated purposes from E1 to an E2 ubiquitin-conjugating enzyme. Finally, E3 ubiquitin ligases mediate ubiquitin transportation onto the substrates either in the

form of directly from E2 to the substrate (RING-type E3s) or by the formation of an E3-ubiquitin intermediate (HECT-type E3s) (Obtained from Zou, Levy-Cohen, and Blank, 2015).

1.3. Ubiquitin signaling

The intracellular signaling by using the covalent attachment of various ubiquitin linkages to protein substrates is important for many cellular pathways (Zhang, Smits, et al., 2017). Protein ubiquitination is induced and performed by a wide range of stimuli and important signaling actions that are performed in cells. These includes a variety of cell surface receptors, which become ubiquitinated at the stage of stimulation by extracellular ligands. Additionally, the functions of ubiquitin ligases are tightly regulated by signal-induced mechanisms (Haglund and Dikic, 2005). The mechanism of mono-ubiquitination is involved in the endocytosis of plasma membrane proteins, the sorting of proteins to the MVB (multivesicular body). Moreover, it is involved in DNA repair, budding of retroviruses, histone activity as well as transcriptional regulation (Haglund, Di Fiore, and Dikic, 2003). Ubiquitination is capable to regulate signaling non-proteolytically as it can be used to recruit proteins, which perform specific signaling pathways by attracting trafficking factors. These factors are used to alter substrate's localization and to control a substrate's activity (Komander and Rape, 2012). Ubiquitination may also change the function of various proteins. For example, mono-ubiquitination can change protein activity and subcellular localization, while K48 poly-ubiquitination targets substrates for proteasomal degradation and K63 or linear polyubiquitin chains provide as protein-protein interaction platforms, which are further used to mediate signal transduction (Zhang, Smits, et al., 2017; Ronai 2016).

There are different types of ubiquitin linkage chains (Figure 4). A chain of polyubiquitin is made of ubiquitin, which contains seven lysine residues (Lys6, Lys11, Lys27, Lys29, Lys33, Lys48, and Lys63) that can be linked by another ubiquitin molecule. The polyubiquitin chains are forked chains of ubiquitin, which are linked either via equal or different lysine residues. Furthermore, many studies show that besides an internal Lys, the ubiquitin can also be attached to other residues, which are found on the substrate; the N-terminal residue, an internal Thr or Ser (to produce an ester bond), or Cys (to produce a thiol ester bond) (Figure 5). The cellular fate of an ubiquitinated protein is normally depending on the form or which type of ubiquitin linkage is found. For example, determination of protein subcellular localization, regulation of

different signaling pathways, transcription factors, protein kinases and controlling the duration as well as magnitude of a protein's activity (Zhang, Smits, et al., 2017; Ronai, 2016; van der Aa et al., 2012; Livneh et al., 2017).

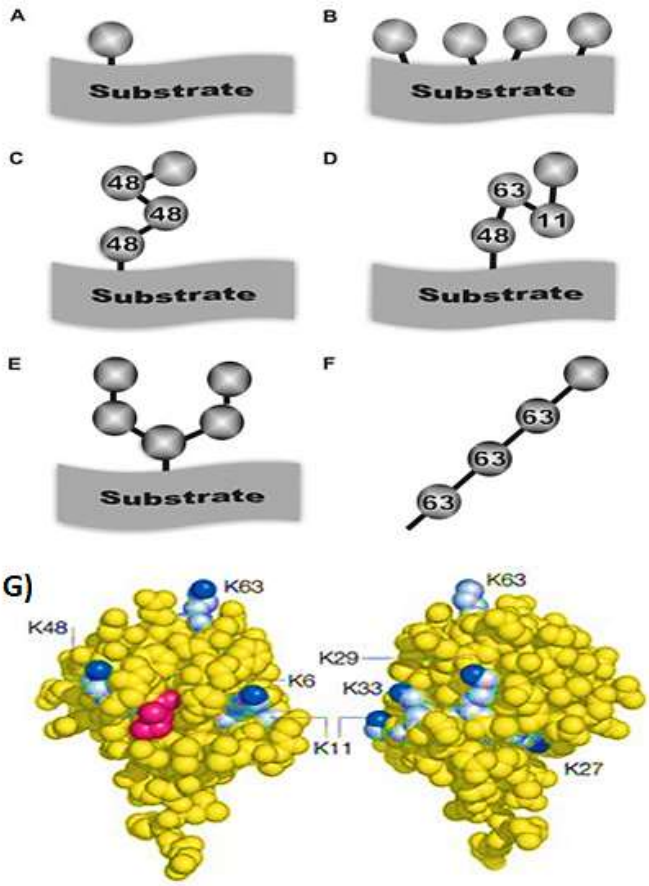

Figure 4: Various kinds of protein ubiquitination. (A) Monoubiquitination, **(B)** Multimonoubiquitination, **(C)** Homogenous polyubiquitin chain, **(D)** Mixed polyubiquitin chain, **(E)** Branched polyubiquitin chain, and **(F)** Unanchored. (Obtained from Bielskienė et al., 2015). (**G)** The two adverse looks of ubiquitin shown. Ubiquitin has seven Lysine residues and all of them can be used for chain formations. The Lys48- and Lys63- connected chains are the best described and are probably the most common. Due to the possible options in the spot and type of ubiquitination, the potential configurations are broad for ubiquitin modifications. All Lysine are shown by white color with the ε-amino-group nitrogen atoms (blue color). All the ubiquitin-binding domains that have been described so far touch an overlapping face ubiquitin that combines Ile44 (red color) (Obtained from Hicke, Schubert, and Hill, 2005).

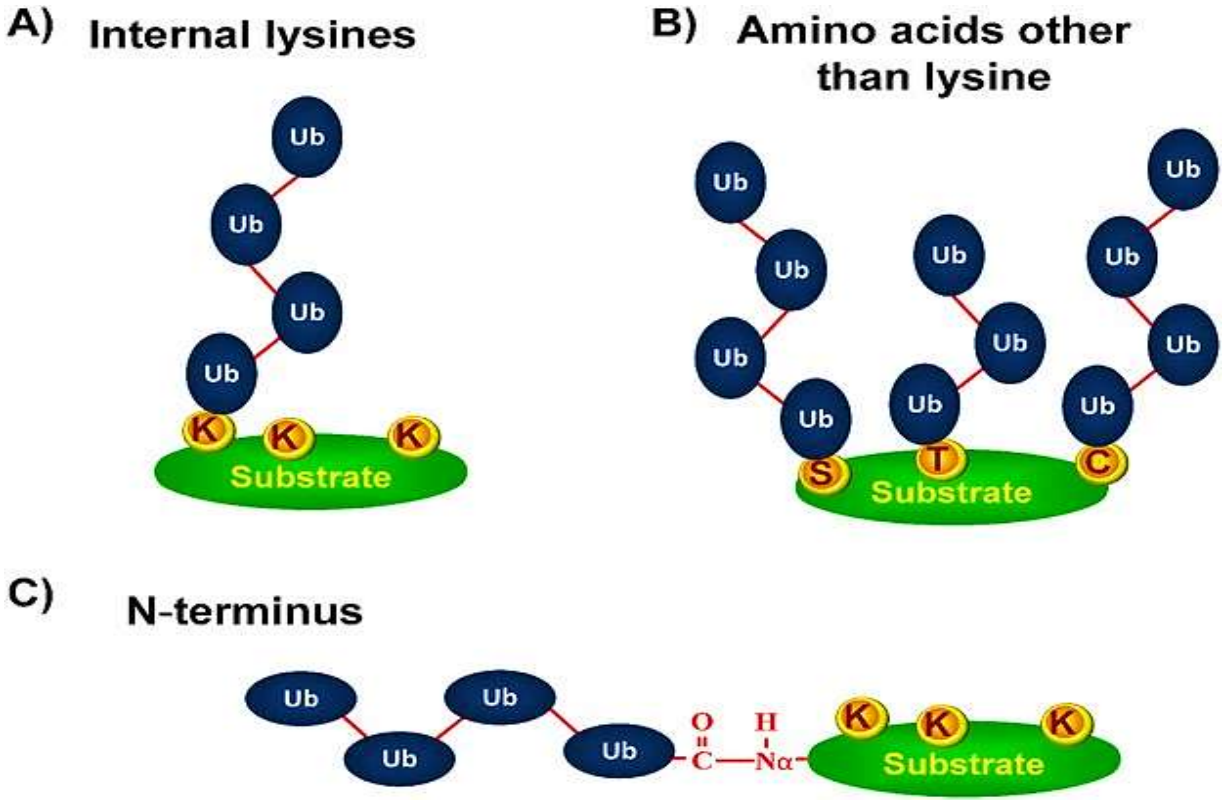

Figure 5: Different sites of ubiquitination. (A) Ubiquitination found on internal Lys residues (B) Ubiquitination found on residues other than Lys such as Ser, Thr, Cys (C) Ubiquitination found on the N-terminal residue (Obtained from Livneh et al., 2017).

1.4. Autophagy

Autophagy is a Greek word in which "auto," meaning oneself and "phagy" meaning to eat ("self-eating"). This word defines an intracellular process in which cytoplasmic components are transported to the lysosome for degradation. The basic term of autophagy was first introduced by the Nobel laureate Christian de Duve on 1963 in London (Bhutia et al., 2013; Barbosa, Grosso, and Fader, 2019). Autophagy is a degradation pathway in which both cellular components and proteins are absorbed by autophagosomes and further digested in the lysosomes. This pathway is important for cellular homeostasis and cellular metabolism (Duffy et al., 2015). There are three main types of autophagy, macroautophagy, microautophagy and chaperone-mediated autophagy. All are used to recognize and degrade various internal cellular constituents (Bhutia et al., 2013; Kimura, Mandell, and Deretic, 2016). Macroautophagy includes the packaging of cytosolic components into a double layered vesicle called autophagosome. The autophagosome fuse with the lysosomes, where the autophagosomal

content is degraded by the lysosomal proteases. The building blocks of the degraded macromolecules are recycled back to the cytosol for reuse. Microautophagy involves the direct absorption of the cytosolic components into the lysosome via invagination of the lysosomal wall. Finally, the Chaperone-mediated autophagy uses chaperone proteins for the direct transfer of cytosolic components across the lysosomal wall (Figure 6) (Wilde et al., 2018).

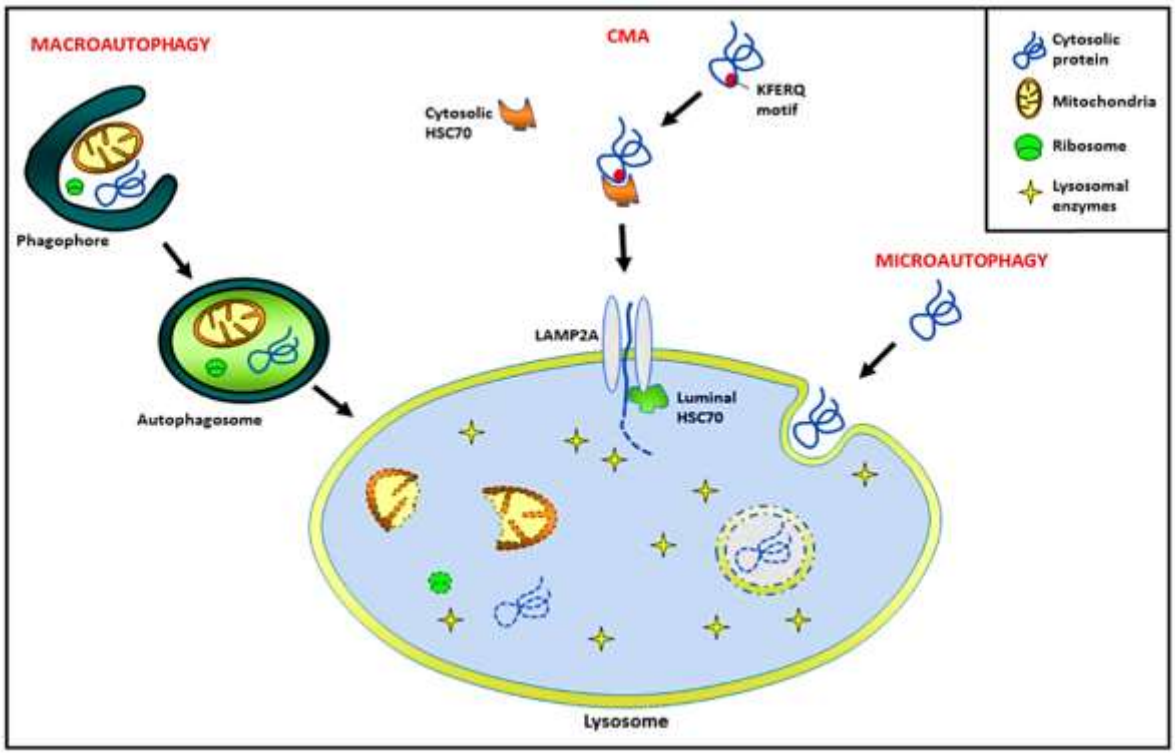

Figure 6: **Three different types of autophagy**. The transfer of cytosolic protein aggregates, organelles and intracellular pathogens into the lysosome bodies for degradation (Obtained from Barbosa, Grosso, and Fader, 2019).

The main role of autophagy is to provide nutrients, which are important for performing cellular activities especially during the condition of fasting and other forms of stress faced by the cell. Autophagy was long considered as a nonselective process. Later autophagy was shown to mediate selective removal of unwanted as well as toxic cytosolic material, such as damaged mitochondria and protein aggregates (Dikic and Elazar, 2018). Several types of pathological conditions such as neurodegeneration, aging, liver failure, inflammatory bowel disease, infection and metabolic disorders, other chronic diseases and especially cancer have been related to dysfunction or defects in autophagy (Barbosa, Grosso, and Fader, 2019; Lozy and Karantza 2012; Choi, 2012). Similarly, deficiency in the autophagy mechanism promotes

genomic instability and the DNA damage response (White, 2016). Dysregulation of autophagy is ultimately connected with the accumulation of oncogenic mutations and also raises chances for susceptibility of tumor growth (Choi, 2012). Autophagy provides a protective and defensive role for the host in the case of immunity, inflammation and the resistance during microbial infections (Dong et al., 2020).

p62 is a ubiquitin-binding protein that is encoded by the SQSTM1 or polyubiquitin-binding protein sequestosome 1 gene (Dong et al., 2020). p62/SQSTM1 is expressed in most cells and tissues and is distributed both in the cytoplasm and in the nucleus. p62/SQSTM act as an autophagy receptor that recognizes and shuttles ubiquitinated proteins to the autophagosome for degradation. This ability of p62/SQSTM1 to act as an autophagy receptor depends on three important interactions. Firstly, p62 directly interacts with selected cargoes and uses its C-terminal ubiquitin associated (UBA) domain to combine with ubiquitinated cargoes. Secondly, p62 interacts with ATG8s (autophagy-related 8 proteins) attached via their lipid tail to the inner membrane of the phagophore. This interaction of autophagy receptors with ATG8s is important for selective autophagy. It is mediated by a motif called LC3-interacting region (LIR). Thirdly, homo polymerization of p62 mediated by its PB1 domain promotes its co-aggregation with the cargo. The polymerization also allows a tight communication of the p62-coated cargo with lipidated ATG8s at the phagophore (Darvekar et al., 2014; Lamark, Svenning, and Johansen, 2017; Ciuffa et al., 2015). p62/SQSTM1 has appeared as a polymeric, modular protein with demanding roles in autophagy, protein aggregation and cell signaling. Similarly, dysregulation of p62 has been involved in various diseases such as cancer and inflammation neurodegenerative disorders (Ciuffa et al., 2015).

1.5. TRIM Proteins

TRIMs (tripartite motif proteins) constitute a family of E3 ligases that are generally dispersed in insects, teleost's and higher level of vertebrates (Luo et al., 2017). The TRIM proteins are also known as RBBC (RING domain, B boxes of the B1 and B2, and a coiled-coil domain) proteins. These proteins are characterized by their common tri-partite domain organization, the highly conserved order of domains in the N-terminal region. The tripartite motif consists of a Really Interesting New Gene (RING) domain, one or two zinc-finger domains that is known as B-boxes (B1 and B2) and a coiled-coil (CC) domain (Figure 7A). Both the RING as well as B-

box domains consist of a zinc-binding motif (Kimura, Mandell, and Deretic, 2016; Lee 2018; Crawford, Johnston, and Irvine, 2018; Zhang et al., 2015). The RING domain is found in hundreds of other proteins whereas the B-box domain is a critical determinant of the tripartite motif (Meroni and Diez-Roux, 2005). Most of the TRIM family proteins have E3 ubiquitin ligase activity due to the N-terminal RING-finger domain. Both the B-Box and CC domains are shown to mediate self-association activity. The CC domain region is approximately 100 residues long and is primarily involved in homo-interactions and establishment of higher level of molecular-mass complexes (Zhang et al., 2015; Lukic and Campbell, 2012). TRIMs gain additional characteristics in the variety of their C-terminal domains. The C-terminal regions, which are found on TRIM proteins are divergent and can constitute of various protein-protein association domains (Gushchina et al., 2018). This C-terminal region includes a specific domain such as the frequently found B30.2 domain, which is also called RFP-like domain. This domain with 170-residues also consists of two types of sub-domains such as PRY and SPRY domains, which mediates protein–protein interactions (Zhang et al., 2015). The TRIM proteins are involved in a huge array of intracellular functions but generally, they function as a part of larger protein complexes and also maintain ubiquitin-protein isopeptide ligase activity (Short and Cox, 2006). Basically, E3 ubiquitin ligases are the form of proteins that perform post-translational modification of targets by ubiquitin-modifying reactions, which result in the combination of a wide range of ubiquitin modifications on a target substrate (Kudryashova et al., 2009).

The human TRIM family of proteins can be categorized into 12 sub-classes based on the domains, which are found in the C-terminal region (Figure 8). The TRIM family in humans has approximately 80 known members (Zhang, Wu, et al., 2017; Boyer et al. 2018; Tomar and Singh 2015; Wang et al. 2011). All the subfamilies of TRIMs comprised of C-I to C-XI groups in which the largest number of TRIMs family members are found in the C-IV group. These TRIMs include the SPRY/B30.2-like domain, a conserved region whose function is considered to be involved in protein-protein interactions or responsible for binding of RNA. The C-XII TRIM proteins lack the RING domain (Tomar and Singh, 2015; Wang et al., 2011). TRIMs have received an increasing research interest due to their important roles in a variety of cellular processes such as intracellular signaling, DNA repair, cell growth, differentiation, development, apoptosis, inherited immunity, protein quality control, autophagy and carcinogenesis (Figure 7B) (Overa et al., 2019; Hatakeyama, 2017; Brigant et al., 2018;

Kimura, Mandell, and Deretic, 2016; Luo et al., 2017). TRIMs also show involvement in defense against viral pathogens or cell-autonomous antiviral defense (Kimura, Mandell, and Deretic, 2016).

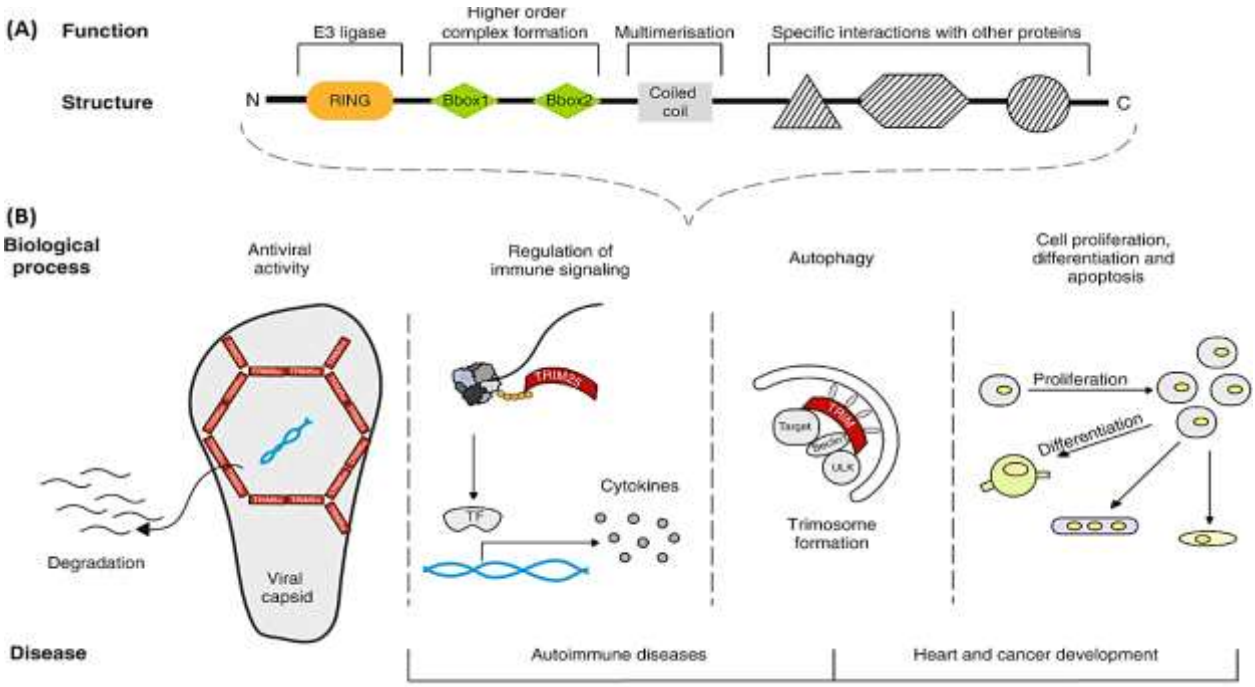

Figure 7: The general overview of TRIM protein domain structure, diverse functions as well as associated diseases. (A) A diagrammatic of the structure of TRIM proteins. TRIMs consist of the RBCC motif (RING domain, B boxes, which contains both the B1 and B2, and a coiled-coil domain) along with the C-terminal domain, which also serves as protein binding domain. The RING domain part of TRIMs have been deliberate E3 ligase activity, while the changeable part of the carboxy-terminal region determinates substrate specificity. (**B)** The biological roles of TRIM proteins are diverse in many respects and includes a direct viral restraint by targeting retroviral capsids for degradation, immune signaling through the processs of polyubiquitination, direct proteins to autophagy, cellular proliferation, differentiation and apoptosis; TF: transcription factor (Obtained from Vunjak and Versteeg, 2019; Khan et al., 2019).

Most of the TRIM proteins display E3 ubiquitin ligase activity (Watanabe and Hatakeyama, 2017) due to the possession of a RING-finger domain (Hatakeyama, 2017). Similarly, the ubiquitination of particular substrates is one of the major mechanisms by which TRIM proteins utilize their biological functions (Lazzari and Meroni, 2016). Mutations in many human TRIM genes result in various kinds of genetic diseases. These genetic diseases include mulibrey (muscle-liver-brain-eye) nanism due to mutations in TRIM37, Opitz syndrome due to the

mutations in TRIM18/MID1, muscular dystrophy limb-girdle Type 2H and Bardet-Biedl syndrome 11 due to various mutations in TRIM32 and familial Mediterranean fever associated with mutations in TRIM20/MEFV (Marin, 2012). Nowadays, both the researchers and clinicians are increasingly concerning TRIMs due to their roles found in cancer development and progression (Chen et al., 2019).

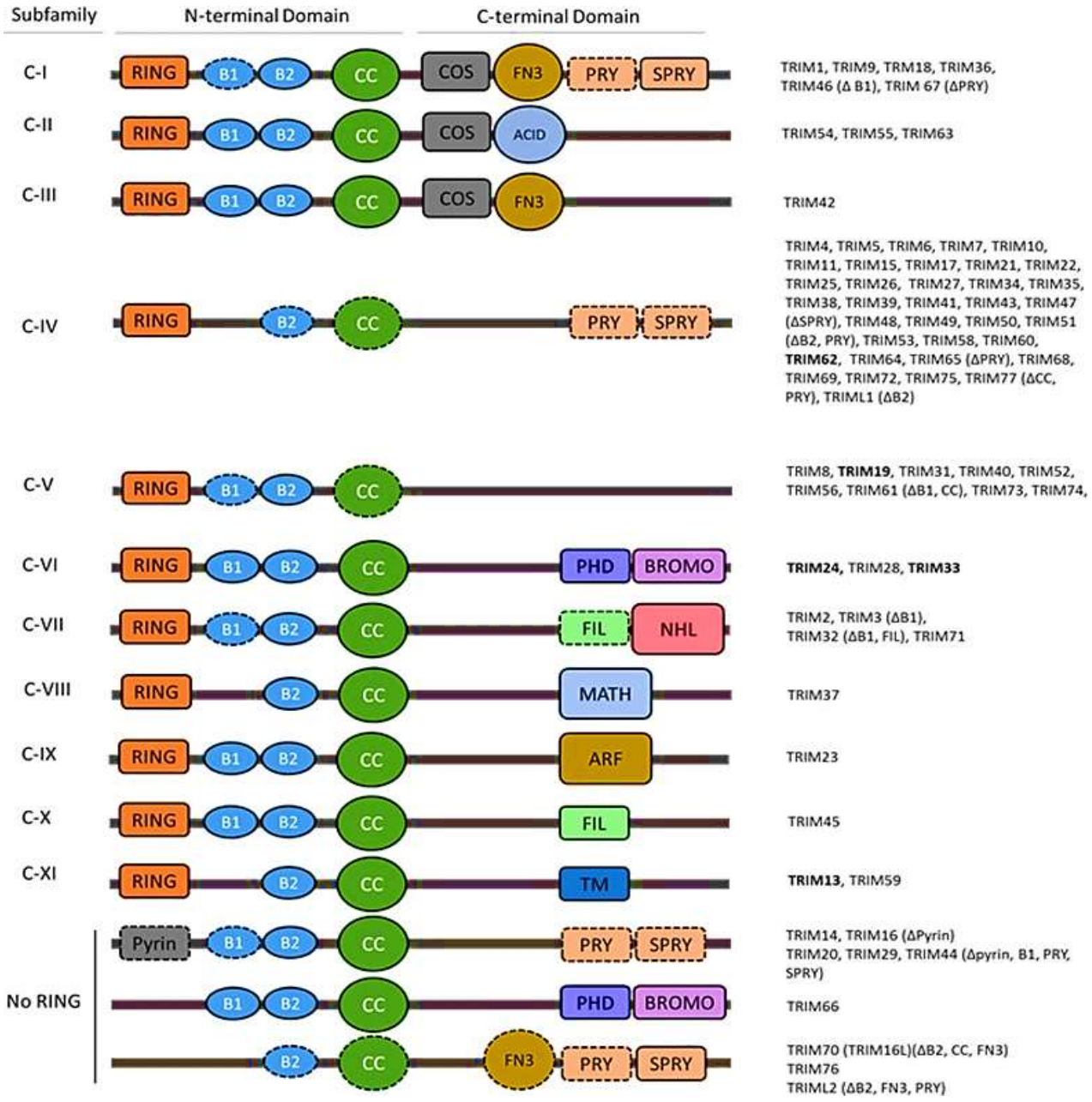

Figure 8: Based on the C-terminal region the structural classification of the TRIM family of proteins are shown. Most of the TRIM family proteins consists of a N-terminal RING domain,

one or two B-box domains (B1 and B2) and a coiled-coil domain (CC). TRIM proteins are classified into 11 subfamilies, which are based on a variable C-terminal domain such as C-I to C-XI. There is also one additional unclassified group, which is lacking a RING finger domain. Those TRIM family members, which are insufficient of one or more domain as shown in dark brackets and illustrated by a dashed outline. The complete list of TRIM proteins, which are found in each class is on the right side. **Pyrin**, Pyrin domain; **FN3,** fibronectin type 3 repeat; **COS,** C-terminal subgroup one signature; **PRY,** PRY domain; **SPRY,** SPRY domain; **PHD,** plant homeodomain; **ACID,** acid-rich region; **FIL,** filamin-type immunoglobulin domain; **NHL, NCL1, HT2A and LIN41** domain; **BROMO,** bromodomain; **ARF,** ADP-ribosylation factor family domain; **MATH,** meprin and tumor-necrosis factor receptor-associated factor homology; **TM,** transmembrane region (Obtained from Crawford, Johnston, and Irvine, 2018).

1.6. TRIM32

TRIM32 is a member of the TRIM family proteins consisting of 653 amino acids and a molecular weight of approximately 72 kDa. It includes a RING finger domain, a B-box region, a coiled-coil domain and six NHL repeats in the C-terminal region, which are involved in protein dimerization and substrate recognitions (Figure 9) (Ito et al., 2017; Shieh, Kudryashova, and Spencer, 2011; Di Rienzo et al., 2019). TRIM32 is a human protein, which was originally named HT2A. This protein was first recognized as a mediator of the biological activity of the lentiviral TAT protein (Tocchini and Ciosk, 2015). The gene of TRIM32 consists of two exons with the full open reading frame included in the second exon (Shieh, Kudryashova, and Spencer, 2011). TRIM32 mutations in the NHL domains are associated with limb-girdle muscular dystrophy 2H (LGMD2H) and sarcotubular myopathy (STM) (Servián-Morilla et al., 2019). TRIM32 plays an important role in skeletal muscle cells and its expression is generally elevated in muscles that are experiencing remodeling and during myogenic differentiation (Meroni, 2012). TRIM32 is shown to have the capability to ubiquitinate actin and thus possibly participates in myofibrillar protein turnover, especially during the period of muscle transformation and adaptation (Meroni, 2012). The Limb-girdle muscular dystrophies (LGMDs) are a heterogeneous group of initial myopathies with both the autosomal dominant and autosomal recessive manner of inheritance (Frosk et al., 2002). LGMD2H affects the muscles especially in the regions of the thighs, shoulders, pelvic area and upper arms area. It is inherited as an autosomal recessive trait (Watanabe and Hatakeyama, 2017). A TRIM32 mutation in the B-Box is associated with Bardet-Biedl syndrome 11 (BBS11) and it is an extremely heterogeneous human obesity syndrome. This syndrome is also distinguished by retinal deterioration, cognitive impairment, renal and cardiovascular abnormalities (Cohen et al., 2012; Chiang et al., 2006; Saccone et al., 2008).

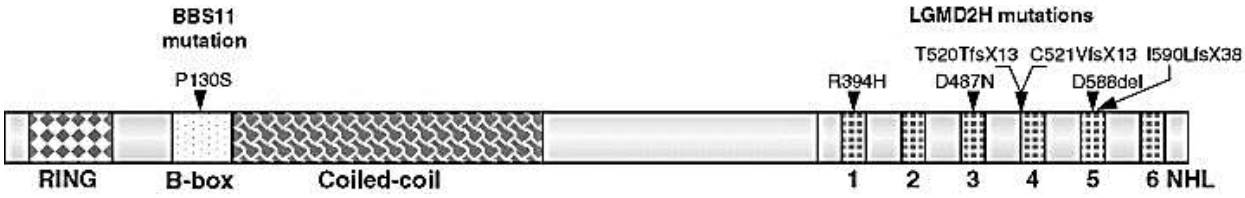

Figure 9: TRIM32 domain structure. The domain structure of TRIM32 along with localization of the human pathogenic mutations, limb-girdle muscular dystrophy 2H at the NHL domain and BBS11 (Bardet–Biedl syndrome 11) at B-box region (Obtained from Shieh, Kudryashova, and Spencer, 2011).

The extended RING domain of TRIM32 is crystallized as a dimer unit. This whole structure forms a four-helix bundle (Figure 10) (Koliopoulos et al., 2016).

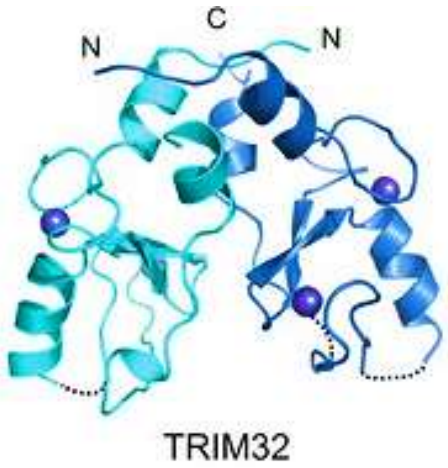

Figure 10: Ring domain structure of TRIM32. TRIM32 RING dimer structure in ribbon illustrates with each RING monomer and colored in cyan and blue and the Zn^{2+} ions as shown in grey spheres (Obtained from Koliopoulos et al., 2016).

TRIM32 is found to be upregulated in various kinds of cancers and its overexpression is shown to promote cell oncogenic transformation as well as tumorigenesis in a largely p53-dependent way. It is found to facilitate degradation of the tumor suppressors Abi2 and thereby act as a proliferative agent (Lazzari and Meroni, 2016; Tocchini and Ciosk, 2015; Liu et al., 2014). TRIM32 overexpression is directly associated with poor prognosis of hepatocellular carcinoma, gastric cancer, and breast cancer (Ito et al., 2017; Du et al., 2018; Cui et al., 2016; Zhao et al., 2018). These findings support that TRIM32 acts as an oncoprotein and a predictor of malignant cancer (Ito et al., 2017). Patients with Alzheimer's disease are shown to display up-regulation of TRIM32 in the occipital lobe and in psoriasis lesions. TRIM32 is shown to

have an influential role in cell polarity, cell division, mobility, neuronal function and metastasis, all of which are dependent upon alterations in the cytoskeleton and actin filament building (Cohen et al., 2012). Identified TRIM32 substrates are muscular proteins as well as proteins, which are involved in cell cycle regulation and cell motility (Lazzari and Meroni, 2016). Recently, various members of the TRIM family proteins were shown to promote autophagy induction via the crucial autophagy initiator proteins ULK1 (Unc-51 like autophagy activating kinase 1) and BECLIN 1. Moreover, some TRIM proteins also serve as cargo receptors for selective autophagy (Di Rienzo et al. 2019). In addition, some of the TRIM family proteins such as TRIM30 and TRIM50 are degraded by autophagy themselves (Overa et al., 2019). Similarly, TRIM32 promotes TAX1BP1-mediated selective autophagic degradation of TLR3/4 adaptor protein TRIF (Yang et al., 2017). Recent research shows that TRIM32 is degraded by autophagy and that it affects the autophagic activity of p62/SQSTM1. Lysosomal degradation of TRIM32 was dependent on the autophagic gene autophagy-related 7 (ATG7) and blocked by knockout of the five autophagy receptors p62, NBR1, NDP52, TAX1BP1 and OPTN, indicating towards degradation by selective autophagy. The p62/SQSTM1 directed TRIM32 for lysosomal degradation, whereas TRIM32 mono-ubiquitylated p62 on lysine residues involved in the regulation of p62/SQSTM1 activity (Overa et al., 2019).

1.7. Generation of knock out cells by CRISPR /Cas9

The CRISPR (Clustered regularly interspaced short palindromic repeats) and Cas proteins form the adaptive CRISPR–Cas immune system in bacteria and archaea. This DNA-encoded as well as RNA-mediated defense system supports the sequence-specific identification, targeting and degradation of external nucleic acids (Barrangou, 2015). The microbial CRISPR-Cas system containing the Cas9 nuclease is conducting specific genomic loci by using a 20-nucleotide guide sequence (gRNA) (Ran, Hsu, Lin, et al., 2013). The Cas9 nuclease is guided by this gRNA molecule to the target DNA molecule by Watson-Crick base pairing. The guide sequences are found inside the CRISPR RNAs usually correlates to phage sequences, which are used for establishing the natural mechanism for CRISPR antiviral defense system. The gRNA sequence can easily be edited to a sequence of interest to target the Cas9 to a specific genomic loci (Hsu, Lander, and Zhang, 2014). The effectiveness and ease of Cas9 endonuclease have led to the production of genomic wide CRISPR-knockout (KO) libraries used for both

mouse and human cells. These libraries are now widely available in public plasmid archives and are typically optimized to gain equal description and performance across all expressed gRNAs and contain an antibiotic or fluorescent selection marker that can be further used to retrieve transduced cells (Yu and Yusa, 2019).

The CRISPR/Cas9 system has been used by thousands of laboratories for targeted genome editing applications in a various range of experimental model systems. The wild-type Cas9 nuclease has facilitated both the effective and targeted genome modification in various species that have been impossible using traditional ways of genetic manipulation techniques. For example, various proteins or RNAs can be restrained to Cas9 to change transcription states of precise genomic loci, control of the chromatin states, or even rearranging the three-dimensional arrangement of the genome. The ease of Cas9 targeting is obtained due to its high efficiency as a site-specific nuclease. Similarly, the possibility for multiplexed modifications have opened a wide range of biological applications for Cas9 in the field of biotechnology and medicine (Hsu, Lander, and Zhang, 2014). For example, some studies show that CRISPR/ Cas9–mediated genome editing technology is possible in adult animals and also provide a promising opportunity for correction and alteration of human genetic diseases (Yin et al., 2014).

2. Aim of the study

The main aims of this study were to:

(a) Identify self-ubiquitination sites in TRIM32.

(b) Generation of myoblast TRIM32 knock-out cell lines by using CRISPR/Cas9.

3. Materials and Methods

3.1. Materials

Table 1: Growth medium used for bacterial cell cultures and mammalian cell lines

Types	Media	Contents
Growth media used for bacterial cultures	LB (Luria-Bertani) medium	10g of Bacto Tryton 5g of Bacto yeast extract 10g NaCl dH_2O up to 1 liter NaOH (pH adjusted to 7.5) Antibiotic used: Ampicillin (100 µg/ml) or Kanamycin (50 µg/ml)
	LB agar Plate	10g of Bacto Trypton 5g of Bacto yeast extract 10g NaCl 15g agar 1 liter of dH_2O NaOH (pH adjusted to 7.5) Antibiotic used: Ampicillin (100 µg/ml) or Kanamycin (50 µg/ml)
	SOC media (Super optimal broth with catabolic repression)	20g of Bacto Trypton 5g of Bacto yeast extract 0.5g NaCl 10ml 250mM KCl 5g $MgCl_2$ 20mM glucose 1 liter of dH_2O NaOH (pH adjusted to 7.5)

Growth media used for Mammalian cell lines	Growth media for mammalian cell culture (HeLa cell, MCF-7 breast cancer cell line, HEK293 FlpIn TRIM32 KO cell line, C2C12 mouse myoblast cell line and the H9c2 rat myoblast cell lines)	Eagles minimum essential medium or MEM (Sigma, M4655) Supplemented with 10% Fetal Bovine Serum (biowest, S181B), 1% penicillin (100 U/ml) and streptomycin (100 g/ml) (Sigma, P4333)
		Dulbecco's Modified Eagle Medium or DMEM (Sigma, D6046) Supplemented with 10% Fetal Bovine Serum (biowest, S181B), 1% penicillin (100 U/ml) and streptomycin (100 g/ml) (Sigma, P4333)
	Growth media for mammalian cell culture (MDA-MB-231 breast cancer cell line)	Roswell Park Memorial Institute or RPMI (Sigma, R8758) Supplemented with 10% Fetal Bovine Serum solution (biowest, S181B), 1% penicillin (100 U/ml) and streptomycin (100 g/ml) (Sigma, P4333)
	Trypsin Solution (Sigma, T3924)	0.25% of Trypsin 0.05% of EDTA in 1x PBS pH adjusted to 7.5
Transfection Reagents	METAFECTENE® PRO	Biontex (T040)
	Trans IT-LT1	Mirus (MIR2300)
	1% Bovine serum albumin	1g bovine serum albumin (Sigma) was mixed with 20 ml of 1x PBS

Table 2: General buffers

Methods	Buffers	Contents
General buffers	TE buffer	10mM Tris-HCL with pH 8 1mM EDTA
	6xT gel loading buffer	0.25% Bromophenol blue 60mM EDTA with pH 8.0 0.6% SDS 40% (W7v) sucrose Sterile filtered
	20x Minigel buffer	193.75 g Tris-Cl 27.22 NaOAc 14.9 g EDTA dH_2O upto the 21
	1x Phosphate buffer saline (PBS)	0.1mM Na-phosphate buffer solution with pH 7.2 0.7% NaCl
	1-kb ladder	1 µl 1-kb ladder stock (1.03 µg/µl) 24 µl TE buffer with pH 8.0 5 µl of 6xT gel loading buffer
SDS- PAGE	4 x Separating gel buffer	181.65g Trizma-base 4g SDS dH_2O up to 11 pH adjusted to 8.8 with HCl
	4 x Concentrating gel buffer	60.55g Trizma-base 4g SDS dH_2O up to 11 pH adjusted to 6.8 with HCl
	8 % Separating gel	5.4 ml of H2O Separating buffer is 2.5 ml 40% acrylamide is 2 ml 10% APS is 100 µl TEMED is 10 µl (Tetramethylethylenediamine)

	10 % Separating gel	4.9 ml of H_2O Separating buffer is 2.5 ml 40% acrylamide is 2.5 ml 100 µl 10% APS 10 µl TEMED (Tetramethylethylenediamine)
	4 % Concentrating gel	H_2O = 6.4 ml Concentarting buffer is 2.5 ml 40% acrylamide 1 ml 10% APS 100 µl TEMED 10 µl (Tetramethylethylenediamine)
	5x loading buffer	312.5mM Tris/HCl 20% Sucrose 10% SDS 0.1% Bromophenol blue
	2 x loading buffer	5x loading buffer (4 ml) dH_2O (6 ml)
Western blotting	1x Transfer buffer	300mM (36.3g) Tris-base 300mM (22.5g) Glycine 200 ml methanol 2.5 ml of 20% SDS 800 ml dH_2O
	5% dried milk solution	2.5 g dried milk 50 ml 1x TBS-T
	5% Ponceau staining Solution	1g Ponceau S staining Acetic Acid 50ml 1000 ml dH_2O
	PBS-T buffer	1000 ml 10x PBS (pH 7.4) 10 ml Tween 8990 ml dH_2O
	1xTBS-T buffer	75ml of 2M NaCl 10ml of 1M Tris-HCl, pH 8.0 1 ml Tween20 (Sigma, P9416) 914 ml dH_2O

Restriction Enzymes Buffer	10x NEBuffer 2.1	50mM HCl 10mM Tris-HCl 10 mM $MgCl_2$ BSA 100 µg/ml (pH 7.9 at 25 ^oC)
	CutSmart Buffer	50mM Potassium Acetate 20mM Tris-Acetate 10 mM Magnesium Acetate BSA 100 µg/ml (pH 7.9 at 25 ^oC)

Table 3: Primers used for site-directed mutagenesis and establishment of CRISPR/Cas9 gRNA plasmids

Name	Primer sequence	Source
TRIM32-K49R	5′-TGCCGCCAGTGCCTGGAGCGCCTATTGGCCAGTAGCATC- 3′ 5′-GATGCTACTGGCCAATAGGCGCTCCAGGCACTGGCGGCA- 3′	This study
TRIM32-K247R	5′-TACTTCCTGGCCAAGATCCGCCAGGCAGATGTAGCACTA- 3′ 5′-TAGTGCTACATCTGCCTGGCGGATCTTGGCCAGGAAGTA- 3′	This study
TRIM32-K401R	5′-ATACAAGTCTTTACCCGCCGCGGCTTTTTGAAGGAAATC- 3′ 5′-GATTTCCTTCAAAAAGCCGCGGCGGGTAAAGACTTGTAT- 3′	This study
CRISPR Mouse T1	5′-CCAGCAGTGTCTGTTTCTCAAG- 3′ 5′-CTATCAGTGACACCAATCAGCC- 3′	This study
CRISPR Mouse T2	5′-GAAGGCACAGTCTACTTCACCC- 3′ 5′-AGGTAAGGCCCTCTCGAATAAG- 3′	This study
CRISPR Rat T1	5′-TGATGCTGAAGGCACAGTCTAT- 3′ 5′-AGGTAAGGCCCTCTCGAATAAG- 3′	This study
CRISPR Rat T2	5′-CTCTGAGAATGAAGATTTCCGC- 3′ 5′-GATCTTGACACAGTGATCCCAA- 3′	This study

Table 4: Primary and Secondary Antibodies

Types	Antibody	Catalogue no.	Dilution	Supplier
Primary Antibodies	GFP-tag antibody (Rabbit)	Ab290	1:5000	Abcam
	TRIM32 antibody (Rabbit)	10326-1-AP	1:2000	Proteintech
	p62 antibody (Mouse)	610833	1:2000	BD Biosciences
	LC3B antibody	L7543	1:1000	Sigma
	PCNA Antibody (Mouse)	M0879	1:2000	DAKO
	Actin Antibody (Rabbit)	A2066	1:1000	Sigma
	GM130 antibody (Rabbit)	ab52649	1:500	Abcam
Secondary Antibodies	HRP-labelled polyclonal anti-mouse IgG	554002	1:2000	Cell signaling
	HRP-labelled polyclonal anti-rabbit IgG	554021	1:2000	BD Biosciences
	HRP-conjugated anti-biotin antibody	#7075	1:2000	Cell signaling
	Alexa Fluor® Rabbit-555 antibody	A-11008	1:5000	Life Technologies
	Alexa Fluor® Mouse-647 antibody	A-21236	1:500	Life Technologies

Table 5: Staining used in Confocal analysis

Staining	Dilution	Supplier
DAPI staining	1:5000	Thermo Scientific

Table 6: Inhibitors used for Western blot

Inhibitors	Concentration/ Quantity used in each well	Catalogue no.	Supplier
BafA1	200 nM	B1793	Sigma
MG132	10 µM	C2759	Sigma
HBBS (Starvation Medium)	2 ml	H8264	Sigma

Table 7: Restriction Enzymes

Name	Catalogue no.	Concentration	Supplier
DpnI	R0176L	20 000 U/ml	New England Biolabs
AgeI	R0552L	50 000 U/ml	New England Biolabs
BbsI	R3539	20 000 U/ml	New England Biolabs

Table 8: Plasmid constructs

Plasmid Construct	Description	Source
pDest-EGFP-TRIM32	Mammalian expression vector for EGFP-tagged TRIM32	(Overa et al., 2019)
pDest-EGFP-TRIM32 K50R	Mammalian expression vector for GFP-TRIM32 with K50R mutation	(Made in this work)
pDest-EGFP-TRIM32 K247R	Mammalian expression vector for GFP-TRIM32 with K247R mutation	(Made in this work)
pDest-EGFP-TRIM32 K401R	Mammalian expression vector for GFP-TRIM32 with K401R mutation	(Made in this work)
pDest-EGFP-TRIM32 K50R/401R	Mammalian expression vector for GFP-TRIM32 with K50R/401R mutations	(Made in this work)
pDest-EGFP-TRIM32 K50R/247R	Mammalian expression vector for GFP-TRIM32 with K50R/247R mutations	(Made in this work)
pDest-EGFP-TRIM32 K401R/K247R	Mammalian expression vector for GFP-TRIM32 with K401R/K247R mutations	(Made in this work)

pDest-EGFP-TRIM32 K50R/401R/K247R	Mammalian expression vector for GFP-TRIM32 with K50R/401R/K247R mutations	(Made in this work)
pDest-mCherry-USP2	Mammalian expression vector for mCherry tagged USP2	(Made in this work)
pDONR-TRIM32 wild type	Entry vector for TRIM32	(Overa et al., 2019)
pDONR-TRIM32 K50R	Entry vector K50R mutated TRIM32	(Made in this work)
pDONR-TRIM32 K247R	Entry vector K247R mutated TRIM32	(Made in this work)
pDONR-TRIM32 K401R	Entry vector K401R mutated TRIM32	(Made in this work)
pX 458	CRISPR/Cas9	(Ran, Hsu, Wright, et al., 2013)

Table 9: Reagents used for sequencing

Reagents	Description	Source
Big dye	DNA Sequencing	Applied Biosystems
6x Sequencing Buffer	DNA Sequencing	Applied Biosystems

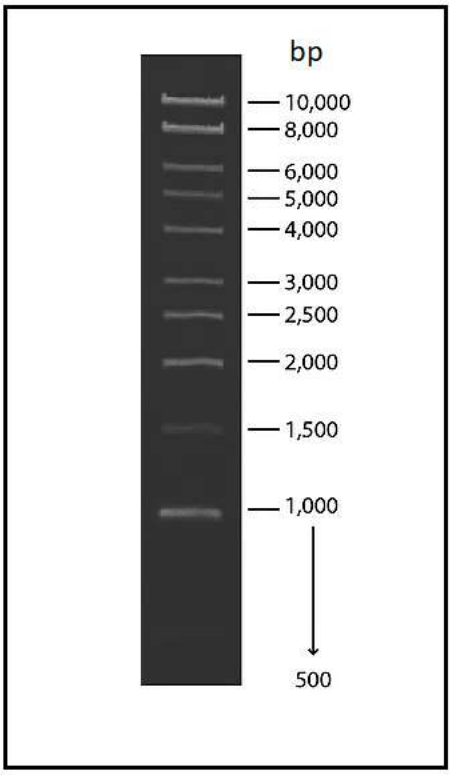

Figure 11: 1-kb DNA ladder (Obtained from www.sigmaaldrich.com).

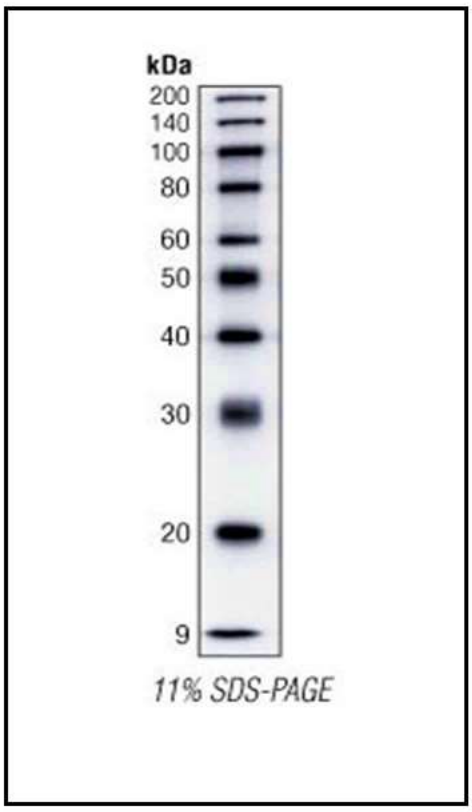

Figure 12: Biotinylated Protein ladder (Obtained from www.cellsignal.com).

3.2. General Methods

3.2.1. Plasmid purification from *E.coli*

The bacterial plasmid DNAs are extensively used as a cloning agent in DNA recombinant technology. A method used for extracting DNA plasmid from bacterial cells was developed and explained by Birnboim and Doly in 1979. The principle of this method is based on the selective alkaline denaturation of high molecular weight chromosomal DNA, whereas the covalently closed circular DNA remains double-stranded. At the time of n eutralization, the chromosomal DNA renatures again to form an insoluble clump, while plasmid DNA remains in the supernatant (Birnboim and Doly, 1979).

In this method, the plasmid-containing cells are treated with sodium dodecyl sulfate (SDS), which diminish the cell wall and then NaOH is used to lyses the cells completely. Then the chromosomal DNA is denatured by turning conditions into alkaline pH value. Neutralization of lysate is obtained by using acidic sodium acetate, which results in renaturation of DNA leading to formation of aggregates in the form of an insoluble network. At the same time, protein-SDS complexes and high molecular weight of RNA precipitates due to the high concentration of sodium acetate. Thus, in this way most of the major contaminating macromolecules are co-precipitated and removed by simple centrifugation. The plasmid DNA or covalently closed circular (CCC) DNA stays in the supernatant and is recovered by binding to a column (Birnboim and Doly, 1979).

Procedure of Plasmid Miniprep

The method of plasmid miniprep were performed at room temperature and all centrifugation steps were performed at maximum speed of 13000 rpm in a tabletop centrifuge machine. The protocol of Gen Elute Plasmid Miniprep kit (Sigma, www.sigmaaldrich.com) have been followed. The following steps were performed during plasmid miniprep.

1. **Harvest and lysate bacteria**

   The overnight bacterial culture of 1500 µl was centrifuged for 1 minute in eppendorf tube and the supernatant was removed. The cells were resuspended in 200 µl resuspension solution by pipetting and vortex in until the pellet was completely dissolved. Afterwards, 200 µl lysis solution was added to the eppendorf tube and inverted gently 4-6 times to mix. This solution in the tube was left to clear for 5 minutes.

2. **Preparation of cleared lysate**

350 µl neutralization solution was added to the tube and inverted this tube gently 4-6 times to mix completely. The debris was pelleted by centrifugation for 10 minutes.

3. **Preparation of binding column**

500 µl column preparation solution was added to the plasmid DNA binding column in a collection tube and centrifuged for 1 minute. The flow through was removed from tube.

4. **Binding of plasmid DNA to the column**

The cleared lysate from step 2 was transferred to the binding column and centrifuged for 1 minute. The flow through was removed.

5. **Wash to remove contaminants**

750 µl wash solution was added to the column and centrifuged for 1 minute. The flow through was removed from tube. This tube was centrifuged again for 1 minute to dry the column.

6. **Eluted purified plasmid DNA**

The column was transferred to a clean eppendorf tube and 100 µl elution solution was added to the column and centrifuged for 1 minute. The eluted plasmid was stored at -20°C.

3.2.2. Measurement of plasmid DNA concentration by Nanodrop

The most commonly used instrument for the measurement of DNA concentration in a solution is the Nanodrop™ spectrophotometer (Thermo Scientific). The determination of the quality and quantity of DNA for this instrument have been facilitated by using a ratio of UV absorbance of 260/280 nm (Brzobohata et al., 2017). Because a common nucleic acid sample will show a very distinctive profile normally in the range of 260/280 nm. To evaluate the sample quality precisely the ratios of 260/280 or 260/230 should be considered in combination along with the general spectral quality. Generally, perfect nucleic acids produce a 260/280 ratio of ~1.8 as well as a 260/280 ratio of ~2.0 for all DNA and RNA respectively. This ratio is totally dependent on

the pH value and ionic strength of that buffer, which is used to make both blank and sample measurements (Desjardins and Conklin, 2010). The Nanodrop Spectrophotometer allows a highly accurate analyses of only1 µl samples with significant reproducibility. Moreover, this instrument has the ability to measure samples with high concentration without dilution (tools.thermofisher.com).

In this work, concentration and purity of eluted plasmid obtained from miniprep was measured by using a Nanodrop device ND-1000 spectrophotometer (Nanodrop Technologies/Thermo Fisher Scientific) in ng/µl.

3.2.3. Gateway LR protocol (From ENTRY clone to DEST vector)

The Gateway system is based onsite-specific recombination reactions, which allows the bacteriophage lambda (λ) to combine and edit itself in and out of a bacterial chromosome. Normally, these Gateway protocols and the recombination reactions are driven by two enzyme blends, which are called BP and LR clonase reactions. Once captured as an entry clone, a DNA fragment can be recombined into a various range of destination vectors that are expression vectors for special applications. The entry/donor vectors can be established by conventional cloning or by a BP reaction on DNA fragments containing attB sites. The BP reaction is catalyzed by the enzyme mix of BP Clonase II that consists of the phage integrase as well as the integration host factor (Karimi, Depicker, and Hilson, 2007; Liang et al., 2013). The LR reaction is catalyzed by the enzyme mix of LR Clonase II that consists of integrase, integration host factor as well as the phage excisionase (Figure 13). The LR reaction includes the recombination of an attL substrate (in an entry/donor clone) with an attR substrate (expression vector) to build an attB-containing expression clone (Karimi, Depicker, and Hilson, 2007; Park, Throop, and Labaer, 2015).

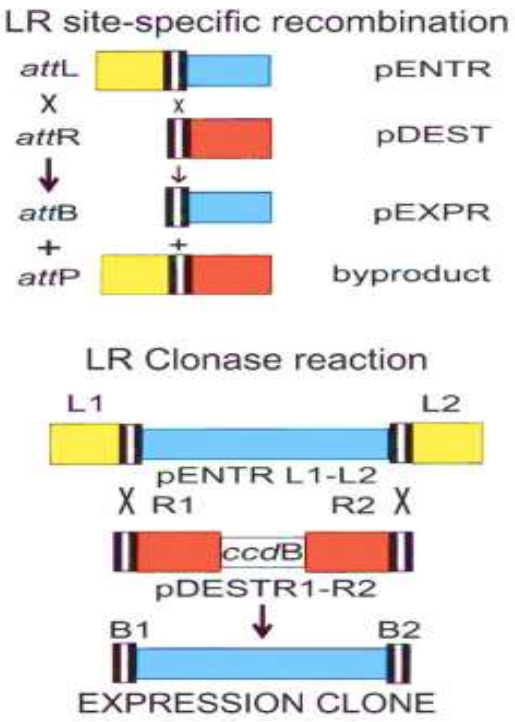

Figure 13: The LR clonase mix is used to transfers the DNA fragment of interest, which are flanked by two attL sites in the entry clone vector (pENTR) that recombine with the corresponding attR sites of a destination vector (pDEST) carrying two attR sites. After recombination of the matching both the attL and attR sites, the DNA fragment of interest is inserted into a new expression clone (pEXPR) to produce attB in a new expression vector (pEXPR) and attP as a byproduct. The ccdB (control of cell death) gene is a standard Gateway cassette (attR1-ccdB-attR2) precedes the ORF coding for an enzyme (Obtained from Karimi, Depicker, and Hilson, 2007).

Procedure

For the conversion of pDONR to pDEST, 100ng pENTR (pDONR) plasmid, 150ng destination vector (pDEST - EGFP), 0.5 µl LR reaction mix and TE buffer up to 10 µl were mixed in an eppendorf tube. The tube was incubated at 25 °C for 2 hours. Afterwards, 1 µl proteinase K was added and incubated at 37 °C for 10 min. The sample was transformed into *E.coli* followed by plasmid miniprep and verified by restriction enzyme digestion and agarose gel electrophoresis.

3.2.4. Agarose gel electrophoresis

Agarose gel electrophoresis is a simple and highly efficient method for separating, analyzing and purifying DNA fragments in the range of 0.5 to 25-kb (Voytas, 2001). By using the method of agarose gel electrophoresis for separation of DNA fragments, the DNA fragments are loaded

into pre-cast wells in the agarose gel and then appropriate current applied. The DNA molecule is negatively charged due to the possession of phosphate backbone, thus when it is placed in an electric field these DNA fragments will move to the positively charged anode. the DNA has a systematic mass/charge ratio, so that DNA molecules are separated by size inside an agarose gel in a pattern such that the distance traveled is inversely proportional to the log value of its molecular weight. The principal model for DNA movement over an agarose gel is followed by "biased reputation model", whereby the prominent line moves forward and drags the rest of the molecule forward. The migration rate of a DNA molecule through an agarose gel is determined by the following factors. Size of the DNA molecule because larger molecules move more slowly due to greater frictional burden as well as they worm their way through the gel pores less efficiently compared than smaller molecules, type and concentration of agarose, voltage applied, DNA conformation, presence of DNA dye (GelRed) and electrophoresis buffer. When separation is done then staining with nucleic acid dye (Gel red) is performed and the DNA molecules can be visualized under UV light (Lee et al., 2012; Smith, 1993).

GelRed is a new fluorescent nucleic acid stain, which is designed for the purpose of replacing ethidium bromide (EtBr) due to its highly toxic nature. GelRed facilitates the method of gel electrophoresis and other experimental methods, which mainly rely upon the fluorescence of stained DNA. When bound to DNA, GelRed shows the same absorption and emission spectra level, which is shown by EtBr (Crisafuli, Ramos, and Rocha, 2015). However, according to its Safety Report from Ames test, it is shown as non-mutagenic. For example, GelRed fails to enter the HeLa cells after 30 min treatment as well as it also produces negative results for the mouse spermatocyte chromosomal aberration test (Sayas, Garcia-Lopez, and Serrano, 2015).

Procedure

1 % agarose gel was prepared by mixing 1 g of agarose with 5 ml of 20x minigel buffer and 94 ml of dH_2O. The solution was completely mixed by boiling in microwave oven. This solution was poured slowly into the casting frame along with insertion of a comb for producing wells. The solution was left for polymerization at room temperature for approximately 20-30 minutes. The comb was removed slowly before placing the gel in a tray. Minigel buffer was added until covering of the gel. In other side, the calculated amount of DNA samples was mixed with TE buffer and 6xT gel loading buffer before employing into the wells along with the ladder (1 kb). The current wires were connected with the tray for applying 90 V current to the gel for 1 hour.

Afterwards, the gel was stained in GelRed for 20 minutes. The DNA bands and 1 kb ladder were visualized on the gel by exposing to the UV light at 302 nm using a UV transilluminator. Finally, images of the gel were obtained by using Multi-Cod Digital imaging system.

3.2.5. Restriction enzyme digestion

The restriction of DNA was first discovered and explained by Arber and Dussoix in 1962 during the analyzing of the molecular mechanisms of host-controlled modifications of bacteriophage. (Arber and Linn, 1969). Restriction enzymes are very useful due to recognition of specific nucleotide sequences and provide a very specific cleavage of DNA (Roberts, 2005; F, Micheli, and Camilloni, 2019).

Procedure

The quantity of 100 ng plasmid DNA was mixed with 1µl 10x cutting buffer. Afterwards, a quantity of 0.5µl of each desired restriction enzyme (EcoRI or Bsr GI) was mixed along with dH_2O to make a total volume of 10 µl in an Eppendorf tube. This was mixed carefully and left for incubation at 37 °C for 1 hour in water bath. Finally, after incubation 2 µl 6xT loading buffer was added and the sample analyzed by agarose gel electrophoresis.

3.2.6. Preparation of bacterial Freeze Stocks

Freezer stocks of bacterial cultures is a way to store *E. coli* transformed with a specific plasmid for later use. 1200 µl of the bacterial overnight culture was mixed with 300 µl 50% glycerol in a 2 ml Cryo tube and stored at -70 ^{o}C.

3.2.7. Site-directed mutagenesis

Quick change site directed mutagenesis (developed by STRATAGENE) is a simple and rapid procedure that includes PCR, DpnI digestion and overlap extension. The important point of this approach is the use of overlap extension to design a circular DNA plasmid with mutations and this all obtained without the use of phosphorylated primers or ligase reactions. The new DNA

is synthesized with nicks between the 3' ends of the synthesized DNA as well as the 5' ends of the first pair of primers during the first round of PCR. Finally, a new pair of mutagenic oligonucleotides leads to the combination of the two DNA sections that anneal together with the overlap sequence inside the two primers during successive rounds of PCR. This new mutated molecule also includes nicks at various positions when compared with those constructs in the first turn of PCR that had been "repaired" by overlap extension. By using this method, mutations can be introduced successfully. Afterwards, the circular DNA is transformed into *E. coli* cells, where the circular plasmid is ligated (Forloni, Liu, and Wajapeyee, 2019).

3.2.7.1. Polymerase chain reaction

The polymerase chain reaction (PCR) is an important tool, which is used to amplify a specific DNA sequence. This method was developed by Kary Mullis in 1983 (Mullis and Faloona, 1987). The PCR reaction can be performed by using a source of DNA obtained from variety of tissues and organisms. PCR facilitate to generate several copies of DNA from a very small amount. PCR based DNA amplification is today used both as a diagnostic tool in the clinic, and in conventional laboratory methods (Garibyan and Avashia, 2013).

Procedure

The following reagents which were mixed in a PCR tube for running in a PCR reaction.

- 0.2 µl Forward primer (10 mM)
- 0.2 µl Reverse primer (10 mM)
- 0.1 µl Template DNA (20-30 ng)
- 2.5 µl PFU reaction buffer (10x)
- 1 µl dNTP mix (10 mM)
- 1 µl DMSO (Dimethyl sulfoxide)
- 0.5 µl Pfu DNA Polymerase
- dH_2O to 25 µl

The following PCR program for site-directed mutagenesis was used:

1. 95 °C 30 sec (Initial denaturing)
2. 95 °C 30 sec (Denaturation)
3. 55 °C 1 min (Annealing)
4. 68 °C 2 min per kb (Elongation)
5. Go back to step 2 for 20 times
6. 68 °C 5 min (Final elongation)
7. 4 °C ∞

To remove template DNA, 0.8 µl DpnI was added and left for incubation at 37 °C in water bath for 1 hour. DpnI restriction enzyme requires methylation at their recognition sites in order to efficiently cleave DNA. Therefore, it will cleave only the template plasmid, and not the mutated plasmids generated by PCR (blog.addgene.org).

3.2.8. Transformation of competent *E. coli* (DH5α)

The artificial method of DNA transfer into Escherichia coli was first demonstrated by Mandel and Higa in1970 (Hanahan, 1983). The transformation of bacteria involves two general phases such as DNA binding to the cell surface, which is followed by uptake of that DNA across the cell envelope into the cytoplasm and establishment as well as expression of that DNA as a stable genetic element in the cell (Hanahan, 1983; Panja et al., 2006). The naturally occurring bacterial transformation are found in various bacterial genus. For example, Micrococcus, Bacillus and Haemophilus organisms shows proteins on their outer surface. The main function of this protein is to bind to DNA in their environment and transfer to the cell. However, it is not common for most of the bacteria to naturally take up DNA from the environment. But when certain artificial conditions are subjected to most bacteria then they become able to take up free DNA and the cells in such artificial state are indicated as competent. *E. coli* has grown and developed into a universal host organism for the purpose of both DNA molecular cloning as well as for a various set of analysis that involve cloned genes (Panja et al., 2006). The competence can be developed in *E. coli* by using different methods. *E. coli* DH5α used in this study is chemically competent. This chemical method involves the treating of bacteria with bacteriophage "λ" DNA in the presence of Ca^{2+} ions by suspending the cells in ice-cold of $CaCl_2$ such as 50–100 mM and then followed by a brief heat shock at 42 °C. This method is known as the "calcium chloride ($CaCl_2$)" method and it is used by our lab as well (Panja et al., 2006; Chan et al., 2013).

Procedure

The chemically competent *E. coli* DH5α cells were thawed on ice around 15-30 minutes. The quantity of 80 µl *E. coli* (DH5α) cells were added in an eppendorf tube. Then an appropriate amount of DNA plasmid was mixed into the tube. This mixture was incubated for 20 minutes on ice. After the incubation, the transformation mixture was heat shocked at 37 °C for 2 minutes in water bath. Afterwards, there was added 250 µl SOC media and left for incubation at 37 °C with 150 rpm shaking for 1 hour. Finally, the incubated mixture was plated by 100-200 µl onto LB plates with ampicillin or kanamycin (Table 1) depending on the plasmid. The plate was left for incubation overnight at 37 °C.

3.2.9. Sanger sequencing

The first sequencing for a complete genome was published by the Nobel Prize winner in Chemistry named Frederick Sanger. Today, the Sanger sequencing method is still broadly used all over the world and is mainly based upon the use of dideoxynucleotides (ddNTPs) that have been used to block DNA polymerization. Basically, the dideoxynucleotides are similar to the deoxynucleotides (dNTPs). The only variation is that the ddNTPs require a hydroxyl group (-OH) on the position of the third carbon of the ribose and this also induces the enzyme to cease the polymerization, since it is not capable to find the chemical group to attach to the next nucleotide. The reaction which is prepared by the DNA polymerase along with a combination of dNTPs as well as ddNTPs, so that at all extensions of a nucleotide, the enzyme can absorb either of them randomly (Figure 14) (Garrido-Cardenas et al., 2017).

In the Big Dye (Applied Biosystem) DNA sequencing kit used here, each ddNTPs is tagged by a specific fluorophore molecule, so that every time one of them is integrated, the produced molecule will discharge a specific signal that will notify on the last integrated nucleotide. In this manner, after a sufficient number of cycles of amplification, the number of molecules will be equivalent to the number of nucleotides that incorporated into the DNA fragment to be sequenced. Later a capillary electrophoresis is carrying out along with these molecules. As a result, they will be arranged according to increasing order of molecular mass in which each molecule can be detected by the fluorophore, which is joined to the reciprocal ddNTPs

terminator of the reaction. The detection method is carried out by a device of Charge-Coupled Device (CCD) spectral detector (Garrido-Cardenas et al., 2017).

In this work, the Big dye V 3.1 DNA sequencing kit (Applied Biosystem) was used. The sequencing reactions was sent to our in-house sequencing lab, where the instrument of ABI PRISM 3130x1 Genetic analyzer (Applied Biosystem) was used for the determination of the DNA sequence.

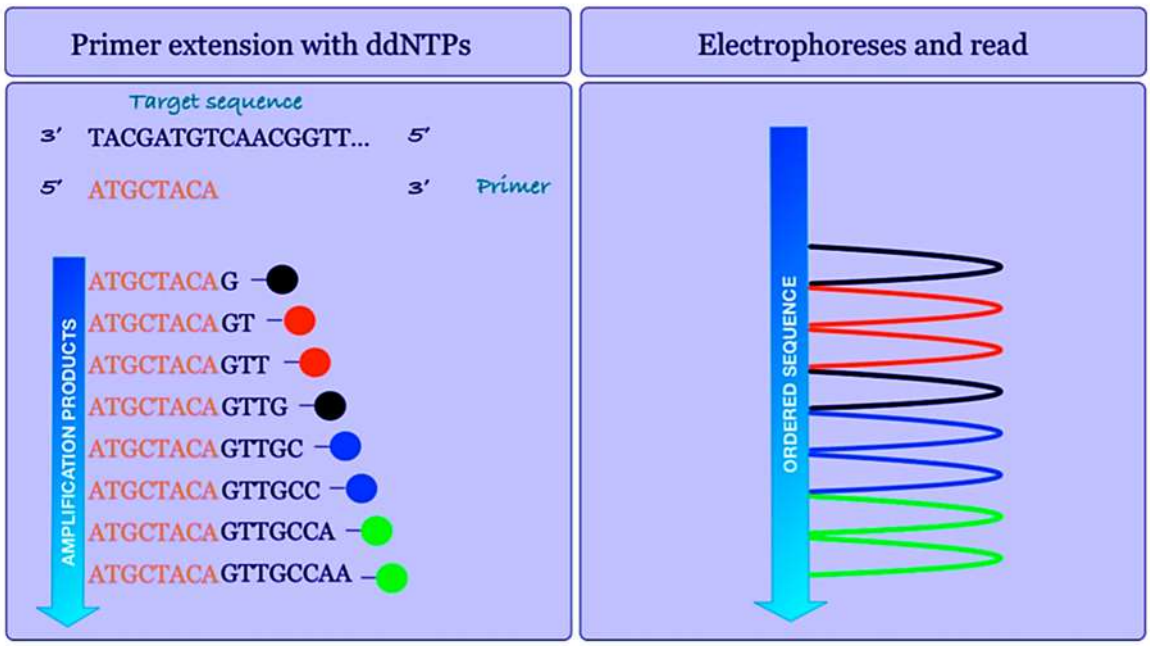

Figure 14: This figure shows the sanger dideoxy sequencing method or chain termination enzymatic method. The fluorescence-labeled ddNTPs have been used to block DNA amplification, which is also shown in figure (Obtained from Garrido-Cardenas et al., 2017).

Procedure

The following reagents were mixed in a 0.2 ml PCR tube on ice.

- 1 µl Plasmid (200-300ng)
- 1 µl Primer (10µM)
- 1 µl Big dye V 3.1(Applied Biosystem)
- 2 µl 5x Sequencing buffer (Applied Biosystem)
- 5 µl dH_2O (Total volume of 10 µl)

The PCR program for sequencing was:

1. 96°C 1 min
2. 96°C 30 sec
3. 50°C 15 sec
4. 60°C 4 min
5. Go back to step 2 for 34 times
6. 4°C ∞

The obtained sequencing result was further analyzed by Chromas software sequence (http://technelysium.com.au/wp/chromas/) and NCBI BLAST (https://blast.ncbi.nlm.nih.gov).

3.2.10. Mammalian cell culture

Mammalian cells were grown in a 5% humidified CO2 incubator at 37°C. All the solutions which were used for growing of cells cultures were preheated to 37°C. The HeLa cells (ATCC, CCL2), MCF-7 breast cancer cell lines (ATCC, HTB-22) and HEK293 FlpIn TRIM32 KO cells (ATCC, CRL-1573) (Overa et al., 2019) cells were grown in MEM with 100 U/ml penicillin and 100 g/ml streptomycin and 10% FCS solution mixture. The MDA-MB-231(ATCC, HTB-26) breast cancer cell line was grown in RPMI with 100 U/ml penicillin and 100 g/ml streptomycin and 10% FCS solution mixture. Similarly, C2C12 mouse myoblast (ATCC, CRL-1772) cell line and the H9c2 rat myoblast (ATCC, CRL-1446) cell line were grown in DMEM with 100 U/ml penicillin and 100 g/ml streptomycin and 10% FCS solution mixture.

3.2.10.1. Splitting and counting of cells

The cells in the cultures have the capability to grow and double in number after every 24 hours. When the cells have grown confluent contact inhibition will make them difficult to transfect and result in stop of growth, detachment and dead.

Therefore, there is need to split the cells when they are confluent. All the mammalian cells used in this lab work were divided and diluted 1:2, 1:4, 1:6 or 1:8 depending on when the next splitting or transfection event was going to take place. All the mammalian cells were grown in

a filter capped flask having a culture area of 75 cm^2 (T75) or 175 cm^2 (T175) (Thermo Fisher scientific).

Procedure

When the cells were confluent, the cell medium removed by suction and these cells in flask (T75 or T175) were washed by 5-10 ml of 1xPBS solution. After washing, 0.5-1ml trypsin was added and evenly distributed over the cells, incubated for 1-2 minute until the cells had detached. Afterwards, culture medium was added to inactivate the trypsin. A small volume of these cells culture solutions, depending on when the next splitting or transfection event take place were transferred to a new flask, 5-10 ml fresh media added, left in incubator for next time use.

3.2.11. Transfection of mammalian cells

Transfection of mammalian cells is the uptake of foreign DNA and is a widely used technique (Cervera and Kamen, 2018). Eukaryotic cells show the capability to take up external DNA under various suitable conditions and this DNA becomes localized in the nucleus. This phenomenon has been used to get both transient and stable expression of different genes (Felgner et al., 1987). The transient transfection has been performed by various kinds of DNA transfection reagents such as calcium phosphate, cationic lipids and cationic polymers (Cervera and Kamen, 2018). An extensive range of cationic lipid reagents for the purpose of lipofection are manufactured, marketed as perfect for various types of cells and diverse types of nucleic acids such as co-transfection of both RNA and DNA (Marwick and Hardingham, 2017). Cationic lipids such as Lipofectamine or METAFECTENE® PRO (Biontex) are very efficient and useful in terms of transfection efficiency (Cervera and Kamen, 2018). In this technique, Lipofection are used to introduce DNA or RNA into the cells by producing a liposome that contain positively charged lipids by encircling the negatively charged nucleic acids. These liposomes are ready to combine with cell membranes allowing the access of nucleic acids inside the cell (Figure 15) (Marwick and Hardingham, 2017).

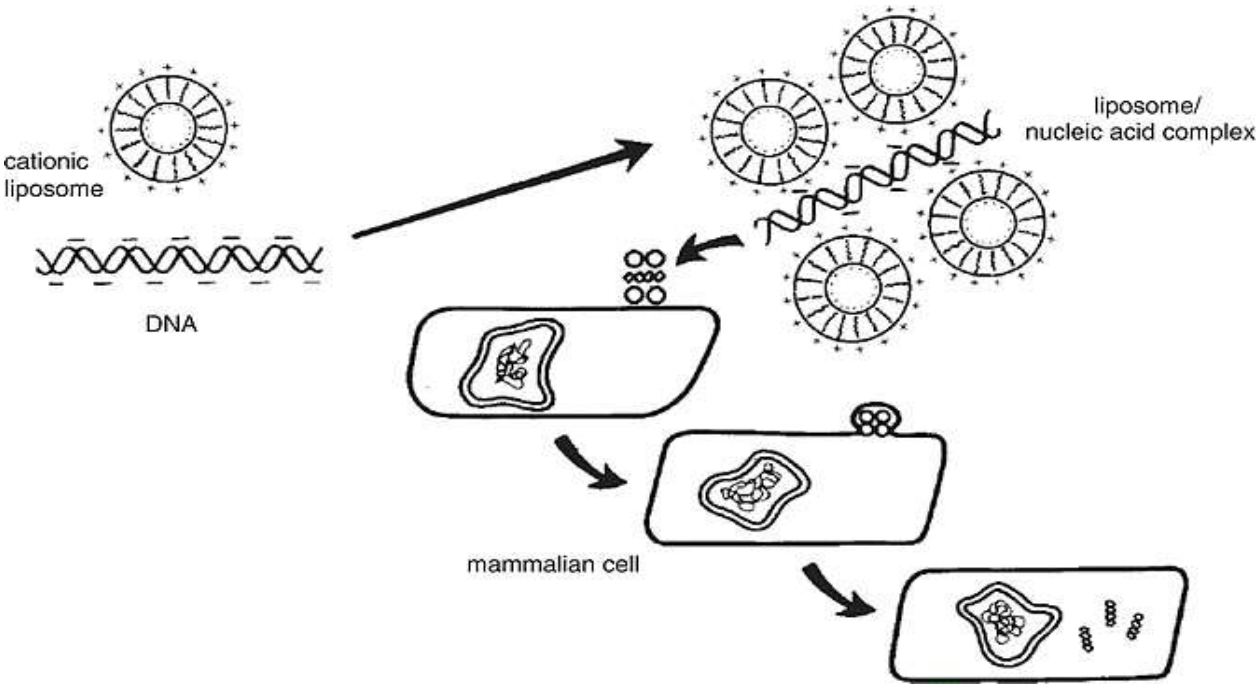

Figure 15: This figure shows the complete mechanism in which lipofection promotes entry of nucleic acid into the mammalian cells. The lipid membrane is surrounding the DNA and merge with the cell membrane by releasing the DNA into the cells (Obtained from Felgner and Ringold, 1989).

Procedure

The number of mammalian cells were counted by using a drop of the cells in the Büchner chamber and counted under a microscope. The number of counted cells in a Büchner square was multiplied with 10^4 value to obtain the number of cells per ml solution. Alternatively, the mammalian cells were counted in TC20 Automatic cell counter. An appropriate number of cells for transfection (300,000 cells per well in 6-well dish) were poured into each well for transfection along with fresh culture media of MEM+10% FCS or RPMI+ 10% FCS(2 ml in each well in a 6 -well dish) and left for incubation for 24 hours.

When the cells were ready for transfection, a mixture for each well were prepared in an eppendorf tube by mixing 150 µl MEM or RPMI media without antibiotic, plasmid DNA (1000ng), 2.5 µl transfection agent (METAFECTENE® PRO (Biontex)) and left for 20 minutes incubation at room temperature. The growth media of cell wells was changed with 2 ml of fresh growth media in each well. After 20 minutes the transfection mix was added to each well. The cells were left for transfection in the incubator for 24 hours. Next day, the cells were checked

under a fluorescence microscope (LECIA CTR 6000) for transfection efficiency (number of cells expressing GFP). When a good transfection efficiency was obtained then the cells are ready for harvesting.

3.2.11.1. Treatment with different inhibitors

The transfected cells were treated with Bafilomycin A1 (0.2 μM) or MG132 (20 μM) inhibitors along with fresh culture media (10% FCS + MEM) or starvation media (HBSS). The MG132 is a powerful, reversible and cell-permeable proteasome inhibitor whereas, Bafilomycin A1 inhibits the lysosome. The cells were treated for 3 hours before harvested by 2x SDS loading buffer with 200mM DTT freshly added. Alternatively, the cells were also treated with Bafilomycin A1 (0.1 μM) or MG132 (5 μM) for 24 hours.

3.2.12. SDS- PAGE

Sodium Dodecyl Sulfate Polyacrylamide Electrophoresis (SDS-PAGE) is widely used technique for analyzing proteins in a mixture (Smith, 1984). This method is also used for determining the molecular weight and analysis of proteins, which are isolated by immunoprecipitation of various cell extracts (Trieu and Targoff, 2019). The percentage of polyacrylamide, which is used in the gel along with the buffer system will control the proteins mobility through the gel when current is applied. In this technique the proteins are reacted with the anionic detergent SDS. The normal size of the target protein is used to select the correct gel and buffer system to produce optimum level of separation and resolution. The protein samples are supported by dye indicator and glycerol in the sample loading buffer. When the current is applied, proteins move through the gel and are separated by charge. The charge of the SDS-protein complex is roughly proportional to protein size. A protein standard is included in one well/lane, which is composed of a pool of proteins with known molecular weights (Smith, 1984; Hnasko and Hnasko, 2015).

Normally, the electrophoresis in SDS-PAGE is run in a discontinuous buffer system provided with two gels such as a lower buffer level, which is used for the separating gel and an upper buffer level, which is used for the stacking gel/concentrating gel. Both gels contain SDS but with various ionic strength and pH level. The staking gel have the capability to concentrates the sample because it does not permit the movement of the SDS-peptide complexes at its own

speed, until they move to the separating gel where they are segregated and separated according to their size. This method allows the separation of comparatively large volumes of samples without falling resolution (Garcia-Solaesa and Abad, 2016).

Procedure

Harvesting of cells for Western Blotting

The growth medium was removed, and the cells washed with 1x PBS two times. 80 µl of 2x SDS loading buffer with 20 % DTT was dropped to each well in a 6-well dish. The cells were scratched from the wells and cell lysates were collected in Eppendorf tubes. These lysate cells were boiled for 10 minutes at 100°C and spun down. The supernatants were now ready for loading on an SDS-PAGE.

Casting and loading of SDS-PAGE

The SDS-PAGE was prepared by collecting two plates, one glass and one plastic which were separated by spacers and mounted in a gel caster. The components of 8% separating gel was mixed (see Table 2) and poured between the fixed plates until 2/3 filled. A small amount of water was added on the top side of separating gel to keep the gel straight. The gel was left for 20 minutes until polymerization. Afterwards, 4 % concentrating gel was mixed (see Table 2) and poured on the upper side of separating gel after removal of water. A piece of comb was placed in this concentrating gel for creation of wells and the gel was left again for 20 minutes until polymerization. The prepared gel was mounted in an electrophoresis apparatus. The comb was removed from the gel and electrophoresis buffer was added to the vertical and bottom side reservoirs. A quantity of 5 µl biotinylated protein ladder and 5 µl blue pre-stained ladder were mixed and this ladder mix was loaded in the gel. Afterwards, cell lysates were loaded onto the wells and the gel was left for 1-2 hours running at 26 mA along with water cooling until the blue staining reached at bottom line.

3.2.13. Western blot

Western blotting or protein immunoblotting is a widely used technique in which an individual protein is visualized in the middle of thousands of other proteins in a sample. This technique

uses SDS-PAGE method to separate proteins in the sample on the basis of size (Roy et al., 2019). This technique was developed in 1979 by several groups independently and was later named 'Western blotting' due to its correlation to southern and northern blotting (Towbin, 1998). This method is based upon using antibody-based examinations to gather important information related to target proteins from complex samples (Najafov and Hoxhaj, 2017). The separated proteins from SDS-PAGE are transferred and immobilized onto a PVDF (polyvinylidene difluoride) or nitrocellulose membrane. The membrane is washed, blocked as well as incubated with an analyte-specific primary antibody. There are two simple approaches involving the use of a direct reporter-labeled primary antibody or a reporter-labeled secondary antibody, which are directed against the present species of the primary antibody. The reporter conjugated to the antibody can be different. For example, an enzyme that produces a reaction product with color or when exposed to a substrate, a luminescent signal was produced at the place of antigen-antibody binding (Hnasko and Hnasko, 2015; Roy et al., 2019). Western blotting can be quantitative or semiquantitative, which is depending on the type of reagents used (Najafov and Hoxhaj, 2017).

It is a regular method that is mainly adopted in the field of molecular biology, biochemistry and cell biology with a vast number of applications. This method can be facilitated to get valuable information about protein quantity, its molecular weight as well as post-translational modifications. Western blotting is a very sensitive method, which is due to the high affinities of antibody approaching their epitopes as well as due to amplificatory nature (Najafov and Hoxhaj, 2017). Western blotting can identify target proteins as low as 1 ng in concentration due to its high-resolution quantity of gel electrophoresis as well as strong sensitivity and specificity provided by the immunoassay (Roy et al., 2019). Even picogram amounts of target proteins can be observed (Najafov and Hoxhaj, 2017).

Procedure

A nitrocellulose blotting membrane (Sigma, GE10600003) along with 6 pieces of filter paper was prepared with the same sizes as separating gel 6.5 x 8.5 cm. A sandwich was made by placing sponge at the bottom followed by three filter paper soaked by 1x Transfer buffer (Table 2), the membrane, the separating gel and finally remaining three filter papers soaked by 1x Transfer buffer. A roller was used to avoid bubbling in the sandwich. The sandwich was locked

in a holder and placed in a blotting chamber (Trans-Blot® Turbo™ Transfer System BIO-RAD). A current of 25 volts was applied for 7 minutes to transfer the proteins from the gel to the membrane.

The blotting membrane was removed from the sandwich and left for 5 minutes with 5% ponceau staining solution and washed with water. This membrane was washed again for 5 minutes by soaking in 1xTBS-T solution at room temperature with shaking. The membrane was blocked by soaking into 5% blocking milk solution at room temperature by shaking for 30 minutes. A quantity of 1.5 ml 5% blocking milk was mixed with primary antibody (Table 4) in a 50 ml tube. The blotting membrane was transferred to the 50 ml tube and left for incubation on rotating roller for ON (overnight) at 4°C. Afterwards, the membrane was washed in 1xTBS-T solution three times for 10 minutes each. A quantity of 1.5 ml with 5% blocking milk was mixed with secondary antibody (Table 4) and ladder antibody (HRP-conjugated anti-biotin antibody) in a 50 ml tube. The blotting membrane was again transferred to the 50 ml tube and left for incubation on rotating roller for 1 hour at RT. The membrane was washed in 1xTBS-T solution three times for 10 minutes each. Finally, the membrane was wrapped in a plastic foil dropped by chemiluminescent peroxidase substrate (Sigma). The membrane signals were detected by Image Quant Las 4000 (GE Lifesciences).

3.2.14. Confocal Microscopy

The most important and diverse application of confocal microscopy in the field of biomedical sciences is the use for imaging either in the form of fixed or living cells that have usually been tagged with one or more kinds of fluorescent probes (Paddock, 1999). These confocal instruments have the capability of revealing fluorescence emissions in the ranges of 400 to 700 nm. This also provide to covers a broad range of frequently available fluorescent probes. The fluorophores consist of various synthetic fluorochromes such as the Alexa dyes and quantum dots, and the naturally occurring fluorescent proteins, which include green fluorescent protein (GFP) and its color mutants such as CFP and YFP (Paddock, 2014). GFP is a spontaneously fluorescent protein, which was isolated from the jellyfish *Aequorea victoria* (Yang, Moss, and Phillips, 1996; Heim, Cubitt, and Tsien, 1995). GFP can provide its role as a protein tag and its expression can be further used to monitor gene expression as well as protein localization in

living organisms. Exogenous GFP is highly expressed in mammalian cells and its fluorescence is generally dispersed throughout the cytoplasm and nucleus. GFP consists of 238 amino acids and it absorbs blue light at 395 nm and emits green light with emission peak at 509 nm (Yang, Moss, and Phillips, 1996; Chalfie et al., 1994). Enhanced Green Fluorescent Protein (EGFP) is a mutant from wild type GFP with an excitation at 490 nm (Masters et al., 2018).

The first confocal microscope was invented by Minsky in 1955 (Prydal and Dilly, 1998). The Confocal laser scanning microscopy is the most suitable method, which is used for visualization of intracellular co-localization of proteins found in intact cells. CLSM also offers important advantages for examining of subcellular localization of proteins when compared with other conventional fluorescence microscopy (Miyashita, 2004). The fluorophores have been designed according to the specific target and helpful to analyze subcellular structures of the cytoplasm, mitochondria, nucleus and co-localization of proteins with multicolor labeling. The laser part of fluorescence confocal microscopy is provided by an excitation light at a wavelength that will also excite a fluorophore of a specific type. The target tissue hits by the excitation laser to produces high intensities of fluorescence at a precise focal point. There is only light coming from the focal plane that is detected because the light approaching from additional planes cannot pass over the pinhole. Both the laser light or the excitation beam and the resultant emission fluorescence light pass over the identical objective of a special mirror, which is known as dichroic mirror. This mirror also reflects the incoming higher-energy with shorter-wavelength laser light but admits the lower-energy with higher-wavelength of fluorescent light to move through the light detector (Figure 16). In fluorescence confocal microscopy, a pinhole is also used to get rid of scattered light. Finally, the light is collected from an extremely focused point and the images of the scanned specimen can then be reorganize point by point. (Miyashita, 2004; Nwaneshiudu et al., 2012; Foldes-Papp, Demel, and Tilz, 2003).

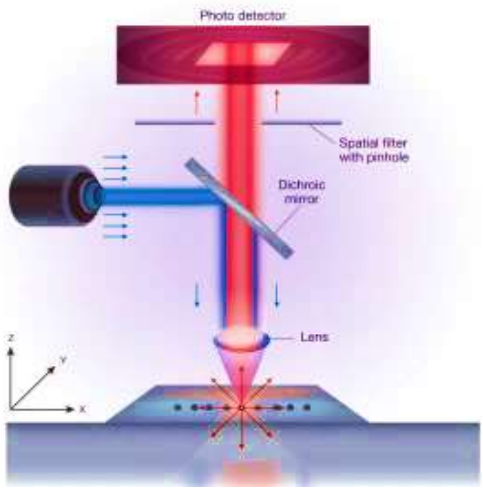

Figure 16: The simplified view of confocal microscopy along with detector, dichroic mirror and lenses (Obtained from Nwaneshiudu et al., 2012).

3.2.14.1. Seeding of cells in 8-well chamber for confocal microscopy

The number of HEK293 FlpIn TRIM32 KO cells were counted in TC20 automatic cell counter cell and calculated the correct number of cells for transfection (4000 cells per well) in 8-well dish (NUNC#155411). The cells were poured into each well for transfection along with 0.5 ml fresh culture media and left for incubation for 24 hours. A mixture for each well were prepared in eppendorf tubes by mixing 25 µl MEM media without antibiotic, plasmid DNA (100 ng), 0.5µ l transfection reagent (Trans IT, Mirus) and left for 15 minutes incubation at RT.

The growth media was changed by 0.5 ml of fresh growth media of MEM+10% FCS in each well. The transfection mix was added dropwise to the wells. The cells were left for transfection in the incubator for 24 hours before fixation, immunostaining and analyses by fluorescence confocal microscopy.

3.2.14.2. Cell fixation and immunostaining

The cell media was removed and 250 µl of 4% Fomaldehyde (GH) was added and cells incubated 15 min at RT to fixate the cells. Afterwards, the cells were washed two times by 1x PBS. The cells were permeabilized by adding 500 µl methanol and left for incubation for 5 minutes at RT before washed two times by 1x PBS. The cells were blocked by 5% Bovine serum albumin (BSA) in PBS for 30 minutes at RT.

The primary antibodies anti-GM130 and anti- p62 were diluted in 1% BSA (Table 4). This primary antibody mixture of 125 µl quantity was added into each well and left for incubation for 1 hour at RT. Afterwards, the cells were washed 3 times with 1x PBS before secondary antibodies treatment. The different secondary antibodies Alexa Rabbit-555 (Anti-rabbit) and Alexa Mouse-647 (Anti-mouse) along with DNA stain DAPI were prepared. This secondary antibody mixture of 125 µl quantity was added into each well and left for incubation for 1 hour, in dark at RT. Afterwards, the cells were washed 2 times with 1x PBS, and the cells were covered by 250 µl 1x PBS for further confocal analysis.

3.2.14.3. Fluorescence Confocal Microscopy

The confocal analysis of 8-well dish was performed by taking confocal images using a 40× NA 1.2 water immersion objective on an LSM780/LSM800 system. There are 4 images per condition, each containing 10-20 cells, were analyzed by using the ZEN software (Zeiss). Each image includes 10-20 cells.

3.3. Generation of knock-out cells by using CRISPR/Cas9

This CRISPR/ Cas9 is a gene-editing technology, which mainly involves two types of important components, a guide RNA component or CRISPR RNA (crRNA), which is used to match a required target gene and Cas9 (CRISPR-associated protein 9), which is an endonuclease. The CRISPR RNA (crRNA) can be used to manage Cas9 to cut DNA and produce double-strand breaks at the position of specific target sites. The following cellular DNA repair process drives to desired insertions, deletions and replacements at the position of target sites. The specificity of the CRISPR/Cas9-mediated DNA cleavage desires target sequences corresponding crRNA and a protospacer neighboring motif (Ran, Hsu, Wright, et al., 2013; Redman et al., 2016; Zhang, Wen, and Guo, 2014). The Cas9 is guided by a small RNAs through Watson-Crick base pairing with the target DNA (Figure 17) (Ran, Hsu, Wright, et al., 2013). For example, by constructing a 20-nucleotide region, which is complementary to a DNA sequence of interest in the sgRNA. The Cas9 can be proposed at any genomic locus with a relevant PAM (proto-spacer adjacent motif) sequence. After the tracking and cleavage of DNA, the repair mechanisms can cause insertion and deletion mutations, which may generate a knock-out (Lentsch et al., 2019).

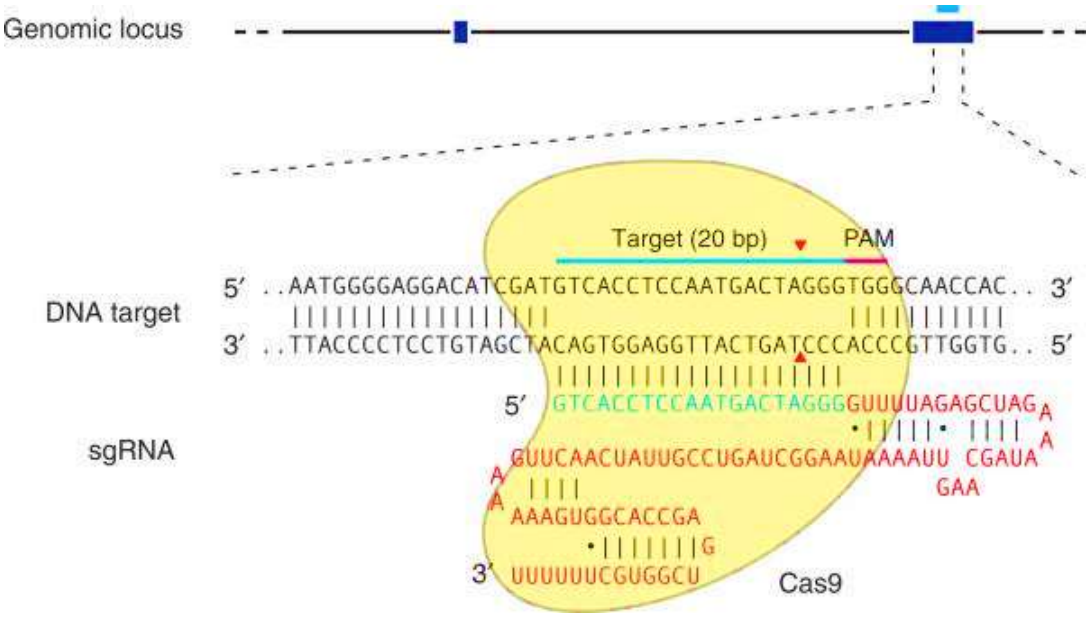

Figure 17: The diagrammatic representation of the RNA-guided Cas9 nuclease is shown. The Cas9 nuclease obtained from S. pyogenes (in yellow) is targeted to genomic DNA (such as human EMX1 locus) by using an sgRNA, which is consisting of a 20-nt guide sequence (blue) and a scaffold (red). The guide sequence pairs with the DNA target (blue bar shown on the top strand) directly upstream of a required 5′-NGG adjoining motif (PAM shown pink). The Cas9 mediates a DSB of ~3 bp is crucial for the PAM (red triangle) (Obtained from Ran, Hsu, Wright, et al., 2013).

Methods performed to establish CRISPR/Cas9 mediated knock out cells

The CRISPR/Cas9 system was used to generate a knockout cell line for TRIM32. The knockout cell line was generated as described by Ran, Hsu, Wright, et al., (2013).

3.3.1. Determination of Cas9 target sites in gene of interest and order Oligos

For determination of target sites in gene of interest, the online CRISPR Design tool software CHOPCHOP (https://chopchop.cbu.uib.no/) that takes an input sequence and identifies suitable target sites was used. We chose the two target sites sequences with top scores for mouse and rat TRIM32 genes.

Mouse Target T1: **5′-CACCGATACGATAGTTGCCCCGGT-3′**

5′-AAACACCGGGGCAACTATCGTATC-3′

Mouse Target T2: **5′-CACCGTGCTCGGGGCGACCTCATTG-3′**

5′-AAACCAATGAGGTCGCCCCGAGCAC-3′

Rat Target T1: **5′-CACCGAAGATTTCCGCTGCATCGC-3′**

5′-AAACGCGATGCAGCGGAAATCTTC-3′

Rat Target T2: **5′-CACCTACAGCGTCCTTATTCGAGA-3′**

5′-AAACTCTCGAATAAGGACGCTGTA-3′

The oligos were ordered from Thermo fisher.

3.3.1.1. Phosphorylation and annealing of Oligoes

The top and bottom strands of oligos were resuspended in dH_2O to a final concentration of 100 μM. The mixture for phosphorylation and annealing of sgRNA oligos were prepared by mixing the following contents in an Eppendorf tube.

1 μl Oligo 1 (100 μM)

1 μl Oligo 2 (100 μM)

1 μl 10x T4 DNA ligase Buffer (NEB)

1 μl T4 Polynucleotide kinase (NEB)

Total: dH_2O to 10 μl

The sample was incubated in a PCR machine with the following program.

37°C 30 min (Phosphorylation)

95°C 5 min (Denaturation)

Temperature ramping down from 95°C to 25°C (Annealing).

3.3.1.2. Linearisation and Ligation in one step

In this step, the phosphorylated and annealed oligoes were inserted in the pX458 plasmid established by Ran, Hsu, Wright, et al., (2013), which encodes the Cas9 endonuclease and GFP.

1 µl 10X NEB2 buffer

1 µl T4 DNA ligase Buffer (NEB)

1 µl annealed oligo (diluted 1:200 in dH_2O)

300 ng pX458 plasmid

0.5 µl Bbsl

0.5 µl T4 DNA ligase (NEB)

Total: dH_2O to 10 µl

The mix was incubated in a PCR machine with the following program.

1. 37°C 20 min
2. 16°C 15 min
3. 37°C 10 min
4. 55°C 15 min
5. 4°C ∞

Step 1 and 2 are repeated 3X.

3.3.2. Transformation of *E.coli* (DH5α)

50 µl of the ligation mix was transformed into 50 µl of competent *E.coli* DH5α. The correct insertion of oligoes into the pX458 plasmid was verified by plasmid miniprep, restriction enzyme digestion, agarose gel electrophoresis and DNA sequencing using the U6 primer. All these methods are described above.

3.3.3. DNA Precipitation

DNA precipitation of plasmids was done to purify the plasmids to increase transfection efficiency. DNA precipitation of the CRISPR pX458 plasmids with inserted sgRNA sequences pX458- m(mouse) TRIM32 (T1), pX458-mTRIM32 (T2), Px458-rat TRIM32 (T1) was performed. 80µl plasmid was mixed with 3M NaOAc pH 5.2 (1:10 vol). This mixture was mixed with 2 vol of 96% EtOH. Afterwards, the mixture was vortex for 10 seconds and left for incubation at RT for 20 minutes. After incubation, the mixture was centrifuged for 30 minutes at maximum speed. The supernatant was removed, and the pellet washed with 200µl 70% EtOH and centrifuged for 10 minutes at maximum speed. The pellet was dried before it was dissolved in 50 µl elution solution. The concentration and purity of the precipitated plasmid were measured by using a Nanodrop device (ND-100 spectrophotometer).

3.3.4. Transfection of mouse myoblast (C2C12) and rat myoblast (H9c2) cells

The transfection of mouse myoblast (C2C12) and rat myoblast (H9c2) cells with transfection agent METAFECTENE® PRO (Biontex) were performed in a similar way as explained above.

3.3.5. Sorting of cells by flow cytometer

One day post transfection the efficiency of the transfection was measured by fluorescence microscopy analysis of EGFP expression in the cells. Wells where the number of transfected cells was more than 35 % were harvested by trypsination, resuspended and filtered to ensure only single cells in the harvested solution. Thereafter, transfected cells were sorted into 96-well dish by using a cell sorter FACSAria cell sorter running FACSDiva software version 5.0 (BD Biosciences) in which the blue laser for excitation of GFP used. The GFP fluorescence was collected through a 530/30 nm bandpass filter in the E detector (Overa et al., 2019). The sorter picks out the green cells in the solution and seeds one green cells in each well of the 96-well dish. Before sorting the 96-well dish was poured by 100 µl DMEM+20% FCS into to each well. The 96 well dishes were incubated for nearly 3 weeks in the cell incubator. Medium was changed once a week, and the wells frequently investigated for cell growth.

When colonies of cells were detected by microscopy of the wells, the cells were detached by trypsination and transferred to a well in a 24-well dish. Each cell clone was given a specific number, and care was taken not to cross-contaminate the cell cultures. When the cells in the 24-well dishes were grown to confluence, the cells were trypsinated and seeded into two wells in a 12-well dish. s and. One well was later harvested in 50 µl 2XSDS+20% DTT for Western Blotting while the other wells were expanded in a cell culture flask for further work and for making freezer stock. The western blotting was performed by using TRIM32 and PCNA antibodies.

4. Results

Previous mass spectrometric (MS) analysis of immunoprecipitated EGFP-TRIM32 from HEK293 FlpIn cells (Overa et al., 2019) identified three lysines that were ubiquitinated or acetylated in cells expressing EGFP-TRIM32 wild type, but not in cell expressing the LGMD2H disease mutant EGFP-TRIM32 D487N that is unable to undergo self-ubiquitination. These lysines were K50, K247 and K401. Bioinformatic analysis using the Phosphosite Plus software (www.phosphosite.org) confirmed that these lysines are potential targets for ubiquitination and acetylation (Figure 18).

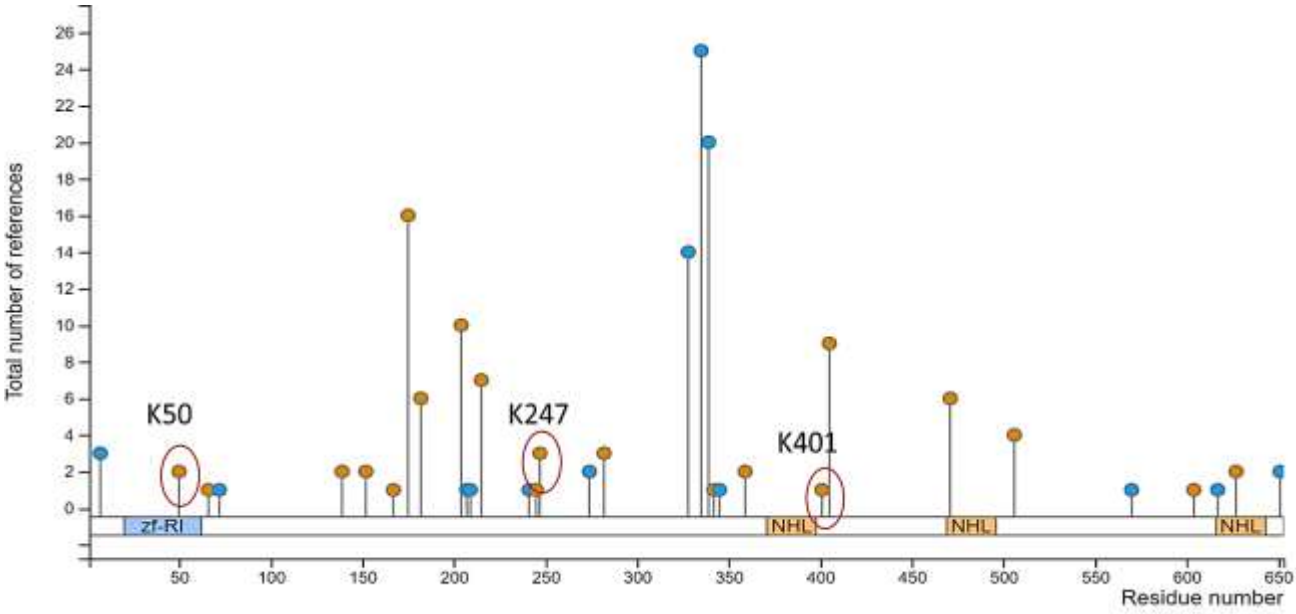

Figure 18: MS data analysis of TRIM32 is shown. The yellow points show ubiquitinated/ acetylated sites and blue points show phosphorylated sites. The circular ubiquitinated sites K50, K401 and K247 were identified in WT TRIM32 in a previous MS study. The LGMD2H disease mutant, which do not undergo self-ubiquitination, displayed no ubiquitination of these residues (Figure is modified from Phosphosite plus).

4.1. Establishment of mammalian expression plasmids for EGFP-TRIM32 K50R, EGFP-TRIM32 K247R and EGFP-TRIM32 K401R

In order to analyze if TRIM32 self-ubiquitination takes place on any of the residues K50, K247 or K401, EGFP-TRIM32 expression plasmids with each of the lysine residues mutated to arginine was established by site directed mutagenesis. The mutagenesis was performed on the mammalian expression vector pDEST-EGFP-TRIM32 and the donor vector pDONR221-TRIM32. The mutagenesis primers were TRIM32-K50R, TRIM32-K247R and TRIM32-K401

R (Table 3). The mutagenesis reaction mixtures were transformed into *E. coli* and plated onto LB+amp plates for the pDEST vectors and LB+kan plates for the pDONR vectors. Plasmids from three *E. coli* colonies from each reaction were purified by plasmid miniprep, before analysis by agarose gel electrophoresis and DNA sequencing.

The DNA sequences were analyzed by Chromas software (technelysium.com.au/wp/chromas) and NCBI BLAST (https://blast.ncbi.nlm.nih.gov). Lysine to arginine mutations was obtained for all three residues as shown in Figure 19.

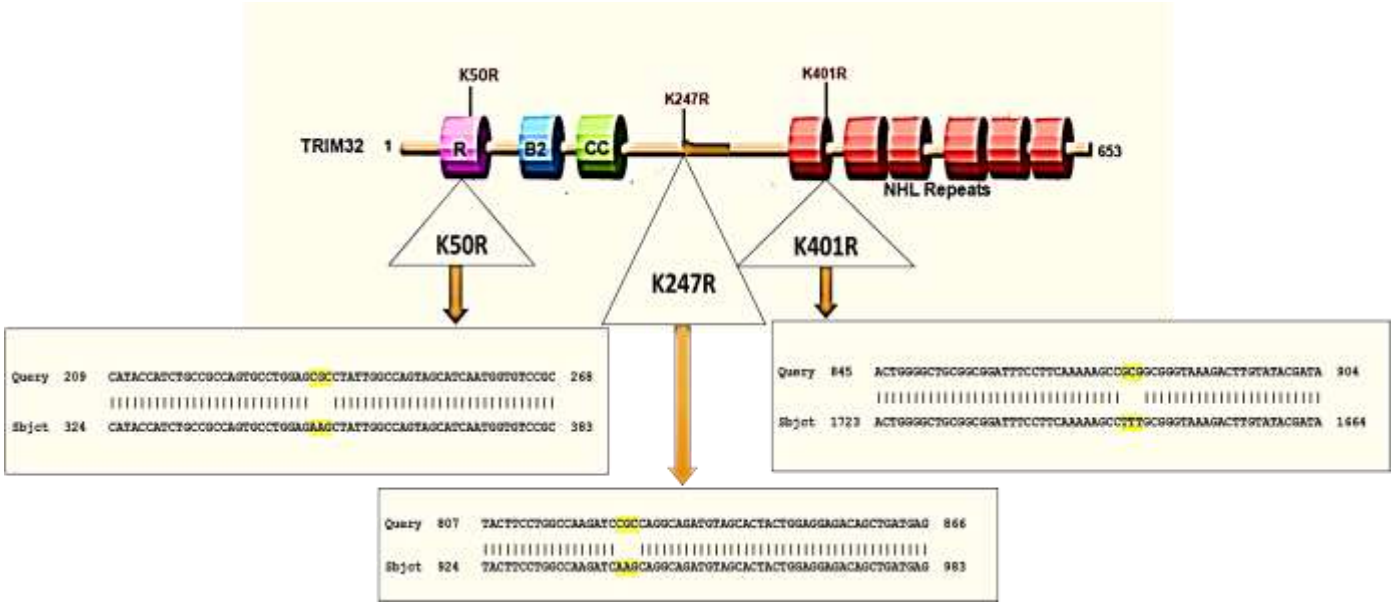

Figure 19: Schematic of TRIM32 domain organization and the location of the three lysines K50, K247 and K401. Below are the sequencing results of the mutated plasmids with the K to R codons marked in yellow (Complete sequencing result found in appendix).

4.2. Introduction of the single mutations K50R, K247R or K401R in TRIM32 did not abolish self-ubiquitination

To investigate if the introduction of the K to R mutations at positions 50, 247 or 401 would affect self-ubiquitination of TRIM32, the pDEST-EGFP-TRIM32 K50R, pDEST-EGFP-TRIM32 K247R and pDEST-EGFP-TRIM32 K401R plasmids were transfected into two different breast cancer cell lines, MDA-MB-231 and MCF-7 along with the pDEST-EGFP-TRIM32 wild type expression plasmid. One day post transfection the cells were harvested in SDS lysis buffer and cell extracts separated by SDS-PAGE. Expression of EGFP-TRIM32 wild type and mutants were detected by Western blotting using an anti-GFP antibody.

When TRIM32 is mono-ubiquitinated by self-ubiquitination, it migrates slower in the SDS-PAGE gel seen as a band just above the band representing un-ubiquitinated TRIM32 (Overa et al., 2019) (Figure 20). EGFP-TRIM32 WT and the three mutants were similarly expressed in both cell lines and the mono-ubiquitin band could be observed in all samples (Figure 20). This shows that mutations of the lysines 50, 247 or 401 in TRIM32 did not abolish self-ubiquitination. The membrane was reblotted by an anti-PCNA antibody, to show that similar amounts of cell extracts were loaded in each well (Figure 20).

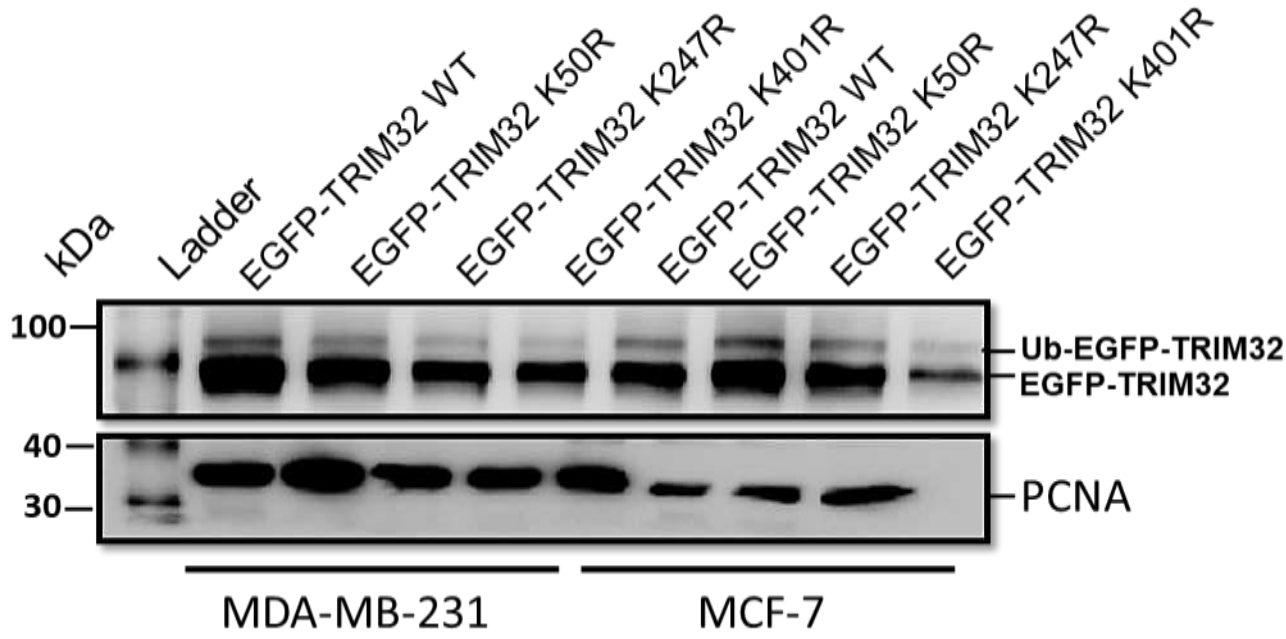

Figure 20: Introductions of K50R, K247R or K401R mutations in TRIM32 did not abolish self-ubiquitination. Western blot analysis of EGFP-TRIM32 WT, EGFP-TRIM32 K50R, EGFP-TRIM32 K247R or EGFP-TRIM32 K401R expressed in MDA-MB-231 and MCF-7 cell lines. The cells were transfected with the indicated pDEST-EGFP-TRIM32 plasmids one day before harvesting for Western blotting. The EGFP-TRIM32 proteins were detected using an anti-GFP antibody. The upper band represents mono-ubiquitinated EGFP-TRIM32, while the lower major band displays un-ubiquitinated EGFP-TRIM32. Blotting using an anti-PCNA antibody was used as loading control.

4.3. Establishment of EGFP-TRIM32 K247R/K401R, K50R/K247R and K50R/K401R expression plasmids

Since mutations of single lysine residues did not impair TRIM32 self-ubiquitination, our next question was if introduction of double K to R mutations would affect its self-ubiquitination activity. EGFP-TRIM32 expression plasmids with the lysine K50/K247, K50/K401 and

K247/K401 residues mutated to arginine were established by site directed mutagenesis as described above. Plasmids from three *E. coli* colonies from each reaction were purified by plasmid miniprep before analysis by DNA sequencing.

The DNA sequences were analyzed by Chromas software (technelysium.com.au/wp/chromas) and NCBI BLAST (https://blast.ncbi.nlm.nih.gov). Lysine to arginine mutations were obtained for all residues as shown in Figure 21.

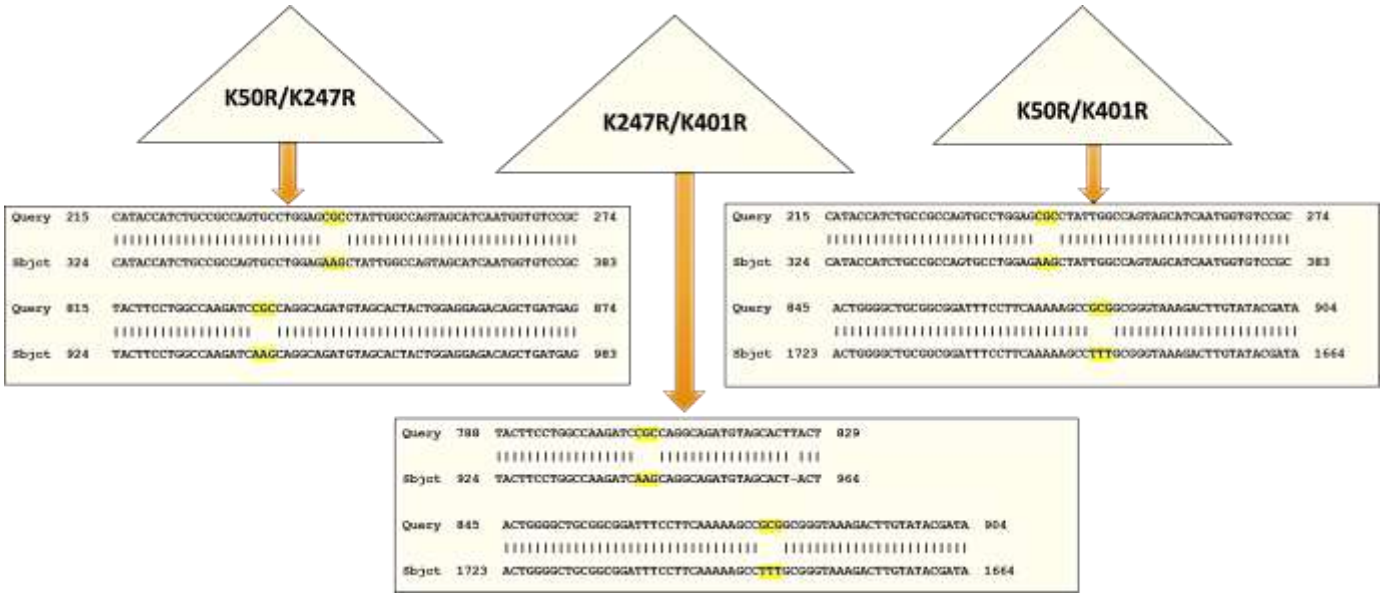

Figure 21: Sequencing results from the introduction of the double lysine mutations K50/K247, K247/K401 and K50/K401 in pDEST-EGFP-TRIM32. Below are the sequencing results of the mutated plasmids with the K to R codons marked in yellow (Complete sequencing result found in appendix).

4.4. Introduction of the K247R/K401R mutations in EGFP-TRIM32 results in an unstable protein

To investigate if the introduction of the K to R double mutations K247R/K401R, K50R /K247R and K50R/K401R would affect self-ubiquitination of TRIM32, the pDEST-EGFP-TRIM32-K247R/K401R, pDEST-EGFP-TRIM32-K50R/K247R and pDEST-EGFP-TRIM32-K50R/ K401R plasmids were transfected into HeLa cell lines along with the pDEST-EGFP-TRIM32 wild type expression plasmid. One day post transfection the cells were harvested in SDS lysis buffer and cell extracts separated by SDS-PAGE. Expression of EGFP-TRIM32 wild type and mutants were detected by Western blotting using an anti-GFP antibody. Figure 22 shows that EGFP-TRIM32 WT and the double mutants K50R/K247R and K50R/K401R are similarly

expressed in HeLa cell lines and the mono-ubiquitin band can be observed in all samples. However, the K247R/K401R mutant displays a weak full-length band, but a strong band with higher mobility in the gel. This indicates that mutations of the lysines K247R/K401R results in an unstable EGFP-TRIM32 protein. Hence, post translational modifications on lysine 247 and lysine 401 seem to be important for the stability of TRIM32. Importantly, the weak bands of full-length EGFP-TRIM32 K247R/K401R suggest that this double mutant still can undergo self-ubiquitination, suggesting that self-ubiquitination as such is not enough to stabilize the protein.

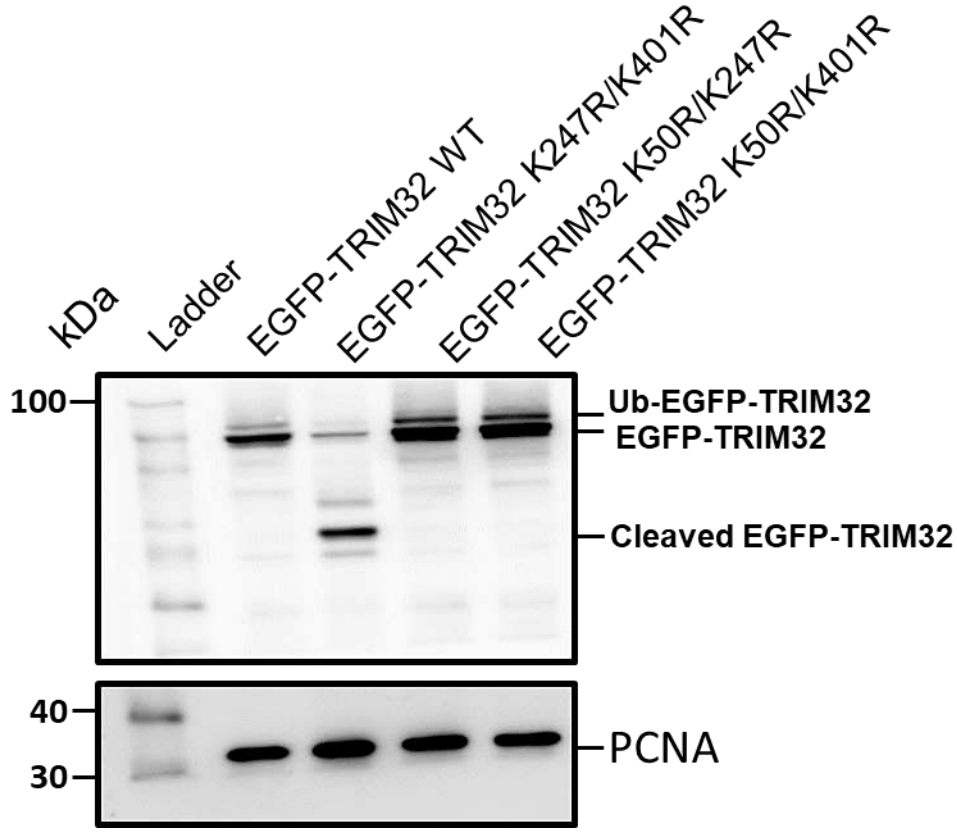

Figure 22: Introduction of the K247R/K401R mutations in EGFP-TRIM32 results in an unstable protein. Western blot analysis of EGFP-TRIM32 WT, EGFP-TRIM32-K247R/K401R, EGFP-TRIM32-K50R/K247R and EGFP-TRIM32-K50R/K401R expressed in HeLa cells. The cells were transfected with the indicated pDEST-EGFP-TRIM32 plasmids one day before harvesting for Western blotting. The EGFP-TRIM32 proteins were detected using an anti-GFP antibody. The upper band represents mono-ubiquitinated EGFP-TRIM32, while the lower major bands display un-ubiquitinated EGFP-TRIM32 along with cleaved EGFP-TRIM32. Blotting using an anti-PCNA antibody was used as loading control.

4.5. Establishment of EGFP-TRIM32 K50/K247R/K401R expression plasmid

As shown above, introduction of the K to R double mutations in TRIM32 did not impair self-ubiquitination activity. We therefore went further to ask if introduction of the triple K to R mutation K50R/K247R/K401R would affect self-ubiquitination. An EGFP-TRIM32 expression plasmid with the three lysine residues mutated to arginine was established by site directed mutagenesis. The mutagenesis was performed on the mammalian expression vector pDEST-EGFP-TRIM32 K247R/K401R and the mutagenesis primers were TRIM32-K50R forward and reverse (Table 3). The mutagenesis reaction mixture was transformed into *E. coli* and plated onto LB+amp plates. Plasmids from three *E. coli* colonies were purified by plasmid miniprep before analysis by DNA sequencing.

The DNA sequences were analyzed by Chromas software (technelysium.com.au/wp/chromas) and NCBI BLAST (https://blast.ncbi.nlm.nih.gov). Lysine to arginine mutations were verified for all three residues K50/K401/K247 as shown in Figure 23.

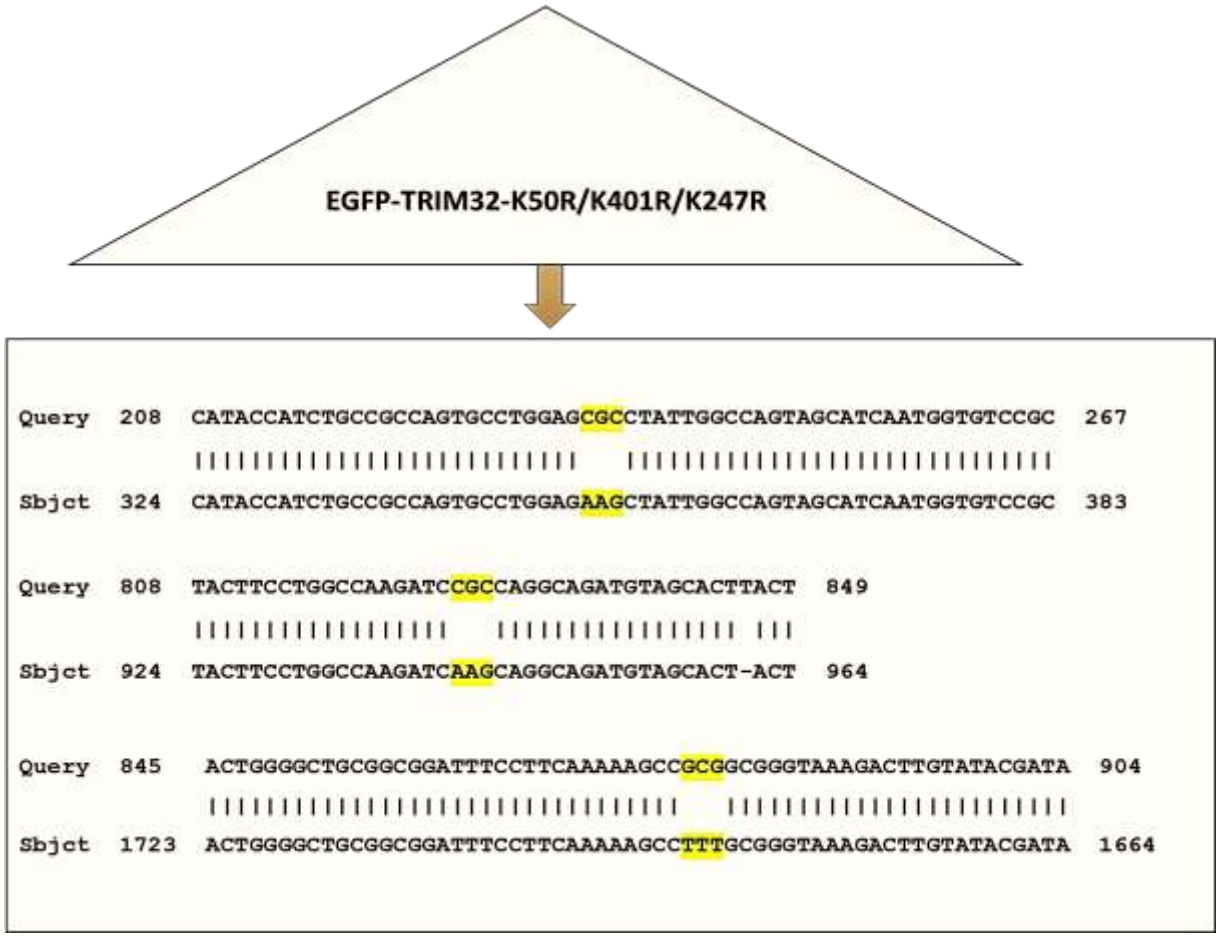

Figure 23: Sequencing results from the introduction of the triple lysine mutations EGFP-TRIM32 K50R/K401R/K247R. Below are the sequencing results of the mutated plasmid with the K to R codons marked in yellow (Complete sequencing result found in appendix).

4.6. Introduction of the triple K50R/K247R/K401R mutation in EGFP-TRIM32 results in cleavage of the protein

To investigate if the introduction of the triple K to R mutations K50R /K247R/K401R would affect self-ubiquitination of TRIM32, the triple mutation plasmid was transfected into HeLa cells along with pDEST-EGFP-TRIM32 WT and the double mutants pDEST-EGFP-TRIM32-K247R/K401R,pDEST-EGFP-TRIM32-K50R/K247R, pDEST-EGFP-TRIM32-K50R/K401R plasmids. In addition, the pDEST-EGFP-TRIM32 WT plasmid was co-transfected with an expression plasmid for the mCherry-tagged de-ubiquitinating enzyme USP2. One day post transfection the cells were harvested in SDS lysis buffer and cell extracts separated by SDS-PAGE. Expression of EGFP-TRIM32 wild type and mutants were detected by Western blotting using an anti-GFP antibody. The results presented in Figure 24 A show that K to R mutations

of the three lysine residues K50, K247 and K401 in TRIM32 make the protein completely unstable. Moreover, Figure 24 A also confirm the previous finding that introduction of the double K to R mutation K247R/K401R result in a partial unstable protein. Interestingly, de-ubiquitination of TRIM32 by USP2 did not affect the stability of TRIM32 (Figure 24 A, last lane). This suggests that another post-translational modification than ubiquitination at K247 and K401 is important for the stability of the protein.

In order to verify these results further, the above experiment was repeated, but this time the TRIM32 proteins were detected by the use of an anti-TRIM32 antibody instead of an anti-GFP antibody (Figure 24 B). Importantly, Western blotting using the anti-TRIM32 antibody resulted in the same band pattern as the anti-GFP antibody. This strongly support our finding that post-translational modifications other than ubiquitination on the lysine residues K50, K247 and K401 are important for the stability of TRIM32.

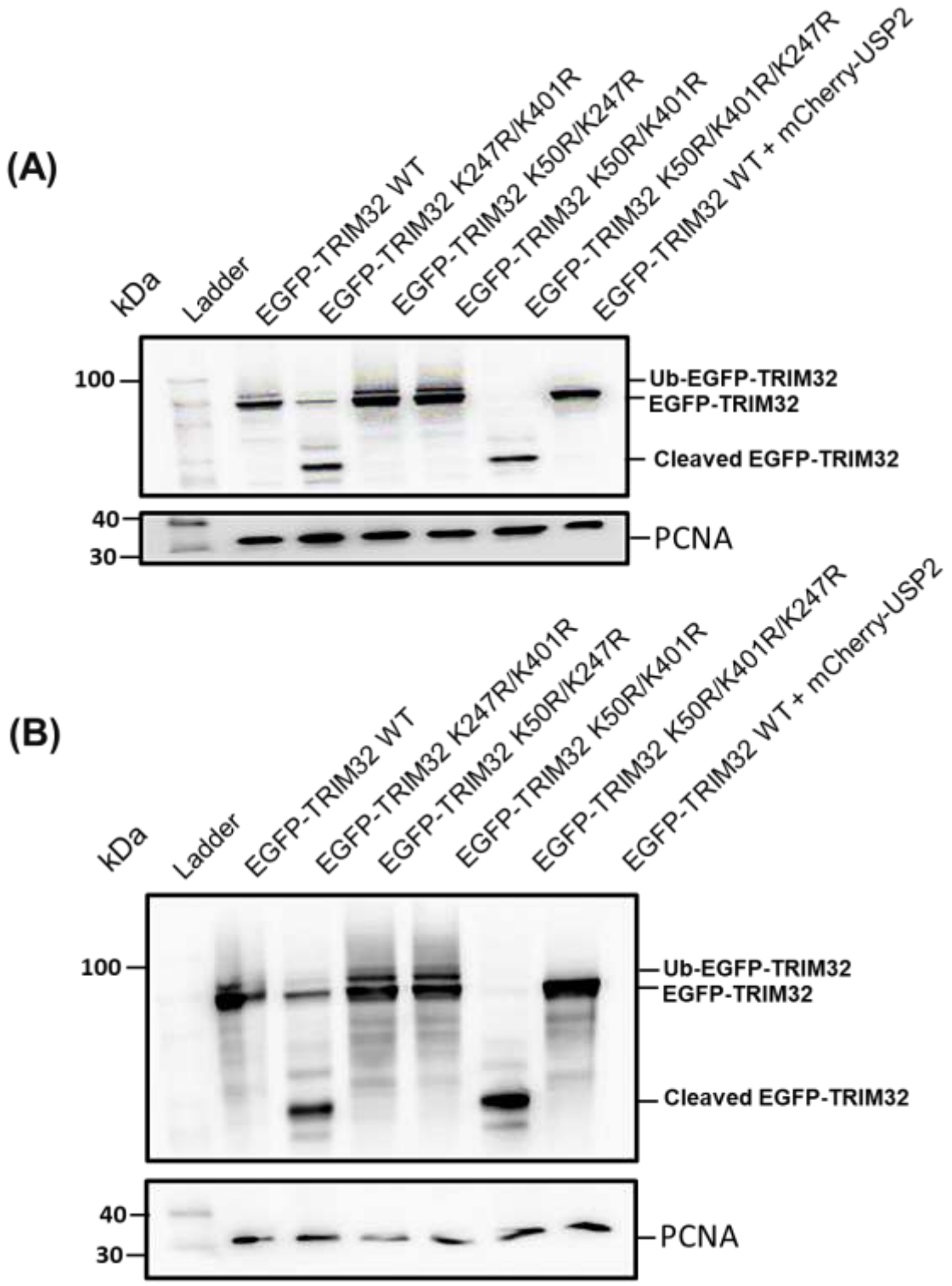

Figure 24: Introduction of the K50R/K247R/K401R mutations in EGFP-TRIM32 results in a completely unstable protein. (A) Western blot analysis of EGFP-TRIM32 WT, EGFP-TRIM32- K247R/K401R, EGFP-TRIM32-K50R/K247R, EGFP-TRIM32- K50R/K401R and EGFP-K50R/K401R/K247R expressed in HeLa cells without or with co-expressed mCherry-USP2 where indicated. The cells were transfected with the plasmids one day before harvesting for Western blotting. The EGFP-TRIM32 proteins were detected using an anti-GFP antibody. The upper band represents

mono-ubiquitinated EGFP-TRIM32, while the lower major band displays un-ubiquitinated EGFP-TRIM32 along with cleaved EGFP-TRIM32. Blotting using an anti-PCNA antibody was used as loading control. (**B)** Western blot analysis of similar experiment as described in 24 A, but the antibody used was an anti-TRIM32 antibody instead of the anti-GFP antibody.

4.7. A PEST sequence is located adjacent to Lysine K247 in TRIM32

The analysis so far has been performed in HeLa or breast cancer cell lines, which express endogenous TRIM32. TRIM32 is a protein that oligomerize, and this oligomerization leads to self-ubiquitination. To investigate if the self-ubiquitination detected in the cell extracts from cells transiently expressing K to R TRIM32 mutants was due to oligomerization with wild-type endogenous TRIM32, the double and triple K to R mutants of TRIM32 were transfected into a HEK293 FlpIn TRIM32 KO cell line (Overa et al., 2019). Western blot analysis displayed similar results as described above (Figure 25 A). The double mutations K50R/K247R, K50R/K401R and K247R/K401R did undergo self-ubiquitination. Moreover, introduction of the double K247R/K401R mutations and the triple K50R/K247R/K401R mutation made TRIM32 unstable, while de-ubiquitination by USP2 did not. Altogether, these results confirm that single and double K to R mutations of K50, K247 and K401 in TRIM32 do not abolish self-ubiquitination.

The results so far indicate that post-translational modifications of K247 and K401, and to a lesser extent also K50 are important for the stability of TRIM32. This prompted us to investigate by bioinformatics if TRIM32 contains a PEST sequence. Interestingly, the PEST prediction software EMBOSS: epestfind identified a putative PEST sequence (PEST score 7.4) at position 248–270, adjacent to the K247 residue (Figure 25 B). The PEST sequence is 100% conserved in mammalian TRIM32 proteins. These results suggest that post-translational modification of lysine K247 protects TRIM32 from degradation directed by the PEST sequence. However, when the lysine 247 residue together with lysine residue K401 is mutated to arginine that cannot be modified by post-translational modifications, TRIM32 is exposed to cleavage.

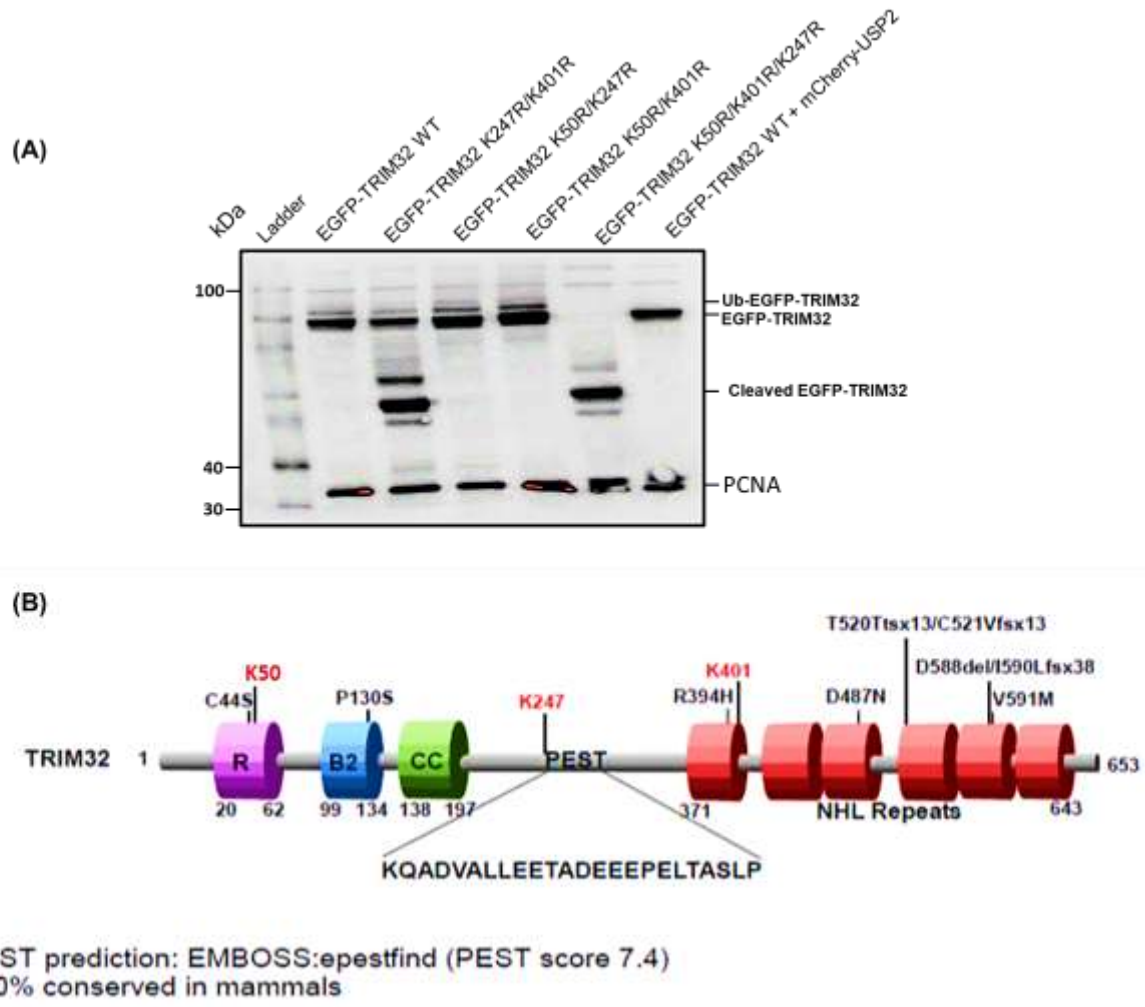

Figure 25: A PEST sequence is located adjacent to K247 in TRIM32. (A) Western blot analysis of EGFP-TRIM32 WT, EGFP-TRIM32- K247R/K401R, EGFP-TRIM32-K50R/K247R, EGFP-TRIM32-K50R/K401R, EGFP-K50R/K401R /K247R and EGFP-TRIM32 WT co-expressed with mCherry-USP2 in HEK293 FlpIn TRIM32 KO cells. The cells were transfected with the indicated pDEST-EGFP-TRIM32 plasmids one day before harvesting for Western blotting. The EGFP-TRIM32 proteins were detected using an anti-TRIM32 antibody. The upper band represents mono-ubiquitinated EGFP-TRIM32, while the lower major band displays un-ubiquitinated EGFP-TRIM32 along with cleaved EGFP-TRIM32. Blotting using an anti-PCNA antibody was used as loading control. **(B)** Schematic of the domain structure of TRIM32 with the conserved putative PEST sequence. TRIM32 domain organization along with the localization of the disease point mutations P130S (BBS11) at the B2 box and D487N (LGMDH2) at NHL repeats domain are shown. The three lysine residues mutate in this work are indicated in red above the schematic. R, Ring finger; B2, Bbox2; CC, Coiled coil (Obtained and modified from (Overa et al., 2019).

4.8. Inhibition of the lysosome or the proteasome does not inhibit cleavage of TRIM32 K50R/K247R/K401R

To investigate if the cleavage of TRIM32 was performed by proteases in the lysosome or proteases in the proteasome, cells were next treated with the proteasomal inhibitor MG132 or

the lysosomal inhibitor Bafilomycin A1 (BafA1). The pDEST-EGFP-TRIM32 WT and the pDEST-EGFP-K50R/K247R/K401R plasmids were transfected into HEK293 FlpIn TRIM32 KO cells. The cells were treated with MG132 (20 μM) or BafA1 (0,2 μM) for three hours one day post transfection (Figure 26 A) or with MG132 (5 μM) or BafA1 (0,1 μM) at the time of transfection for 24 hrs (Figure 26 B). The cells were grown in Full Medium or starvation medium (HBSS) for three hrs before harvesting. The cells were harvested in SDS lysis buffer and cell extracts separated by SDS-PAGE. Expression of EGFP-TRIM32 wild type and triple mutants were detected by Western blotting using an anti-GFP antibody. Neither 3 hours nor 24 hours treatments with the MG132 inhibitor or BafA1 inhibited cleavage of the triple K to R, K50R/K247R/K401R, mutant of TRIM32. This may suggest that TRIM32 is cleaved by a protease not associated with the proteasome or with the lysosome, or by both.

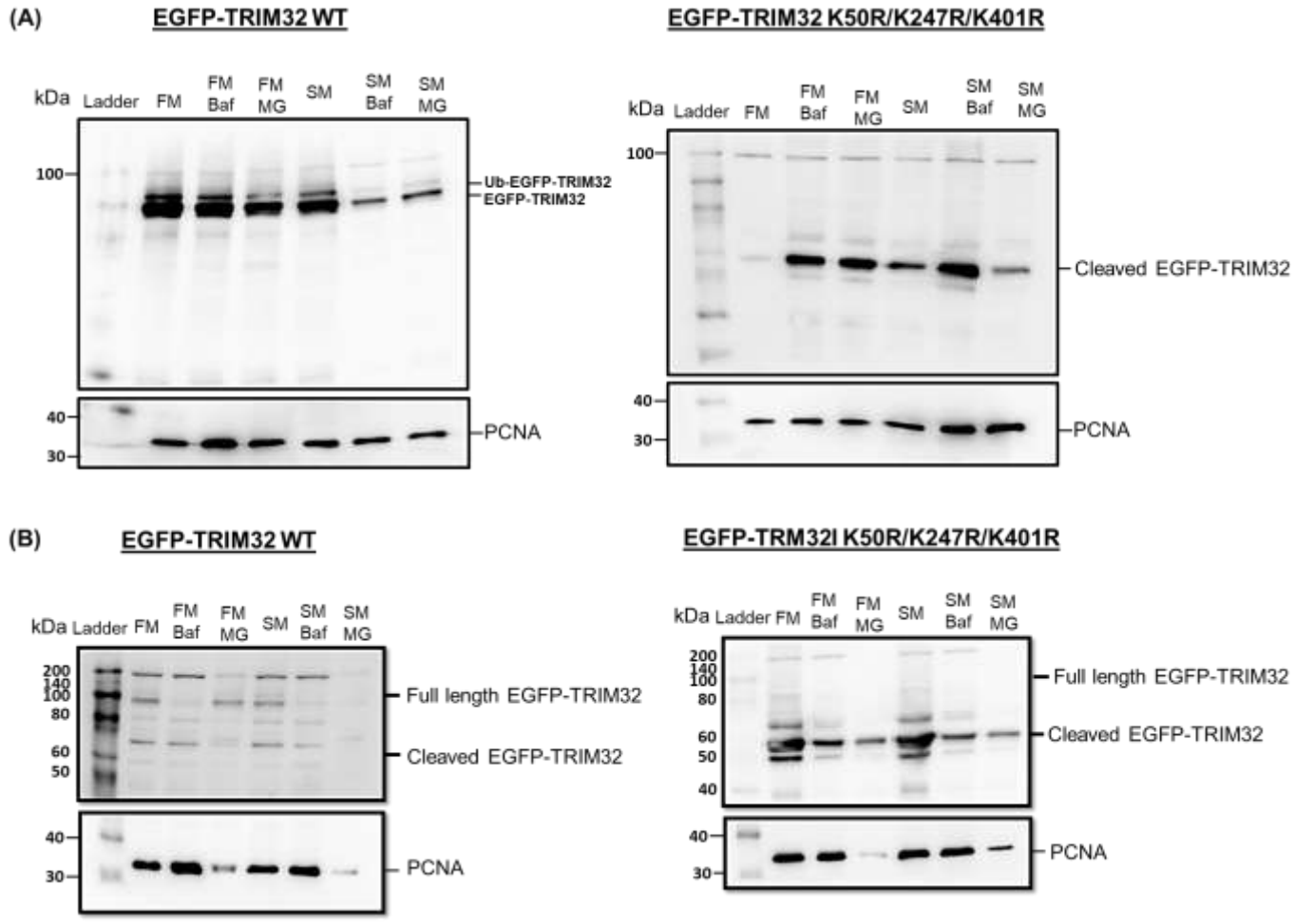

Figure 26: Inhibition of the lysosome or the proteasome does not inhibit cleavage of EGFP-TRIM32 K50R/K247R/K401R. (A) Western blot analysis of EGFP-TRIM32 WT and EGFP-K50R/K401R /K247R expressed in HEK293 FlpIn TRIM32 KO cells lines. The cells were

transfected with the indicated pDEST-EGFP-TRIM32 plasmids one day before harvesting for Western blotting. The EGFP-TRIM32 proteins were detected using an anti-GFP antibody. Blotting using an anti-PCNA antibody was used as loading control. Inhibitor treatment of MG132 (20 µM) or BafA1 (0,2 µM) for three hours and one day post transfection (FM: Full Media, SM: Starvation Media, Baf: Bafilomycin A1, MG: MG132). **(B)** Western blot analysis of EGFP-TRIM32 WT and EGFP-TRIM32-K49R/K401R /K247R expressed in HEK293 FlpIn TRIM32 KO cells lines. The cells were transfected with the indicated pDEST-EGFP-TRIM32 plasmids one day before harvesting for Western blotting. The EGFP-TRIM32 proteins were detected using an anti-GFP antibody. Blotting using an anti-PCNA antibody was used as loading control. The inhibitors MG132 (5 µM) and BafA1 (0,1 µM) were added at the time of transfection and stayed for 24 hrs. Starvation (HBSS) was performed for 3 hrs before harvesting. (FM: Full Media, SM: Starvation Media, Baf: Bafilomycin A1, MG: MG132).

4.9. EGFP-TRIM32 WT and mutants colocalize with Golgi marker GM130 and autophagy receptor p62/SQSTM1

Previous studies have shown that TRIM32 localizes to cytoplasmic dots, and that it co-localizes with the autophagy receptor p62/SQSTM1 in some of these dots. To investigate if introduction of the double K to R mutations and the triple K to R mutation in TRIM32 would affect the localization of TRIM32, fluorescent confocal imaging was applied.

The pDEST-EGFP-TRIM32-K247R/K401R, pDEST-EGFP-TRIM32-K50R/K247R, pDEST-EGFP-TRIM32- K50R/K401R and pDEST-EGFP-K50R/K401R /K247R plasmids were transfected into HEK293 FlpIn TRIM32 KO cells along with the pDEST-EGFP-TRIM32 wild type and pDEST-EGFP expression plasmids. One day post transfection cell fixation and immunostaining were performed with antibodies against the Golgi protein GM130 and the autophagy receptor p62/SQSTM1. The cell nucleus was visualized by DAPI staining.

Figure 27 A shows the distribution of GFP, and the normal staining of Golgi GM130 and p62/SQSTM1. Aggregation is not a general trait of EGFP, and most cells displayed a diffused EGFP localized all over the nucleus and cytoplasm. GM130 stained a perinuclear structure indicative of the Golgi apparatus, while p62/SQSTM1 appeared as dots dispersed throughout the cytoplasm.

EGFP-TRIM32 displayed a localization pattern as described by others. It forms several cytoplasmic dots, and when over-expressed it has a tendency to form large cytoplasmic aggregates. Both p62/SQSTM1 and GM130 colocalized with TRIM32 in some small dots, and in the large aggregates (Figure 27 B).

The K to R triple mutant EGFP-TRIM32 K50R/K247R/K401R formed larger and more cytoplasmic aggregates than TRIM32 WT (Figure 27 C). Some of the aggregates displayed colocalization with GM130 and p62/SQSTM1. However, the colocalization seemed to be much less prominent, indicating that the cleaved form of TRIM32 has less ability to aggregate the Golgi protein GM130 and autophagy receptor p62/SQSTM1. The K to R double mutant EGFP-TRIM32 K50R/K247R displayed a localization and colocalization pattern very similar to EGFP-TRIM32 WT (Figure 27 D). The K to R double mutants EGFP-TRIM32 K50R/K401R (Figure 27 E) and EGFP-TRIM32 K247R/K401R (Figure 27 F) showed a very similar localization pattern. In some cells they displayed a diffuse staining throughout the cytoplasm in addition to some cytoplasmic aggregates, while in other cells they accumulated to large aggregates. Both the small and the large aggregates showed colocalization of GM130 and p62/SQSTM1.

Altogether, these results may indicate that full-length TRIM32 has a strong tendency to aggregate the Golgi protein GM130 and the autophagy receptor p62/SQSTM1, while the cleaved TRIM32 protein has a strong tendency to formed aggregates, but less ability to co-aggregate GM130 and p62/SQSTM1.

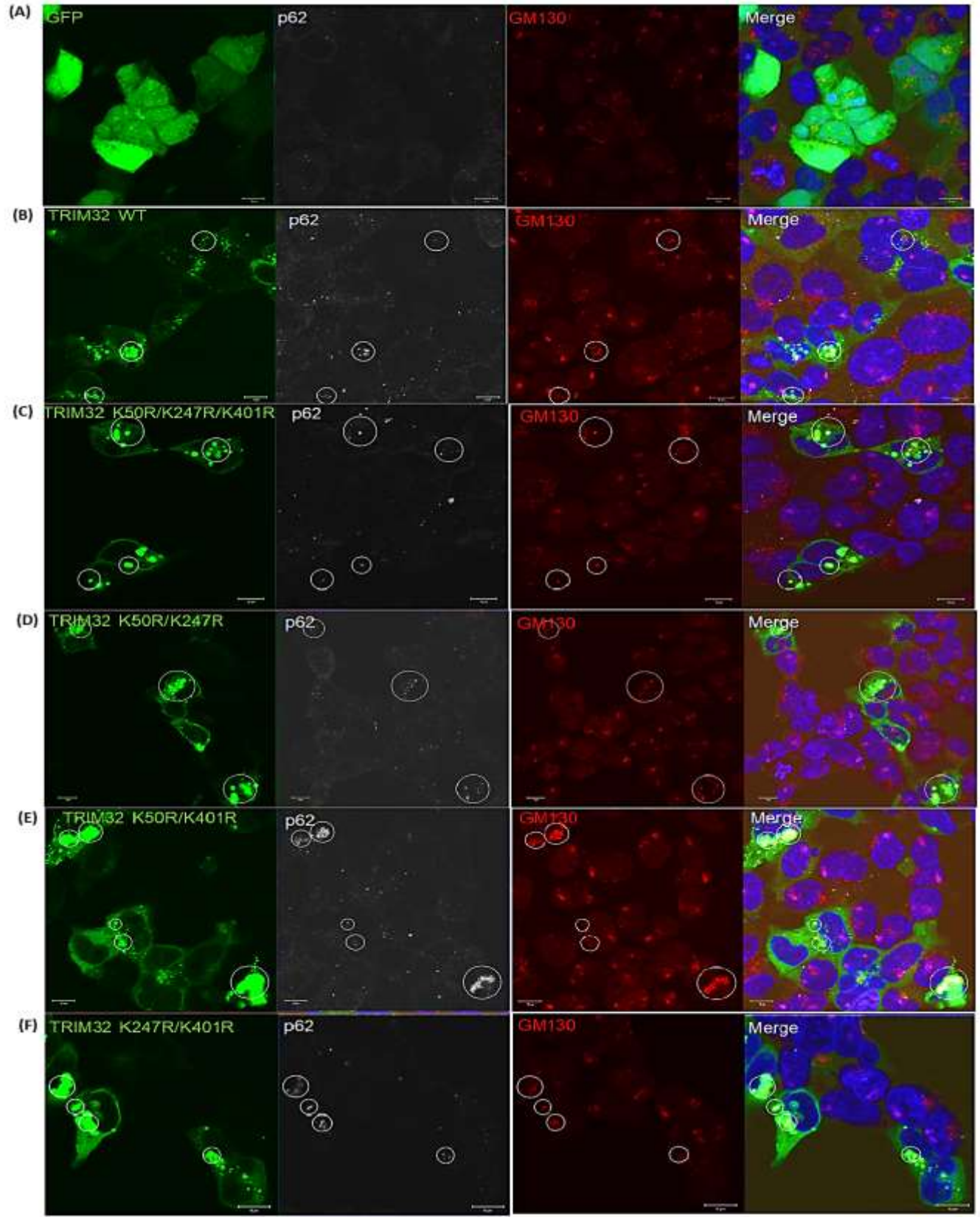

Figure 27: EGFP-TRIM32 WT and mutants colocalize with Golgi marker GM130 and autophagy receptor p62/SQSTM1. HEK293 FlpIn EGFP-TRIM32 KO cells transfected with EGFP (A), EGFP-TRIM32 WT (B), EGFP-TRIM32 K50R/K247R/K401R (C), EGFP-TRIM32

K50R/K247R (D), EGFP-TRIM32 K50R/ K401R (E), EGFP-TRIM32 K247R/K401R (F) expression plasmids. One day post transfection the cells were fixed and stained with antibodies against GM130 (Golgi: red) and p62 (white). The images were obtained by using a ZEISS780 confocal laser scanning microscope and the colocalization monitored by using the ZEN software. Scale bars: 10 µm.

4.9. Establishment of CRISPR/Cas9 plasmids directed against T1 and T2 target sites in mouse TRIM32 and T1 target site in rat TRIM32

Since mutations in TRIM32 are implicated in the development of muscle dystrophy, myoblast cell lines that have the ability to differentiate into muscle cells would be a promising model system for studying the functionality of TRIM32. Here the mouse myoblast cell line C2C12 and the rat myoblast cell line H9c2 were chosen for an attempt to make a myoblast TRIM32 KO cell line. For this purpose, the bioinformatics tool CHOPCHOP (https://chopchop .cbu.uib.no/) was applied to identify promising Cas9 target sites in the mouse and rat TRIM32 genes. Two gRNA sequences were selected for each gene (mouse T1 and T2, and rat T1 and T2). Forward and reverse oligoes for each target site were phosphorylated and annealed, before they were ligated into the CRISPR/Cas9 plasmid pX458 (Ran, Hsu, Wright, et al., 2013), which also expresses the EGFP protein. The ligation mix was transformed into *E. coli* and plated on LB+amp plates. Three colonies from each plate were purified by plasmid miniprep and successful cloning verified by restriction enzyme digestion and DNA sequencing. Analysis of the DNA sequences showed that the gRNAs directed against mouse T1 and T2 targets sites, and the gRNA directed to the rat T1 target site were successfully cloned into the pX458 vector (Figure 28).

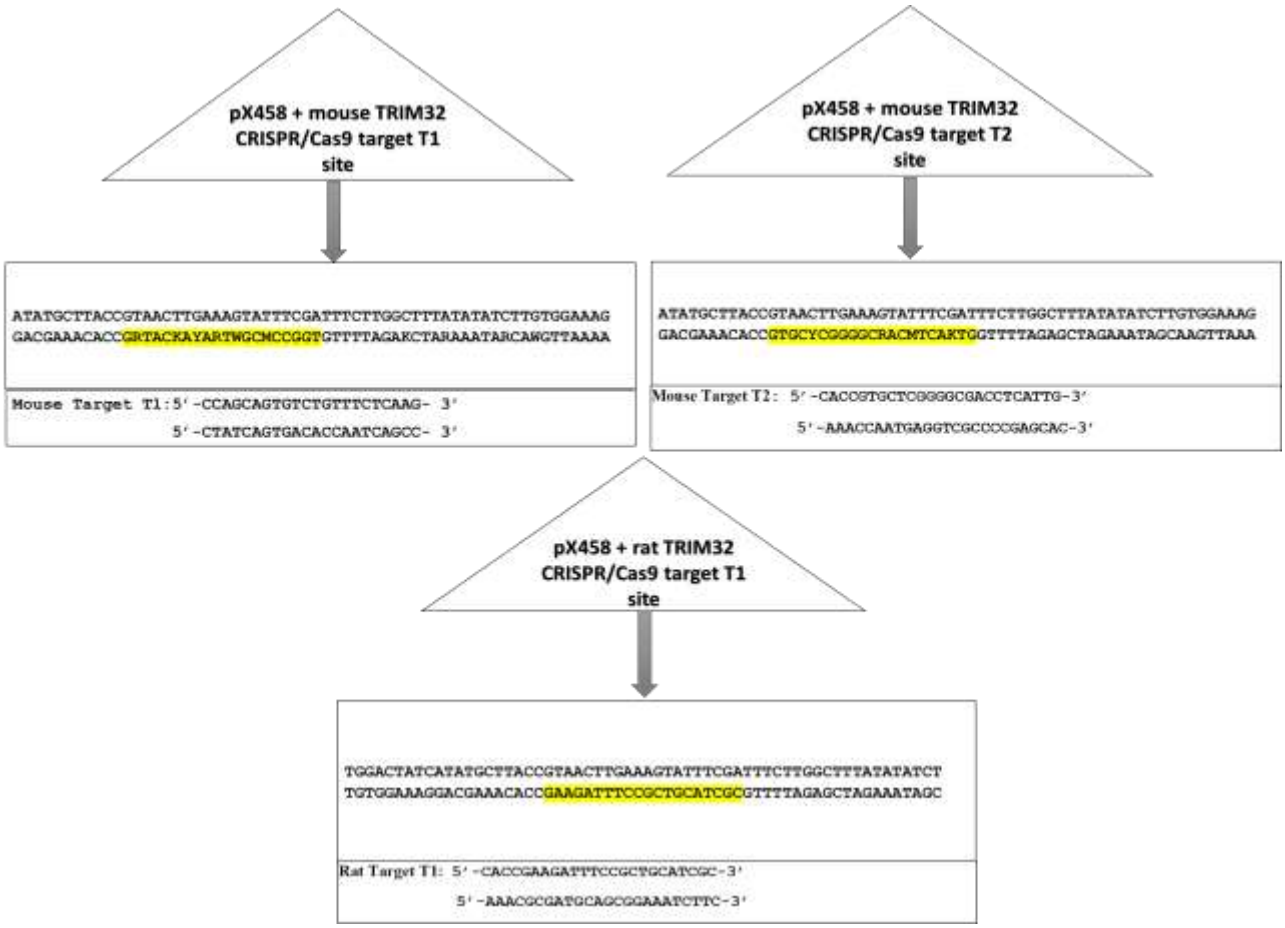

Figure 28: gRNA sequences against mouse TRIM32 and rat TRIM32 were successfully cloned into the pX458 CRISPR/Cas9 vector. DNA Sequencing results of the pX458 plasmids with inserted gRNAs directed against mouse T1 and T2 targets sites and the gRNA directed against the rat T1 target site are marked in yellow (Complete sequencing result found in appendix).

4.10. Establishment of myoblast C2C12 TRIM32 KO cell lines

To investigate if these three CRISPR/Cas9 plasmids had the ability to generate TRIM32 KO cell lines, the plasmids were transfected into the mouse myoblast C2C12 cell line, and the rat H9c2 cell line, respectively. Successfully transfected cells were selected based on the expression of EGFP and sorted as single cells into a well in a 96 well dish. The C2C12 cells grew well, and around 20 cell colonies for each of the target sites were picked and amplified further for analysis by Western blotting. The rat H9c2 cell cultures did not grow well, and no colonies were picked for further analysis. When the selected colonies were expanded up to a 12-well dish, the cells were harvested in SDS lysis buffer and cell extracts separated by SDS-PAGE. The presence or absence of TRIM32 in the cell extracts were analyzed by using an anti-TRIM32 antibody. Extracts from HEK293 cells were used as positive controls.

Figure 29 shows that the expression level of TRIM32 varies significantly between the different clones. However, the two clones T1-16 and T2-1 seem to completely lack the expression of TRIM32, and hence are potential candidates for establishment of myoblast TRIM32 KO cell lines. Freezer stocks were made of these two potential clones for further analysis by the MCRG.

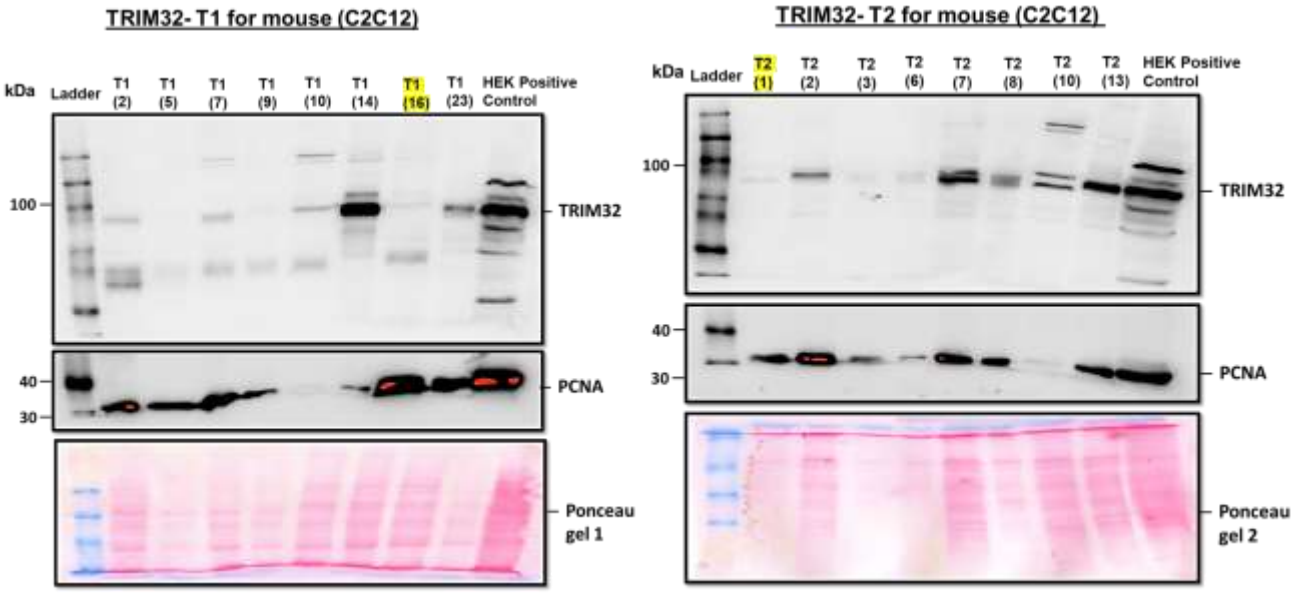

Figure 29: **Establishment of TRIM32 KO clones in the myoblast C2C12 cell line.** Western blot of cell extracts from the various expanded CRISPR/Cas9 clones of the C2C12 cell line. Extracts were blotted against an anti-TRIM32 antibody, and extracts from a HEK293 cell line were run in parallel as a positive control. Reblotting using the PCNA antibody shows the amount of cell extracts loaded in each lane. The two putative KO clones (T1-16 and T2-1) are marked in yellow.

5. Discussion

LGMD2H is a muscle dystrophy disease, which is caused by mutations in the ubiquitin ligase TRIM32, whose function in the muscles is not completely understood (Di Rienzo et al., 2019). However, it is shown that activation of TRIM32 is regulated by oligomerization and self-ubiquitination. The LGMD2H mutant form of TRIM32 is unable to undergo self-ubiquitination, and it is shown that it is unable to ubiquitinate the autophagy receptor p62/SQSTM1 and to be an autophagic substrate itself (Overa et al., 2019). LGMD2H (MIM 254110) is a gentle mode of autosomal recessive muscular dystrophy with a changeable clinical

presentation. The beginning is commonly within the 2d or 3d decade of life, and advancement is slow. The greater number of patients have continued ambulatory into the 6th decade of life. There is no indication of cardiac or facial symptoms (Frosk et al., 2002).

TRIM32 due to its E3 ubiquitin ligase activity has been demonstrated to direct degradation of various targets, so the absence or abnormal function of TRIM32, which is caused by recessive mutations would lead to the loss of ubiquitination as well as aggregation of the TRIM32 substrates (Servián-Morilla et al., 2019). This ubiquitously expressed nature of TRIM32 suggests that it plays an important role in other tissues, such as cardiac and smooth muscle but also in epithelia and brain tissues, where its expression is at high level (Cohen et al., 2012). The ubiquitin proteasome system (UPS) has been shown to play a significant role in mediating muscle wasting (Bilodeau, Coyne, and Wing, 2016). The purpose of this work was to identify, which lysine residues in TRIM32 are targets for its self-ubiquitination activity. Three lysine residues that were previously identified as potential targets by mass spectrophotometry analysis were mutated to arginine, which are unable to be modified by ubiquitin. Unfortunately, mutation of all three lysine residues did not abolish self-ubiquitination activity. This do not rule out that these lysines are targets for self-ubiquitination. However, it shows that also other lysine residues in TRIM32 are targets for self-ubiquitination. Identification of these residues needs further mutational analysis followed by Western Blotting in further study.

5.1. PEST sequences role in protein stability

Surprisingly, introduction of the K247R/K401R mutations in TRIM32 resulted in an unstable protein, giving a cleavage product of TRIM32 of around 30 kDa in the SDS gel. Bioinformatic analysis predicted a conserved PEST sequences adjacent to the K247 residue. The PEST hypothesis was first proposed in 1986 by Rechsteiner and his colleagues, which is based upon the presence of polypeptide sequence regions enriched in proline (P), glutamic acid (E), aspartic acid (D), serine (S), and threonine (T) confined by two positively charged amino acids, lysine (K), arginine (R) or histidine (H) in many short-lived proteins. These regions are hydrophilic and at least 12 amino acids long, while being not present in more stable proteins with half-lives of more than 20 h. Hence, PEST sequences are signals for rapid degradation of target proteins (Spencer, Theodosiou, and Noonan, 2004; Pakdel, Le Goff, and Katzenellenbogen, 1993; Qile

et al., 2019; Reverte, Ahearn, and Hake, 2001). Certainly, in many short living proteins, the mutation of the PEST domain sequences results in the stabilization of the proteins and might affect nuclear localization of some proteins. Moreover, in many proteins PEST sequences appear to function as anchor sites of E3 ubiquitin ligases, which are required for ubiquitin dependent protein degradation (Qile et al., 2019; Park, Jeong, and Kim, 2014). Generally, the PEST regions are flanked by clusters that contain various positively charged amino acids. Based on these observations, there are developed algorithms that identify putative PEST regions in protein sequences (Rogers, Wells, and Rechsteiner, 1986; Chen and Clarke, 2002).

A lot of evidence supports the idea that PEST sequences target proteins for degradation by the 26S proteasome (Rechsteiner and Rogers, 1996; Chen and Clarke, 2002). A strong connection has been established between nuclear protein stability and the existence of PEST regions (Chevaillier, 1993). Ramakrishna et al., (2011) results suggest that a PEST motif found in the NANOG protein is necessary for an effective NANOG ubiquitination and the deletion of this PEST motif result in increased stability of NANOG protein by abolishing its ubiquitination (Ramakrishna et al., 2011).

Here we find that K247 in TRIM32 is located at the start of a PEST sequence (Figure 25 B). Introduction of lysine to arginine mutations of K247 and K401 resulted in an unstable protein. This suggests that post translational modifications on lysine 247 and lysine 401 are important for the stability of TRIM32. Importantly, presence of the self-ubiquitination band in the Western blot of EGFP-TRIM32 K247R/K401R suggests that this double mutant still can undergo self-ubiquitination. Furthermore, de-ubiquitination of TRIM32 by USP2 did not affect the stability of TRIM32 (Figure 24A, last lane). Hence, ubiquitination of these residues seems not to be enough to stabilize the protein (Figure 22), suggesting that other post-translational modifications such as acetylation, methylation or sumoylation might important for protecting TRIM32 from degradation mediated by the PEST sequence. This will be an interesting topic for further studies.

The identification of a PEST sequence in TRIM32 raised the question whether this sequence directs TRIM32 cleavage by the proteasome or in the lysosome. In order to analyze this, proteasomal inhibitor MG132 and lysosomal inhibitor BafA1 were applied on cells expressing the triple K to R mutant form of TRIM32. Bafilomycin A1 is a member of the family of

macrolide antibiotic, which was among the first of this class segregated from Streptomyces gresius. It is an effective inhibitor of the Vacuolar H+ ATPase, which controls pH activity in the lysosome (V-ATPase). By using this mechanism Bafilomycin A1 is capable of preventing autophagic flux by inhibiting the acidification of endosomes as well lysosomes bodies (Redmann et al., 2017).

The cells were treated with MG132 or BafA1 for three hours one day post transfection (Figure 26 A) or with MG132 or BafA1 at the time of transfection and for 24 hrs (Figure 26 B). The cells were incubated in Full Medium or starvation medium (HBSS, 3 hrs) before harvesting. However, neither 3 hours nor 24 hours treatments with the MG132 inhibitor or BafA1 inhibited cleavage of the TRIM32 K50R/K247R/K401R mutant. This suggests that TRIM32 is cleaved by a protease not associated with the proteasome or with the lysosome or can be cleaved by both. Hence, treatment with both MG132 and BafA1 in the same cell culture should be performed in future studies. According to Overa et al., (2019) endogenous wild type TRIM32 is degraded by both lysosomal pathways and the proteasome in HEK293 cells. The treatment of both the lysosomal and the proteasomal inhibitor increased the amount of TRIM32 to a similar extent under starvation conditions, whereas the proteasomal pathway appears to be most important under normal cellular conditions (Overa et al., 2019).

5.2. Mouse myoblast (C2C12) TRIM32-KO cell lines as model system to study the function of TRIM32 in muscle cells

The mouse myoblast (C2C12) cells are used as a model system to study the various kinds of muscular dystrophies such as Duchenne muscular dystrophy (DMD), Emery–Dreifuss muscular dystrophy (EDMD) and limb–girdle muscular dystrophy (LGMD) *in vitro.* The mouse myoblast (C2C12) cells myotube or fibrin gel system has been grown to show that the cells in fibrin gels draw out better level of contractile activity compared than mouse myoblast (C2C12) cultures on conventional two-dimensional surfaces. The mouse myoblast (C2C12) when deprived of serum go through cell cycle capture and start to combine and form a multinucleated myotubes. The myotubes serve as the building blocks for skeletal muscle, so in this manner understanding of the differentiation process of mouse skeletal myoblasts (C2C12) in vitro has the possibility to resolve the mechanisms of the myogenic differentiation process in vivo as well (Bajaj et al., 2011). The study conducted by Bajaj et al., (2011) showed that the

geometrical hints deliberated by the protein micropatterns possibly manage to various tractional stresses and cytoskeletal restructuring of C2C12 myoblast cells, which further produced various degrees of differentiation on the distinct geometries. They found that geometrical hints influence the differentiation process of C2C12 myoblasts cells, and that the differentiation of C2C12 myoblasts cells are found on three main geometries; a linear, a circular and a hybrid pattern. The hybrid 30° pattern appeared as the best geometry to expand the differentiation of C2C12 myotubes (Bajaj et al., 2011).

It is demonstrated that TRIM32 is involved in the managing of differentiation and self-regeneration of neural progenitor cells during mouse embryonic brain development. Furthermore, the Drosophila orthologs of TRIM32, Brat and the Brat-like protein called Mei-p26 control stem cell proliferation, which is found in the Drosophila nervous system and ovaries, respectively. So, in this manner, the control of stem cell proliferation might be a typical function of TRIM-NHL proteins and deregulation of muscle stem cell activity upon failure of TRIM32 could provide to the development of LGMD2H (Nicklas et al., 2012). According to Nicklas et al., (2012) TRIM32 is enough to induce muscular differentiation of mouse myoblast (C2C12) cells, while upon knock-down of TRIM32 the differentiation of C2C12 cells is restricted. Similarly, it is demonstrated that TRIM32 is implicated in muscle differentiation and that differentiation possibly depends upon the ubiquitination and degradation of c-Myc (Oncogene). Overall, it is proved that TRIM32 knock-out mice produces a myopathy that conferred by LGMD2H patients and that muscle transformation in these mice was highly delayed and damaged. Based on these experimental findings, it was proposed that loss of TRIM32 function in the muscle stem cells will diminish their functionality. This dysfunction of the muscle stem cells could lead to the etiology of LGMD2H (Nicklas et al., 2012).

Mokhonova et al., (2015) created a genetically modified mice that were deficient of TRIM32 (T32KO) and noticed that they exhibited both the myopathic and neurogenic phenotypes. The muscles of these mice showed a mild muscular dystrophy and presented dystrophic characteristics, which are similar to those found in patients with the muscular disorders LGMD2H. Similarly, the T32KO mice showed a decline in the concentration of neurofilament proteins, which are found in the brain and a decreased motor axon diameter. these neurogenic features are also visible in LGMD2H patients (Mokhonova et al., 2015). TRIM32 knockout mouse was also created by Kudryashova, Kramerova, and Spencer, (2012), which proved to be

a good model for studying the pathogenic mechanisms of LGMD2H. In this TRIM32 KO mouse model, the absence of TRIM32 resulted in a similar kind of myopathic phenotype as demonstrated in LGMD2H along with similar type of muscle morphology and muscle weakness on grip strength (Kudryashova, Kramerova, and Spencer, 2012; Kudryashova et al., 2011).

In this work, mouse myoblast (C2C12) TRIM32-KO cell lines were established by CRISPR/Cas9. The knockout of TRIM32 expression in the cell lines was verified by Western blotting. The expression level of TRIM32 varied between the different clones. However, the two clones T1-16 and T2-1 (Figure 29) seem to completely lack the expression of TRIM32, and hence are potential candidates for further studies. First, verification of the TRIM32 KO has to be performed by sequencing the genomic region in TRIM32 targeted by the gRNA sequences. Thereafter, stable TRIM32 KO cells with expression of tagged TRIM32 wild-type, LGMD2H disease mutant or BBS11 disease mutant forms can be established by virus transduction. These cell lines, together with the TRIM32 KO cell lines and the normal C2C12 cell line, will be applied in various studies to understand the pathogenic role of the disease mutations for the development of the related disease.

Conclusion

In this work self-ubiquitination of the K50, K247 and K401 sites in TRIM32 was analyzed by site-directed mutagenesis. Introduction of single or double K to R mutations did not seem to abolish self-ubiquitination. However, the introduction of the double K247R/K401R mutations in EGFP-TRIM32 results in an unstable protein and the introduction of the triple K50R/K247R/K401R mutation in EGFP-TRIM32 results in cleavage of the protein. The inhibition of the lysosome or the proteasome did not inhibit cleavage of TRIM32 K50R/K247R/K401R. This suggest that post-translational modifications of TRIM32 at the K247 and K401 residues protects TRIM32 from proteolytic cleavage, and this protection is further enhanced by modifications on K50. Localization studies in HEK293 FlpIn TRIM32 KO cells showed that EGFP-TRIM32 WT and the K to R double and triple mutants had a tendency to aggregate in the cytoplasm, clustering with the Golgi protein GM130 and the autophagy receptor p62/SQSTM1. Finally, two myoblast C2C12 TRIM32 KO cell lines were successfully established.

6. Future work

For the future work, it would be interesting to investigate the effect of expressing the TRIM32 disease mutations in the C2C12 myoblast cell line compared to expression of wild type TRIM32. Especially, it will be interesting to analyze the autophagy process in these cells, and to determine whether the pathology of the LGMD2H mutation is due to dysfunctional degradation of specific muscle proteins. Furthermore, since the C2C12 cells can be induced to differentiate into muscle fibers, the TRIM32 KO cell line can be used to study whether TRIM32 affects protein degradation during differentiation.

The lysine residues in TRIM32 involved in self-ubiquitination were not mapped in this work. Thus, it would be interesting to investigate more ubiquitinated sites that are found in EGFP-TRIM32.

In this work we identified K247 and K401 as important residues for protection of TRIM32 against proteolytic cleavage directed by a predicted PEST sequence. Our data suggest that post-translational modifications other that ubiquitination is important for this protection. It will be interesting in further studies to identify, which post-translational modification (acetylation, methylation, sumoylation) that takes place on these lysine residues, and also to identify under which conditions the modifications take place.

7. References

Arber, W., and S. Linn. 1969. 'DNA modification and restriction', *Annu Rev Biochem*, 38: 467-500.

Addgene,https://blog.addgene.org/plasmids-101-methylation-and-restriction-enzymes (04 March, 2020).

Bajaj, Piyush, Bobby Reddy, Jr., Larry Millet, Chunan Wei, Pinar Zorlutuna, Gang Bao, and Rashid Bashir. 2011. 'Patterning the differentiation of C2C12 skeletal myoblasts', *Integrative Biology*, 3: 897-909.

Balch, W. E., R. I. Morimoto, A. Dillin, and J. W. Kelly. 2008. 'Adapting proteostasis for disease intervention', *Science*, 319: 916-9.

Barbosa, María Carolina, Rubén Adrián Grosso, and Claudio Marcelo Fader. 2019. 'Hallmarks of Aging: An Autophagic Perspective', *Frontiers in Endocrinology*, 9.

Barrangou, Rodolphe. 2015. 'The roles of CRISPR–Cas systems in adaptive immunity and beyond', *Curr Opin Immunol*, 32: 36-41.

Bhutia, Sujit K., Subhadip Mukhopadhyay, Niharika Sinha, Durgesh Nandini Das, Prashanta Kumar Panda, Samir K. Patra, Tapas K. Maiti, Mahitosh Mandal, Paul Dent, Xiang-Yang Wang, Swadesh K. Das, Devanand Sarkar, and Paul B. Fisher. 2013. 'Autophagy: cancer's friend or foe?', *Advances in cancer research*, 118: 61-95.

Bielskienė, Kristina, Lida Bagdonienė, Julija Mozūraitienė, Birutė Kazbarienė, and Ernestas Janulionis. 2015. 'E3 ubiquitin ligases as drug targets and prognostic biomarkers in melanoma', *Medicina*, 51: 1-9.

Bilodeau, P. A., E. S. Coyne, and S. S. Wing. 2016. 'The ubiquitin proteasome system in atrophying skeletal muscle: roles and regulation', *Am J Physiol Cell Physiol*, 311: C392-403.

Birnboim, H. C., and J. Doly. 1979. 'A rapid alkaline extraction procedure for screening recombinant plasmid DNA', *Nucleic Acids Res*, 7: 1513-23.

Borlepawar, A., N. Frey, and A. Y. Rangrez. 2019. 'A systematic view on E3 ligase Ring TRIMmers with a focus on cardiac function and disease', *Trends Cardiovasc Med*, 29: 1-8.

Boyer, N. P., C. Monkiewicz, S. Menon, S. S. Moy, and S. L. Gupton. 2018. 'Mammalian TRIM67 Functions in Brain Development and Behavior', *eNeuro*, 5.

Brigant, B., V. Metzinger-Le Meuth, J. Rochette, and L. Metzinger. 2018. 'TRIMming down to TRIM37: Relevance to Inflammation, Cardiovascular Disorders, and Cancer in MULIBREY Nanism', *Int J Mol Sci*, 20.

Brzobohata, K., E. Drozdova, J. Smutny, T. Zeman, and R. Benus. 2017. 'Comparison of Suitability of the Most Common Ancient DNA Quantification Methods', *Genet Test Mol Biomarkers*, 21: 265-71.

Budenholzer, L., C. L. Cheng, Y. Li, and M. Hochstrasser. 2017. 'Proteasome Structure and Assembly', *J Mol Biol*, 429: 3500-24.

Cervera, L., and A. A. Kamen. 2018. 'Large-Scale Transient Transfection of Suspension Mammalian Cells for VLP Production', *Methods Mol Biol*, 1674: 117-27.

Cell signal, https://www.cellsignal.com/products/experimental-controls/biotinylated-protein-ladder-detection-pack/7727 (10 March, 2020).

Chalfie, M., Y. Tu, G. Euskirchen, W. W. Ward, and D. C. Prasher. 1994. 'Green fluorescent protein as a marker for gene expression', *Science*, 263: 802-5.

Chan, Weng-Tat, Chandra S. Verma, David P. Lane, and Samuel Ken-En Gan. 2013. 'A comparison and optimization of methods and factors affecting the transformation of Escherichia coli', *Biosci Rep*, 33: e00086.

Chen, Eva Y., and David M. Clarke. 2002. 'The PEST sequence does not contribute to the stability of the cystic fibrosis transmembrane conductance regulator', *BMC Biochemistry*, 3: 29.

Chen, W. X., L. Cheng, L. Y. Xu, Q. Qian, and Y. L. Zhu. 2019. 'Bioinformatics analysis of prognostic value of TRIM13 gene in breast cancer', *Biosci Rep*, 39.

Chevaillier, Philippe. 1993. 'Pest sequences in nuclear proteins', *International Journal of Biochemistry*, 25: 479-82.

Chiang, A. P., J. S. Beck, H. J. Yen, M. K. Tayeh, T. E. Scheetz, R. E. Swiderski, D. Y. Nishimura, T. A. Braun, K. Y. Kim, J. Huang, K. Elbedour, R. Carmi, D. C. Slusarski, T. L. Casavant, E. M. Stone, and V. C. Sheffield. 2006. 'Homozygosity mapping with SNP arrays identifies TRIM32, an E3 ubiquitin ligase, as a Bardet-Biedl syndrome gene (BBS11)', *Proc Natl Acad Sci U S A*, 103: 6287-92.

Choi, Kyeong Sook. 2012. 'Autophagy and cancer', *Experimental & molecular medicine*, 44: 109-20.

CHOPCHOP, https://chopchop.cbu.uib.no/ (24 March, 2020).

Chromas, http://technelysium.com.au/wp/chromas/ (24 March, 2020).

Ciuffa, R., T. Lamark, A. K. Tarafder, A. Guesdon, S. Rybina, W. J. Hagen, T. Johansen, and C. Sachse. 2015. 'The selective autophagy receptor p62 forms a flexible filamentous helical scaffold', *Cell Rep*, 11: 748-58.

Cohen, Shenhav, Bo Zhai, Steven P. Gygi, and Alfred L. Goldberg. 2012. 'Ubiquitylation by Trim32 causes coupled loss of desmin, Z-bands, and thin filaments in muscle atrophy', *J Cell Biol*, 198: 575-89.

Crawford, L. J., C. K. Johnston, and A. E. Irvine. 2018. 'TRIM proteins in blood cancers', *J Cell Commun Signal*, 12: 21-29.

Crisafuli, F. A., E. B. Ramos, and M. S. Rocha. 2015. 'Characterizing the interaction between DNA and GelRed fluorescent stain', *Eur Biophys J*, 44: 1-7.

Cui, X., Z. Lin, Y. Chen, X. Mao, W. Ni, J. Liu, H. Zhou, X. Shan, L. Chen, J. Lv, Z. Shen, C. Duan, B. Hu, and R. Ni. 2016. 'Upregulated TRIM32 correlates with enhanced cell proliferation and poor prognosis in hepatocellular carcinoma', *Mol Cell Biochem*, 421: 127-37.

Darvekar, S. R., J. Elvenes, H. B. Brenne, T. Johansen, and E. Sjottem. 2014. 'SPBP is a sulforaphane induced transcriptional coactivator of NRF2 regulating expression of the autophagy receptor p62/SQSTM1', *PLoS One*, 9: e85262.

Desjardins, Philippe, and Deborah Conklin. 2010. 'NanoDrop microvolume quantitation of nucleic acids', *Journal of visualized experiments : JoVE*: 2565.

Di Rienzo, M., M. Antonioli, C. Fusco, Y. Liu, M. Mari, I. Orhon, G. Refolo, F. Germani, M. Corazzari, A. Romagnoli, F. Ciccosanti, B. Mandriani, M. T. Pellico, R. De La Torre, H. Ding, M. Dentice, M. Neri, A. Ferlini, F. Reggiori, M. Kulesz-Martin, M. Piacentini, G. Merla, and G. M. Fimia. 2019. 'Autophagy induction in atrophic muscle cells requires ULK1 activation by TRIM32 through unanchored K63-linked polyubiquitin chains', *Sci Adv*, 5: eaau8857.

Dikic, I., and Z. Elazar. 2018. 'Mechanism and medical implications of mammalian autophagy', *Nat Rev Mol Cell Biol*, 19: 349-64.

Dong, Ying, Jingzhuang Zhao, Xiaoyu Chen, Miao Liu, Guangming Ren, Tongyan Lu, Yizhi Shao, and Liming Xu. 2020. 'Autophagy induced by infectious pancreatic necrosis virus promotes its multiplication in the Chinook salmon embryo cell line CHSE-214', *Fish & Shellfish Immunology*, 97: 375-81.

Du, Y., W. Zhang, B. Du, S. Zang, X. Wang, X. Mao, and Z. Hu. 2018. 'TRIM32 overexpression improves chemoresistance through regulation of mitochondrial function in non-small-cell lung cancers', *Onco Targets Ther*, 11: 7841-52.

Duffy, A., J. Le, E. Sausville, and A. Emadi. 2015. 'Autophagy modulation: a target for cancer treatment development', *Cancer Chemother Pharmacol*, 75: 439-47.

F, D. I. Felice, G. Micheli, and G. Camilloni. 2019. 'Restriction enzymes and their use in molecular biology: An overview', *J Biosci*, 44.

Felgner, P. L., T. R. Gadek, M. Holm, R. Roman, H. W. Chan, M. Wenz, J. P. Northrop, G. M. Ringold, and M. Danielsen. 1987. 'Lipofection: a highly efficient, lipid-mediated DNA-transfection procedure', *Proc Natl Acad Sci U S A*, 84: 7413-7.

Felgner, P. L., and G. M. Ringold. 1989. 'Cationic liposome-mediated transfection', *Nature*, 337: 387-8.

Foldes-Papp, Z., U. Demel, and G. P. Tilz. 2003. 'Laser scanning confocal fluorescence microscopy: an overview', *Int Immunopharmacol*, 3: 1715-29.

Forloni, M., A. Y. Liu, and N. Wajapeyee. 2019. 'Multisite-Directed Mutagenesis', *Cold Spring Harb Protoc*, 2019: pdb.prot097816.

Frosk, Patrick, Tracey Weiler, Edward Nylen, Thangirala Sudha, Cheryl R. Greenberg, Kenneth Morgan, T. Mary Fujiwara, and Klaus Wrogemann. 2002. 'Limb-Girdle Muscular Dystrophy Type 2H Associated with Mutation in TRIM32, a Putative E3-Ubiquitin–Ligase Gene', *The American Journal of Human Genetics*, 70: 663-72.

Garcia-Solaesa, V., and S. C. Abad. 2016. 'SDS-Polyacrylamide Electrophoresis and Western Blotting Applied to the Study of Asthma', *Methods Mol Biol*, 1434: 107-20.

Garibyan, Lilit, and Nidhi Avashia. 2013. 'Polymerase chain reaction', *The Journal of investigative dermatology*, 133: 1-4.

Garrido-Cardenas, J. A., F. Garcia-Maroto, J. A. Alvarez-Bermejo, and F. Manzano-Agugliaro. 2017. 'DNA Sequencing Sensors: An Overview', *Sensors (Basel)*, 17.

Gushchina, Liubov V., Thomas A. Kwiatkowski, Sayak Bhattacharya, and Noah L. Weisleder. 2018. 'Conserved structural and functional aspects of the tripartite motif gene family point towards therapeutic applications in multiple diseases', *Pharmacology & Therapeutics*, 185: 12-25.

Haglund, Kaisa, Pier Paolo Di Fiore, and Ivan Dikic. 2003. 'Distinct monoubiquitin signals in receptor endocytosis', *Trends Biochem Sci*, 28: 598-604.

Haglund, Kaisa, and Ivan Dikic. 2005. 'Ubiquitylation and cell signaling', *The EMBO journal*, 24: 3353-59.

Hanahan, D. 1983. 'Studies on transformation of Escherichia coli with plasmids', *J Mol Biol*, 166: 557-80.

Hatakeyama, S. 2017. 'TRIM Family Proteins: Roles in Autophagy, Immunity, and Carcinogenesis', *Trends Biochem Sci*, 42: 297-311.

Heim, R., A. B. Cubitt, and R. Y. Tsien. 1995. 'Improved green fluorescence', *Nature*, 373: 663-4.

Hicke, L., H. L. Schubert, and C. P. Hill. 2005. 'Ubiquitin-binding domains', *Nat Rev Mol Cell Biol*, 6: 610-21.

Hnasko, T. S., and R. M. Hnasko. 2015. 'The Western Blot', *Methods Mol Biol*, 1318: 87-96.

Hsu, Patrick D., Eric S. Lander, and Feng Zhang. 2014. 'Development and applications of CRISPR-Cas9 for genome engineering', *Cell*, 157: 1262-78.

Ito, M., K. Migita, S. Matsumoto, K. Wakatsuki, T. Tanaka, T. Kunishige, H. Nakade, M. Nakatani, and Y. Nakajima. 2017. 'Overexpression of E3 ubiquitin ligase tripartite motif 32 correlates with a poor prognosis in patients with gastric cancer', *Oncol Lett*, 13: 3131-38.

Karimi, Mansour, Anna Depicker, and Pierre Hilson. 2007. 'Recombinational cloning with plant gateway vectors', *PLANT PHYSIOLOGY*, 145: 107.106989.

Khalil, R. 2018. 'Ubiquitin-Proteasome Pathway and Muscle Atrophy', *Adv Exp Med Biol*, 1088: 235-48.

Khan, Ramisha, Amna Khan, Amjad Ali, Muhammad Idrees, and Ramisha Khan. 2019. 'The interplay between viruses and TRIM family proteins', *Reviews in medical virology*: e2028-e28.

Kimura, T., M. Mandell, and V. Deretic. 2016. 'Precision autophagy directed by receptor regulators - emerging examples within the TRIM family', *J Cell Sci*, 129: 881-91.

Klaips, C. L., G. G. Jayaraj, and F. U. Hartl. 2018. 'Pathways of cellular proteostasis in aging and disease', *J Cell Biol*, 217: 51-63.

Koliopoulos, M. G., D. Esposito, E. Christodoulou, I. A. Taylor, and K. Rittinger. 2016. 'Functional role of TRIM E3 ligase oligomerization and regulation of catalytic activity', *Embo j*, 35: 1204-18.

Komander, David, and Michael Rape. 2012. 'The Ubiquitin Code', *Annu Rev Biochem*, 81: 203-29.

Kudryashova, E., J. Wu, L. A. Havton, and M. J. Spencer. 2009. 'Deficiency of the E3 ubiquitin ligase TRIM32 in mice leads to a myopathy with a neurogenic component', *Hum Mol Genet*, 18: 1353-67.

Kudryashova, Elena, Irina Kramerova, and Melissa J. Spencer. 2012. 'Satellite cell senescence underlies myopathy in a mouse model of limb-girdle muscular dystrophy 2H', *The Journal of Clinical Investigation*, 122: 1764-76.

Kudryashova, Elena, Arie Struyk, Ekaterina Mokhonova, Stephen C. Cannon, and Melissa J. Spencer. 2011. 'The common missense mutation D489N in TRIM32 causing limb girdle muscular dystrophy 2H leads to loss of the mutated protein in knock-in mice resulting in a Trim32-null phenotype', *Hum Mol Genet*, 20: 3925-32.

Lamark, T., S. Svenning, and T. Johansen. 2017. 'Regulation of selective autophagy: the p62/SQSTM1 paradigm', *Essays Biochem*, 61: 609-24.

Lazzari, Elisa, and Germana Meroni. 2016. 'TRIM32 ubiquitin E3 ligase, one enzyme for several pathologies: From muscular dystrophy to tumours', *The International Journal of Biochemistry & Cell Biology*, 79: 469-77.

Lee, H. J. 2018. 'The Role of Tripartite Motif Family Proteins in TGF-beta Signaling Pathway and Cancer', *J Cancer Prev*, 23: 162-69.

Lee, P. Y., J. Costumbrado, C. Y. Hsu, and Y. H. Kim. 2012. 'Agarose gel electrophoresis for the separation of DNA fragments', *Journal of visualized experiments : JoVE*.

Lentsch, Eva, Lifei Li, Susanne Pfeffer, Arif B. Ekici, Leila Taher, Christian Pilarsky, and Robert Grützmann. 2019. 'CRISPR/Cas9-Mediated Knock-Out of Kras(G12D) Mutated Pancreatic Cancer Cell Lines', *Int J Mol Sci*, 20: 5706.

Liang, X., L. Peng, C. H. Baek, and F. Katzen. 2013. 'Single step BP/LR combined Gateway reactions', *Biotechniques*, 55: 265-8.

Liu, Ju, C. Zhang, X. L. Wang, P. Ly, V. Belyi, Z. Y. Xu-Monette, K. H. Young, W. Hu, and Z. Feng. 2014. 'E3 ubiquitin ligase TRIM32 negatively regulates tumor suppressor p53 to promote tumorigenesis', *Cell death and differentiation*, 21: 1792-804.

Livneh, I., Y. Kravtsova-Ivantsiv, O. Braten, Y. T. Kwon, and A. Ciechanover. 2017. 'Monoubiquitination joins polyubiquitination as an esteemed proteasomal targeting signal', *Bioessays*, 39.

Lozy, F., and V. Karantza. 2012. 'Autophagy and cancer cell metabolism', *Semin Cell Dev Biol*, 23: 395-401.

Lukic, Z., and E. M. Campbell. 2012. 'The cell biology of TRIM5alpha', *Curr HIV/AIDS Rep*, 9: 73-80.

Luo, Kai, Youshen Li, Lihai Xia, Wei Hu, Weihua Gao, Liwei Guo, Guangming Tian, Zhitao Qi, Hanwen Yuan, and Qiaoqing Xu. 2017. 'Analysis of the expression patterns of the novel large multigene TRIM gene family (finTRIM) in zebrafish', *Fish & Shellfish Immunology*, 66: 224-30.

Marin, I. 2012. 'Origin and diversification of TRIM ubiquitin ligases', *PLoS One*, 7: e50030.

Marwick, K. F. M., and G. E. Hardingham. 2017. 'Transfection in Primary Cultured Neuronal Cells', *Methods Mol Biol*, 1677: 137-44.

Masters, T. A., R. J. Marsh, T. S. Blacker, D. A. Armoogum, B. Larijani, and A. J. Bain. 2018. 'Polarized two-photon photoselection in EGFP: Theory and experiment', *J Chem Phys*, 148: 134311.

Meroni, G., and G. Diez-Roux. 2005. 'TRIM/RBCC, a novel class of 'single protein RING finger' E3 ubiquitin ligases', *Bioessays*, 27: 1147-57.

Meroni, Germana. 2012. *TRIM/RBCC Proteins* (New York, NY: Springer New York: New York, NY).

Miyashita, T. 2004. 'Confocal microscopy for intracellular co-localization of proteins', *Methods Mol Biol*, 261: 399-410.

Mokhonova, Ekaterina I., Nuraly K. Avliyakulov, Irina Kramerova, Elena Kudryashova, Michael J. Haykinson, and Melissa J. Spencer. 2015. 'The E3 ubiquitin ligase TRIM32 regulates myoblast proliferation by controlling turnover of NDRG2', *Hum Mol Genet*, 24: 2873-83.

Mullis, K. B., and F. A. Faloona. 1987. 'Specific synthesis of DNA in vitro via a polymerase-catalyzed chain reaction', *Methods Enzymol*, 155: 335-50.

Najafov, Ayaz, and Gerta Hoxhaj. 2017. 'Chapter 1 - Introduction.' in Ayaz Najafov and Gerta Hoxhaj (eds.), *Western Blotting Guru* (Academic Press).

Nandi, D., P. Tahiliani, A. Kumar, and D. Chandu. 2006. 'The ubiquitin-proteasome system', *J Biosci*, 31: 137-55.

NCBI BLAST, https: //blast. ncbi.nlm. nih.gov/ Blast.cgi?PROGRAM= blastn&PAGE_ TYPE=BlastSearch &LINK _LOC=blasthome (24 March, 2020).

Nicklas, Sarah, Anthony Otto, Xiaoli Wu, Pamela Miller, Sandra Stelzer, Yefei Wen, Shihuan Kuang, Klaus Wrogemann, Ketan Patel, Hao Ding, and Jens C. Schwamborn. 2012. 'TRIM32 regulates skeletal muscle stem cell differentiation and is necessary for normal adult muscle regeneration', *PLoS One*, 7: e30445-e45.

Nwaneshiudu, A., C. Kuschal, F. H. Sakamoto, R. R. Anderson, K. Schwarzenberger, and R. C. Young. 2012. 'Introduction to confocal microscopy', *The Journal of investigative dermatology*, 132: e3.

Overa, K. S., J. Garcia-Garcia, Z. Bhujabal, A. Jain, A. Overvatn, K. B. Larsen, V. Deretic, T. Johansen, T. Lamark, and E. Sjottem. 2019. 'TRIM32, but not its muscular dystrophy-associated mutant, positively regulates and is targeted to autophagic degradation by p62/SQSTM1', *J Cell Sci*, 132.

Paddock, Stephen W. 1999. "Confocal Microscopy : Methods and Protocols." In. Totowa, NJ: Humana Press : Imprint: Humana.

Paddock, S.W. 2014. "Confocal Microscopy : Methods and Protocols." In. New York, NY: Springer New York : Imprint: Humana.

Pakdel, F., P. Le Goff, and B. S. Katzenellenbogen. 1993. 'An assessment of the role of domain F and PEST sequences in estrogen receptor half-life and bioactivity', *J Steroid Biochem Mol Biol*, 46: 663-72.

Panja, Subrata, Swati Saha, Bimal Jana, and Tarakdas Basu. 2006. 'Role of membrane potential on artificial transformation of E. coli with plasmid DNA', *Journal of Biotechnology*, 127: 14-20.

Park, Jaehong, Andrea L. Throop, and Joshua Labaer. 2015. 'Site-specific recombinational cloning using gateway and in-fusion cloning schemes', *Current protocols in molecular biology*, 110: 3.20.1-3.20.23.

Park, K. C., J. Jeong, and K. I. Kim. 2014. 'Regulation of mIkappaBNS stability through PEST-mediated degradation by proteasome', *Biochem Biophys Res Commun*, 443: 1291-5.

Prydal, J. I., and P. N. Dilly. 1998. 'Advances in confocal microscopy of the cornea', *Eye (Lond)*, 12 (Pt 3a): 331-2.

Phosphosite plus, Available from: https:// www.phosphosite.org /proteinAction.action ?id = 1298502&showAllSites=true (07 January, 2020).

Qile, Muge, Yuan Ji, Marien J. C. Houtman, Marlieke Veldhuis, Fee Romunde, Bart Kok, and Marcel A. G. van der Heyden. 2019. 'Identification of a PEST Sequence in Vertebrate K(IR)2.1 That Modifies Rectification', *Frontiers in physiology*, 10: 863-63.

Ramakrishna, S., B. Suresh, K. H. Lim, B. H. Cha, S. H. Lee, K. S. Kim, and K. H. Baek. 2011. 'PEST motif sequence regulating human NANOG for proteasomal degradation', *Stem Cells Dev*, 20: 1511-9.

Ran, F. Ann, Patrick D. Hsu, Chie-Yu Lin, Jonathan S. Gootenberg, Silvana Konermann, Alexandro E. Trevino, David A. Scott, Azusa Inoue, Shogo Matoba, Yi Zhang, and Feng Zhang. 2013. 'Double nicking by RNA-guided CRISPR Cas9 for enhanced genome editing specificity', *Cell*, 154: 1380-89.

Ran, F. Ann, Patrick D. Hsu, Jason Wright, Vineeta Agarwala, David A. Scott, and Feng Zhang. 2013. 'Genome engineering using the CRISPR-Cas9 system', *Nat Protoc*, 8: 2281-308.

Rechsteiner, Martin, and Scott W. Rogers. 1996. 'PEST sequences and regulation by proteolysis', *Trends Biochem Sci*, 21: 267-71.

Redman, Melody, Andrew King, Caroline Watson, and David King. 2016. 'What is CRISPR/Cas9?', *Archives of disease in childhood. Education and practice edition*, 101: 213-15.

Redmann, M., G. A. Benavides, T. F. Berryhill, W. Y. Wani, X. Ouyang, M. S. Johnson, S. Ravi, S. Barnes, V. M. Darley-Usmar, and J. Zhang. 2017. 'Inhibition of autophagy with bafilomycin and chloroquine decreases mitochondrial quality and bioenergetic function in primary neurons', *Redox Biol*, 11: 73-81.

Reverte, Carlos G., Michael D. Ahearn, and Laura E. Hake. 2001. 'CPEB Degradation during Xenopus Oocyte Maturation Requires a PEST Domain and the 26S Proteasome', *Developmental Biology*, 231: 447-58.

Roberts, Richard J. 2005. 'How restriction enzymes became the workhorses of molecular biology', *Proc Natl Acad Sci U S A*, 102: 5905-08.

Rogers, S., R. Wells, and M. Rechsteiner. 1986. 'Amino acid sequences common to rapidly degraded proteins: the PEST hypothesis', *Science*, 234: 364-8.

Ronai, Z. A. 2016. 'Monoubiquitination in proteasomal degradation', *Proc Natl Acad Sci U S A*, 113: 8894-6.

Roy, Jyoti, Neha Jain, Garima Singh, Basudeb Das, and Bibekanand Mallick. 2019. 'Chapter 5 - Small RNA proteome as disease biomarker: An incognito treasure of clinical utility.' in Bibekanand Mallick (ed.), *AGO-Driven Non-Coding RNAs* (Academic Press).

Saccone, V., M. Palmieri, L. Passamano, G. Piluso, G. Meroni, L. Politano, and V. Nigro. 2008. 'Mutations that impair interaction properties of TRIM32 associated with limb-girdle muscular dystrophy 2H', *Hum Mutat*, 29: 240-7.

Sayas, E., F. Garcia-Lopez, and R. Serrano. 2015. 'Toxicity, mutagenicity and transport in Saccharomyces cerevisiae of three popular DNA intercalating fluorescent dyes', *Yeast*, 32: 595-606.

Servián-Morilla, E., M. Cabrera-Serrano, E. Rivas-Infante, A. Carvajal, P. J. Lamont, A. L. Pelayo-Negro, G. Ravenscroft, R. Junckerstorff, J. M. Dyke, S. Fletcher, A. M. Adams, F. Mavillard, M. A. Fernández-García, J. L. Nieto-González, N. G. Laing, and C. Paradas. 2019. 'Altered myogenesis and premature senescence underlie human TRIM32-related myopathy', *Acta Neuropathologica Communications*, 7: 30.

Shieh, P. B., E. Kudryashova, and M. J. Spencer. 2011. 'Limb-girdle muscular dystrophy 2H and the role of TRIM32', *Handb Clin Neurol*, 101: 125-33.

Short, K. M., and T. C. Cox. 2006. 'Subclassification of the RBCC/TRIM superfamily reveals a novel motif necessary for microtubule binding', *J Biol Chem*, 281: 8970-80.

SIGMA, https://www.sigmaaldrich.com/content/dam/sigma-aldrich /docs /Sigma /Bulletin / pln70bul.pdf (19 February 2020).

Sigmaaldrich, https://www.sigmaaldrich.com/catalog/product/sigma/d0428?lang=en&region =NO (10 March 2020).

Smith, B. J. 1984. 'SDS Polyacrylamide Gel Electrophoresis of Proteins.' in John M. Walker (ed.), *Proteins* (Humana Press: Totowa, NJ).

Smith, D. R. 1993. 'Agarose gel electrophoresis', *Methods Mol Biol*, 18: 433-8.

Sommer, Thomas, and Dieter H. Wolf. 2014. 'The ubiquitin–proteasome-system', *Biochimica et Biophysica Acta (BBA) - Molecular Cell Research*, 1843: 1.

Spencer, M. L., M. Theodosiou, and D. J. Noonan. 2004. 'NPDC-1, a novel regulator of neuronal proliferation, is degraded by the ubiquitin/proteasome system through a PEST degradation motif', *J Biol Chem*, 279: 37069-78.

Thermo Scientific, http://tools.thermofisher.com/content/sfs/manuals/nd-1000-v3.8-users-manual-8%205x11.pdf (21 February, 2020).

Tocchini, Cristina, and Rafal Ciosk. 2015. 'TRIM-NHL proteins in development and disease', *Seminars in Cell & Developmental Biology*, 47-48: 52-59.

Tomar, D., and R. Singh. 2015. 'TRIM family proteins: emerging class of RING E3 ligases as regulator of NF-kappaB pathway', *Biol Cell*, 107: 22-40.

Towbin, Harry. 1998. 'Western Blotting.' in Peter J. Delves (ed.), *Encyclopedia of Immunology (Second Edition)* (Elsevier: Oxford).

Trieu, E. P., and I. N. Targoff. 2019. 'SDS-PAGE for (35)S Immunoprecipitation and Immunoprecipitation Western Blotting', *Methods Mol Biol*, 1855: 417-36.

van der Aa, Lieke M., Luc Jouneau, Emmanuel Laplantine, Olivier Bouchez, Lidy Van Kemenade, and Pierre Boudinot. 2012. 'FinTRIMs, fish virus-inducible proteins with E3 ubiquitin ligase activity', *Developmental & Comparative Immunology*, 36: 433-41.

van Tol, S., A. Hage, M. I. Giraldo, P. Bharaj, and R. Rajsbaum. 2017. 'The TRIMendous Role of TRIMs in Virus-Host Interactions', *Vaccines (Basel)*, 5.

Voytas, D. 2001. 'Agarose gel electrophoresis', *Curr Protoc Immunol*, Chapter 10: Unit 10.4.

Vunjak, Milica, and Gijs A. Versteeg. 2019. 'TRIM proteins', *Current Biology*, 29: R42-R44.

Wang, J., B. Liu, N. Wang, Y. M. Lee, C. Liu, and K. Li. 2011. 'TRIM56 is a virus- and interferon-inducible E3 ubiquitin ligase that restricts pestivirus infection', *J Virol*, 85: 3733-45.

Watanabe, M., and S. Hatakeyama. 2017. 'TRIM proteins and diseases', *J Biochem*, 161: 135-44.

White, E. 2016. 'Autophagy and p53', *Cold Spring Harb Perspect Med*, 6: a026120.

White, E., and R. S. DiPaola. 2009. 'The double-edged sword of autophagy modulation in cancer', *Clin Cancer Res*, 15: 5308-16.

Wilde, Lindsay, Katherina Tanson, Joseph Curry, Ubaldo Martinez-Outschoorn, and Lindsay Wilde. 2018. "Autophagy in cancer: a complex relationship." In, 1939-54.

Yang, F., L. G. Moss, and G. N. Phillips, Jr. 1996. 'The molecular structure of green fluorescent protein', *Nat Biotechnol*, 14: 1246-51.

Yang, Q., T. T. Liu, H. Lin, M. Zhang, J. Wei, W. W. Luo, Y. H. Hu, B. Zhong, M. M. Hu, and H. B. Shu. 2017. 'TRIM32-TAX1BP1-dependent selective autophagic degradation of TRIF negatively regulates TLR3/4-mediated innate immune responses', *PLoS Pathog*, 13: e1006600.

Yin, H., W. Xue, S. Chen, R. L. Bogorad, E. Benedetti, M. Grompe, V. Koteliansky, P. A. Sharp, T. Jacks, and D. G. Anderson. 2014. 'Genome editing with Cas9 in adult mice corrects a disease mutation and phenotype', *Nat Biotechnol*, 32: 551-3.

Yu, J. S. L., and K. Yusa. 2019. 'Genome-wide CRISPR-Cas9 screening in mammalian cells', *Methods*, 164-165: 29-35.

Zhang, F., Y. Wen, and X. Guo. 2014. 'CRISPR/Cas9 for genome editing: progress, implications and challenges', *Hum Mol Genet*, 23: R40-6.

Zhang, X., A. H. Smits, G. B. van Tilburg, P. W. Jansen, M. M. Makowski, H. Ovaa, and M. Vermeulen. 2017. 'An Interaction Landscape of Ubiquitin Signaling', *Mol Cell*, 65: 941-55.e8.

Zhang, Xinshang, Heng Zhao, Yeyu Chen, Huiying Luo, Peilong Yang, and Bin Yao. 2015. 'A zebrafish (Danio rerio) bloodthirsty member 20 with E3 ubiquitin ligase activity involved in immune response against bacterial infection', *Biochemical and Biophysical Research Communications*, 457: 83-89.

Zhang, Y., S. S. Wu, X. H. Chen, Z. H. Tang, Y. S. Yu, and G. Q. Zang. 2017. 'Tripartite Motif Containing 52 (TRIM52) Promotes Cell Proliferation in Hepatitis B Virus-Associated Hepatocellular Carcinoma', *Med Sci Monit*, 23: 5202-10.

Zhao, T. T., F. Jin, J. G. Li, Y. Y. Xu, H. T. Dong, Q. Liu, P. Xing, G. L. Zhu, H. Xu, S. C. Yin, and Z. F. Miao. 2018. 'TRIM32 promotes proliferation and confers chemoresistance to breast cancer cells through activation of the NF-kappaB pathway', *J Cancer*, 9: 1349-56.

Zou, Xiao, Gal Levy-Cohen, and Michael Blank. 2015. 'Molecular functions of NEDD4 E3 ubiquitin ligases in cancer', *Biochimica et Biophysica Acta (BBA) - Reviews on Cancer*, 1856: 91-106.

Appendix

List of single, double and triple mutated cloned sequences

Clone 1: pDEST-EGFP-TRIM32-K50R

```
Query  89    ATGGCTGCAGCAGCAGCTTCTCACCTGAACCTGGATGCCCTCCGGGAAGTGCTAGAATGC  148
             ||||||||||||||||||||||||||||||||||||||||||||||||||||||||||||
Sbjct  204   ATGGCTGCAGCAGCAGCTTCTCACCTGAACCTGGATGCCCTCCGGGAAGTGCTAGAATGC  263

Query  149   CCCATCTGCATGGAGTCCTTCACAGAAGAGCAGCTGCGTCCCAAGCTTCTGCACTGTGGC  208
             ||||||||||||||||||||||||||||||||||||||||||||||||||||||||||||
Sbjct  264   CCCATCTGCATGGAGTCCTTCACAGAAGAGCAGCTGCGTCCCAAGCTTCTGCACTGTGGC  323

Query  209   CATACCATCTGCCGCCAGTGCCTGGAGCGCCTATTGGCCAGTAGCATCAATGGTGTCCGC  268
             ||||||||||||||||||||||||||   ||||||||||||||||||||||||||||||
Sbjct  324   CATACCATCTGCCGCCAGTGCCTGGAGAAGCTATTGGCCAGTAGCATCAATGGTGTCCGC  383

Query  269   TGTCCCTTTTGCAGCAAGATTACCCGCATAACCAGCTTGACCCAGCTGACAGACAATCTG  328
             ||||||||||||||||||||||||||||||||||||||||||||||||||||||||||||
Sbjct  384   TGTCCCTTTTGCAGCAAGATTACCCGCATAACCAGCTTGACCCAGCTGACAGACAATCTG  443

Query  329   ACAGTGCTAAAGATCATTGATACAGCTGGGCTCAGCGAGGCTGTGGGGCTGCTCATGTGT  388
             ||||||||||||||||||||||||||||||||||||||||||||||||||||||||||||
Sbjct  444   ACAGTGCTAAAGATCATTGATACAGCTGGGCTCAGCGAGGCTGTGGGGCTGCTCATGTGT  503

Query  389   CGGTCCTGTGGGCGGCGTCTGCCCCGGCAATTCTGCCGGAGCTGTGGTTTGGTGTTATGT  448
             ||||||||||||||||||||||||||||||||||||||||||||||||||||||||||||
Sbjct  504   CGGTCCTGTGGGCGGCGTCTGCCCCGGCAATTCTGCCGGAGCTGTGGTTTGGTGTTATGT  563

Query  449   GAGCCCTGCCGGGAGGCAGACCATCAGCCTCCTGGCCCACTGTACACCTCCCCTGTTCAA  508
             |||||||||||||||||||||||||||||||||| ||||||||| |||| || ||||
Sbjct  564   GAGCCCTGCCGGGAGGCAGACCATCAGCCTCCTGGCC-ACTGTACAC-TCCC-TG-TCAA  619
```

Clone 2: pDEST- EGFP-TRIM32-K247R

```
Query  87    ATGGCTGCAGCAGCAGCTTCTCACCTGAACCTGGATGCCCTCCGGGAAGTGCTAGAATGC  146
             ||||||||||||||||||||||||||||||||||||||||||||||||||||||||||||
Sbjct  204   ATGGCTGCAGCAGCAGCTTCTCACCTGAACCTGGATGCCCTCCGGGAAGTGCTAGAATGC  263

Query  147   CCCATCTGCATGGAGTCCTTCACAGAAGAGCAGCTGCGTCCCAAGCTTCTGCACTGTGGC  206
             ||||||||||||||||||||||||||||||||||||||||||||||||||||||||||||
Sbjct  264   CCCATCTGCATGGAGTCCTTCACAGAAGAGCAGCTGCGTCCCAAGCTTCTGCACTGTGGC  323

Query  207   CATACCATCTGCCGCCAGTGCCTGGAGAAGCTATTGGCCAGTAGCATCAATGGTGTCCGC  266
```

```
                ||||||||||||||||||||||||||||||||||||||||||||||||||||||||||||
Sbjct  324   CATACCATCTGCCGCCAGTGCCTGGAGAAGCTATTGGCCAGTAGCATCAATGGTGTCCGC  383

Query  267   TGTCCCTTTTGCAGCAAGATTACCCGCATAACCAGCTTGACCCAGCTGACAGACAATCTG  326
                ||||||||||||||||||||||||||||||||||||||||||||||||||||||||||||
Sbjct  384   TGTCCCTTTTGCAGCAAGATTACCCGCATAACCAGCTTGACCCAGCTGACAGACAATCTG  443

Query  327   ACAGTGCTAAAGATCATTGATACAGCTGGGCTCAGCGAGGCTGTGGGGCTGCTCATGTGT  386
                ||||||||||||||||||||||||||||||||||||||||||||||||||||||||||||
Sbjct  444   ACAGTGCTAAAGATCATTGATACAGCTGGGCTCAGCGAGGCTGTGGGGCTGCTCATGTGT  503

Query  387   CGGTCCTGTGGGCGGCGTCTGCCCCGGCAATTCTGCCGGAGCTGTGGTTTGGTGTTATGT  446
                ||||||||||||||||||||||||||||||||||||||||||||||||||||||||||||
Sbjct  504   CGGTCCTGTGGGCGGCGTCTGCCCCGGCAATTCTGCCGGAGCTGTGGTTTGGTGTTATGT  563

Query  447   GAGCCCTGCCGGGAGGCAGACCATCAGCCTCCTGGCCACTGTACACTCCCTGTCAAAGAA  506
                ||||||||||||||||||||||||||||||||||||||||||||||||||||||||||||
Sbjct  564   GAGCCCTGCCGGGAGGCAGACCATCAGCCTCCTGGCCACTGTACACTCCCTGTCAAAGAA  623

Query  507   GCAGCTGAGGAGCGGCGTCGGGACTTTGGAGAGAAGTTAACTCGTCTGCGGGAACTTATG  566
                ||||||||||||||||||||||||||||||||||||||||||||||||||||||||||||
Sbjct  624   GCAGCTGAGGAGCGGCGTCGGGACTTTGGAGAGAAGTTAACTCGTCTGCGGGAACTTATG  683

Query  567   GGGGAGCTGCAGCGGCGGAAGGCAGCCTTGGAAGGTGTCTCCAAGGACCTTCAGGCAAGG  626
                ||||||||||||||||||||||||||||||||||||||||||||||||||||||||||||
Sbjct  684   GGGGAGCTGCAGCGGCGGAAGGCAGCCTTGGAAGGTGTCTCCAAGGACCTTCAGGCAAGG  743

Query  627   TATAAAGCAGTTCTCCAGGAGTATGGGCATGAGGAGCGCAGGGTCCAGGATGAGCTGGCT  686
                ||||||||||||||||||||||||||||||||||||||||||||||||||||||||||||
Sbjct  744   TATAAAGCAGTTCTCCAGGAGTATGGGCATGAGGAGCGCAGGGTCCAGGATGAGCTGGCT  803

Query  687   CGCTCTCGGAAGTTCTTCACAGGCTCTTTGGCTGAAGTTGAGAAGTCCAATAGTCAAGTG  746
                ||||||||||||||||||||||||||||||||||||||||||||||||||||||||||||
Sbjct  804   CGCTCTCGGAAGTTCTTCACAGGCTCTTTGGCTGAAGTTGAGAAGTCCAATAGTCAAGTG  863

Query  747   GTAGAGGAGCAGAGTTACCTGCTTAACATTGCAGAGGTGCAGGCTGTGTCTCGCTGTGAC  806
                ||||||||||||||||||||||||||||||||||||||||||||||||||||||||||||
Sbjct  864   GTAGAGGAGCAGAGTTACCTGCTTAACATTGCAGAGGTGCAGGCTGTGTCTCGCTGTGAC  923

Query  807   TACTTCCTGGCCAAGATCCGCCAGGCAGATGTAGCACTACTGGAGGAGACAGCTGATGAG  866
                ||||||||||||||||||   ||||||||||||||||||||||||||||||||||||||
Sbjct  924   TACTTCCTGGCCAAGATCAAGCAGGCAGATGTAGCACTACTGGAGGAGACAGCTGATGAG  983
```

Clone 3: pDONR- EGFP-TRIM32-K401 (Transfer into pDest by GATEWAY LR reaction)

```
Query  665   TGGTTTGCTCAGCTGGCTCCTGTGACAGGCCACGCAGTGGCCATCCAAGGTATATACCTT  724
             ||||||||||||||||||||||||||||||||||||||||||||||||||||||||||||
Sbjct  1903  TGGTTTGCTCAGCTGGCTCCTGTGACAGGCCACGCAGTGGCCATCCAAGGTATATACCTT  1844

Query  725   GAGGGAGTTATCATAGCTGTCAGTCACACCAATCAGCCCCTGGCAGTTCATTGCCACTGA  784
             ||||||||||||||||||||||||||||||||||||||||||||||||||||||||||||
Sbjct  1843  GAGGGAGTTATCATAGCTGTCAGTCACACCAATCAGCCCCTGGCAGTTCATTGCCACTGA  1784

Query  785   GAGAGGAGTGAGGTTGGGTAGATCTGCCCCAAGGAAGCTTAGCACAAAGCTATCAATGCC  844
             ||||||||||||||||||||||||||||||||||||||||||||||||||||||||||||
Sbjct  1783  GAGAGGAGTGAGGTTGGGTAGATCTGCCCCAAGGAAGCTTAGCACAAAGCTATCAATGCC  1724

Query  845   ACTGGGGCTGCGGCGGATTTCCTTCAAAAAGCCGCGGCGGGTAAAGACTTGTATACGATA  904
             ||||||||||||||||||||||||||||||||  ||||||||||||||||||||||||
Sbjct  1723  ACTGGGGCTGCGGCGGATTTCCTTCAAAAAGCCTTTGCGGGTAAAGACTTGTATACGATA  1664

Query  905   GTTACCACGGTCAGCGACTAGTACTTCACCTTGACTGGTCACGTAGAGACTGACTGGAAG  964
             ||||||||||||||||||||||||||||||||||||||||||||||||||||||||||||
Sbjct  1663  GTTACCACGGTCAGCGACTAGTACTTCACCTTGACTGGTCACGTAGAGACTGACTGGAAG  1604

Query  965   ATTGAACATTCCTGGGAGTGCTGCCTTTGGCCCCCATCTTCTTTGAGAAAGAGGCACTGC  1024
             |||||||||||||| |||||||||||||||||||||||||| ||||||||||||||||
Sbjct  1603  ATTGAACATTCCTGG-AGTGCTGCCTTTGGCCCCCATCTTCTT-GAGAAAGAGGCACTGC  1546
```

Clone 4: pDEST- EGFP-TRIM32-K247/K401R

```
Query  69    ATGGCTGCAGCAGCAGCTTCTCACCTGAACCTGGATGCCCTCCGGGAAGTGCTAGAATGC  128
             ||||||||||||||||||||||||||||||||||||||||||||||||||||||||||||
Sbjct  204   ATGGCTGCAGCAGCAGCTTCTCACCTGAACCTGGATGCCCTCCGGGAAGTGCTAGAATGC  263

Query  129   CCCATCTGCATGGAGTCCTTCACAGAAGAGCAGCTGCGTCCCAAGCTTCTGCACTGTGGC  188
             ||||||||||||||||||||||||||||||||||||||||||||||||||||||||||||
Sbjct  264   CCCATCTGCATGGAGTCCTTCACAGAAGAGCAGCTGCGTCCCAAGCTTCTGCACTGTGGC  323

Query  189   CATACCATCTGCCGCCAGTGCCTGGAGAAGCTATTGGCCAGTAGCATCAATGGTGTCCGC  248
             ||||||||||||||||||||||||||||||||||||||||||||||||||||||||||||
Sbjct  324   CATACCATCTGCCGCCAGTGCCTGGAGAAGCTATTGGCCAGTAGCATCAATGGTGTCCGC  383

Query  249   TGTCCCTTTTGCAGCAAGATTACCCGCATAACCAGCTTGACCCAGCTGACAGACAATCTG  308
             ||||||||||||||||||||||||||||||||||||||||||||||||||||||||||||
```

```
Sbjct  384  TGTCCCTTTTGCAGCAAGATTACCCGCATAACCAGCTTGACCCAGCTGACAGACAATCTG  443

Query  309  ACAGTGCTAAAGATCATTGATACAGCTGGGCTCAGCGAGGCTGTGGGGCTGCTCATGTGT  368
            ||||||||||||||||||||||||||||||||||||||||||||||||||||||||||||
Sbjct  444  ACAGTGCTAAAGATCATTGATACAGCTGGGCTCAGCGAGGCTGTGGGGCTGCTCATGTGT  503

Query  369  CGGTCCTGTGGGCGGCGTCTGCCCCGGCAATTCTGCCGGAGCTGTGGTTTGGTGTTATGT  428
            ||||||||||||||||||||||||||||||||||||||||||||||||||||||||||||
Sbjct  504  CGGTCCTGTGGGCGGCGTCTGCCCCGGCAATTCTGCCGGAGCTGTGGTTTGGTGTTATGT  563

Query  429  GAGCCCTGCCGGGAGGCAGACCATCAGCCTCCTGGCCACTGTACACTCCCTGTCAAAGAA  488
            ||||||||||||||||||||||||||||||||||||||||||||||||||||||||||||
Sbjct  564  GAGCCCTGCCGGGAGGCAGACCATCAGCCTCCTGGCCACTGTACACTCCCTGTCAAAGAA  623

Query  489  GCAGCTGAGGAGCGGCGTCGGGACTTTGGAGAGAAGTTAACTCGTCTGCGGGAACTTATG  548
            ||||||||||||||||||||||||||||||||||||||||||||||||||||||||||||
Sbjct  624  GCAGCTGAGGAGCGGCGTCGGGACTTTGGAGAGAAGTTAACTCGTCTGCGGGAACTTATG  683

Query  549  GGGGAGCTGCAGCGGCGGAAGGCAGCCTTGGAAGGTGTCTCCAAGGACCTTCAGGCAAGG  608
            ||||||||||||||||||||||||||||||||||||||||||||||||||||||||||||
Sbjct  684  GGGGAGCTGCAGCGGCGGAAGGCAGCCTTGGAAGGTGTCTCCAAGGACCTTCAGGCAAGG  743

Query  609  TATAAAGCAGTTCTCCAGGAGTATGGGCATGAGGAGCGCAGGGTCCAGGATGAGCTGGCT  668
            ||||||||||||||||||||||||||||||||||||||||||||||||||||||||||||
Sbjct  744  TATAAAGCAGTTCTCCAGGAGTATGGGCATGAGGAGCGCAGGGTCCAGGATGAGCTGGCT  803

Query  669  CGCTCTCGGAAGTTCTTCACAGGCTCTTTGGCTGAAGTTGAGAAGTCCAATAGTCAAGTG  728
            ||||||||||||||||||||||||||||||||||||||||||||||||||||||||||||
Sbjct  804  CGCTCTCGGAAGTTCTTCACAGGCTCTTTGGCTGAAGTTGAGAAGTCCAATAGTCAAGTG  863

Query  729  GTAGAGGAGCAGAGTTACCTGCTTAACATTGCAGAGGTGCA-GCTGTGTCTCGCTGTGAC  787
            |||||||||||||||||||||||||||||||||||||||| |||||||||||||||||||
Sbjct  864  GTAGAGGAGCAGAGTTACCTGCTTAACATTGCAGAGGTGCAGGCTGTGTCTCGCTGTGAC  923

Query  788  TACTTCCTGGCCAAGATCCGCCAGGCAGATGTAGCACTTACT  829
            ||||||||||||||||||   |||||||||||||||| |||
Sbjct  924  TACTTCCTGGCCAAGATCAAGCAGGCAGATGTAGCACT-ACT  964
```

Clone 5: pDONR -TRIM32-K50R/K247 (Transfer into pDest by GATEWAY LR reaction)

```
Query  95    ATGGCTGCAGCAGCAGCTTCTCACCTGAACCTGGATGCCCTCCGGGAAGTGCTAGAATGC  154
             ||||||||||||||||||||||||||||||||||||||||||||||||||||||||||||
Sbjct  204   ATGGCTGCAGCAGCAGCTTCTCACCTGAACCTGGATGCCCTCCGGGAAGTGCTAGAATGC  263

Query  155   CCCATCTGCATGGAGTCCTTCACAGAAGAGCAGCTGCGTCCCAAGCTTCTGCACTGTGGC  214
             ||||||||||||||||||||||||||||||||||||||||||||||||||||||||||||
Sbjct  264   CCCATCTGCATGGAGTCCTTCACAGAAGAGCAGCTGCGTCCCAAGCTTCTGCACTGTGGC  323

Query  215   CATACCATCTGCCGCCAGTGCCTGGAGCGCCTATTGGCCAGTAGCATCAATGGTGTCCGC  274
             |||||||||||||||||||||||||   ||||||||||||||||||||||||||||||
Sbjct  324   CATACCATCTGCCGCCAGTGCCTGGAGAAGCTATTGGCCAGTAGCATCAATGGTGTCCGC  383

Query  275   TGTCCCTTTTGCAGCAAGATTACCCGCATAACCAGCTTGACCCAGCTGACAGACAATCTG  334
             ||||||||||||||||||||||||||||||||||||||||||||||||||||||||||||
Sbjct  384   TGTCCCTTTTGCAGCAAGATTACCCGCATAACCAGCTTGACCCAGCTGACAGACAATCTG  443

Query  335   ACAGTGCTAAAGATCATTGATACAGCTGGGCTCAGCGAGGCTGTGGGGCTGCTCATGTGT  394
             ||||||||||||||||||||||||||||||||||||||||||||||||||||||||||||
Sbjct  444   ACAGTGCTAAAGATCATTGATACAGCTGGGCTCAGCGAGGCTGTGGGGCTGCTCATGTGT  503

Query  395   CGGTCCTGTGGGCGGCGTCTGCCCCGGCAATTCTGCCGGAGCTGTGGTTTGGTGTTATGT  454
             ||||||||||||||||||||||||||||||||||||||||||||||||||||||||||||
Sbjct  504   CGGTCCTGTGGGCGGCGTCTGCCCCGGCAATTCTGCCGGAGCTGTGGTTTGGTGTTATGT  563

Query  455   GAGCCCTGCCGGGAGGCAGACCATCAGCCTCCTGGCCACTGTACACTCCCTGTCAAAGAA  514
             ||||||||||||||||||||||||||||||||||||||||||||||||||||||||||||
Sbjct  564   GAGCCCTGCCGGGAGGCAGACCATCAGCCTCCTGGCCACTGTACACTCCCTGTCAAAGAA  623

Query  515   GCAGCTGAGGAGCGGCGTCGGGACTTTGGAGAGAAGTTAACTCGTCTGCGGGAACTTATG  574
             ||||||||||||||||||||||||||||||||||||||||||||||||||||||||||||
Sbjct  624   GCAGCTGAGGAGCGGCGTCGGGACTTTGGAGAGAAGTTAACTCGTCTGCGGGAACTTATG  683

Query  575   GGGGAGCTGCAGCGGCGGAAGGCAGCCTTGGAAGGTGTCTCCAAGGACCTTCAGGCAAGG  634
             ||||||||||||||||||||||||||||||||||||||||||||||||||||||||||||
Sbjct  684   GGGGAGCTGCAGCGGCGGAAGGCAGCCTTGGAAGGTGTCTCCAAGGACCTTCAGGCAAGG  743

Query  635   TATAAAGCAGTTCTCCAGGAGTATGGGCATGAGGAGCGCAGGGMCCAGGATGAGCTGGCT  694
             |||||||||||||||||||||||||||||||||||||||||| ||||||||||||||||
Sbjct  744   TATAAAGCAGTTCTCCAGGAGTATGGGCATGAGGAGCGCAGGGTCCAGGATGAGCTGGCT  803

Query  695   CGCTCTCGGAAGTTCTTCACAGGCTCTTTGGCTGAMGTTGAGAAGTCCAATAGTCAAGTG  754
             |||||||||||||||||||||||||||||||||| ||||||||||||||||||||||||
```

```
Sbjct  804   CGCTCTCGGAAGTTCTTCACAGGCTCTTTGGCTGAAGTTGAGAAGTCCAATAGTCAAGTG  863

Query  755   GTAGAGGAGCAGAGTTACCTGCTTAACATTGCAGAGGTGCAGGCTGTGTCTCGCTGTGAC  814
              ||||||||||||||||||||||||||||||||||||||||||||||||||||||||||||
Sbjct  864   GTAGAGGAGCAGAGTTACCTGCTTAACATTGCAGAGGTGCAGGCTGTGTCTCGCTGTGAC  923

Query  815   TACTTCCTGGCCAAGATCCGCCAGGCAGATGTAGCACTACTGGAGGAGACAGCTGATGAG  874
              ||||||||||||||||||   ||||||||||||||||||||||||||||||||||||||
Sbjct  924   TACTTCCTGGCCAAGATCAAGCAGGCAGATGTAGCACTACTGGAGGAGACAGCTGATGAG  983

Query  875   GAGGAGCCAGAGCTCACTGCCAGCTTGCCTCGGGAGCTCACCCTGCAAGATGTGGAGCTC  934
              ||||||||||||||||||||||||||||||||||||||||||||||||||||||||||||
Sbjct  984   GAGGAGCCAGAGCTCACTGCCAGCTTGCCTCGGGAGCTCACCCTGCAAGATGTGGAGCTC  1043

Query  935   CTTAAGGTAGGTCATGTTGG-CCCCTCCAAATTGGAC  970
              |||||||||||||||||||| ||||||||||||||||
Sbjct  1044  CTTAAGGTAGGTCATGTTGGCCCCCTCCAAATTGGAC  1080
```

Clone 6: pDONR -TRIM32-K50/K401R (Transfer into pDest by GATEWAY LR reaction)

```
Query  95    ATGGCTGCAGCAGCAGCTTCTCACCTGAACCTGGATGCCCTCCGGGAAGTGCTAGAATGC  154
             ||||||||||||||||||||||||||||||||||||||||||||||||||||||||||||
Sbjct  204   ATGGCTGCAGCAGCAGCTTCTCACCTGAACCTGGATGCCCTCCGGGAAGTGCTAGAATGC  263

Query  155   CCCATCTGCATGGAGTCCTTCACAGAAGAGCAGCTGCGTCCCAAGCTTCTGCACTGTGGC  214
             ||||||||||||||||||||||||||||||||||||||||||||||||||||||||||||
Sbjct  264   CCCATCTGCATGGAGTCCTTCACAGAAGAGCAGCTGCGTCCCAAGCTTCTGCACTGTGGC  323

Query  215   CATACCATCTGCCGCCAGTGCCTGGAGCGCCTATTGGCCAGTAGCATCAATGGTGTCCGC  274
             ||||||||||||||||||||||||||   ||||||||||||||||||||||||||||||
Sbjct  324   CATACCATCTGCCGCCAGTGCCTGGAGAAGCTATTGGCCAGTAGCATCAATGGTGTCCGC  383

Query  275   TGTCCCTTTTGCAGCAAGATTACCCGCATAACCAGCTTGACCCAGCTGACAGACAATCTG  334
             ||||||||||||||||||||||||||||||||||||||||||||||||||||||||||||
Sbjct  384   TGTCCCTTTTGCAGCAAGATTACCCGCATAACCAGCTTGACCCAGCTGACAGACAATCTG  443

Query  335   ACAGTGCTAAAGATCATTGATACAGCTGGGCTCAGCGAGGCTGTGGGGCTGCTCATGTGT  394
             ||||||||||||||||||||||||||||||||||||||||||||||||||||||||||||
Sbjct  444   ACAGTGCTAAAGATCATTGATACAGCTGGGCTCAGCGAGGCTGTGGGGCTGCTCATGTGT  503

Query  395   CGGTCCTGTGGGCGGCGTCTGCCCCGGCAATTCTGCCGGAGCTGTGGTTTGGTGTTATGT  454
```

```
            ||||||||||||||||||||||||||||||||||||||||||||||||||||||||||||
Sbjct  504  CGGTCCTGTGGGCGGCGTCTGCCCCGGCAATTCTGCCGGAGCTGTGGTTTGGTGTTATGT  563

Query  455  GAGCCCTGCCGGGAGGCAGACCATCAGCCTCCTGGCCACTGTACACTCCCTGTCAAAGAA  514
            ||||||||||||||||||||||||||||||||||||||||||||||||||||||||||||
Sbjct  564  GAGCCCTGCCGGGAGGCAGACCATCAGCCTCCTGGCCACTGTACACTCCCTGTCAAAGAA  623

Query  515  GCAGCTGAGGAGCGGCGTCGGGACTTTGGAGAGAAGTTAACTCGTCTGCGGGAACTTATG  574
            ||||||||||||||||||||||||||||||||||||||||||||||||||||||||||||
Sbjct  624  GCAGCTGAGGAGCGGCGTCGGGACTTTGGAGAGAAGTTAACTCGTCTGCGGGAACTTATG  683

Query  575  GGGGAGCTGCAGCGGCGGAAGGCAGCCTTGGAAGGTGTCTCCAAGGACCTTCAGGCMAGG  634
            |||||||||||||||||||||||||||||||||||||||||||||||||||||||| |||
Sbjct  684  GGGGAGCTGCAGCGGCGGAAGGCAGCCTTGGAAGGTGTCTCCAAGGACCTTCAGGCAAGG  743

Query  635  TATAAAGCAGTTCTCCAGGAGTATGGGCATGAGGAGCGCAGGGTCCAGGATGAGCTGGCT  694
            ||||||||||||||||||||||||||||||||||||||||||||||||||||||||||||
Sbjct  744  TATAAAGCAGTTCTCCAGGAGTATGGGCATGAGGAGCGCAGGGTCCAGGATGAGCTGGCT  803

Query  695  CGCTCTCGGAAGTTCTTCACAGGCTCTTTGGCTGAAAGMTGAGAAGTCCAATAGTCAAGT  754
            |||||||||||||||||||||||||||||||| ||| ||||||||||||||||||||||
Sbjct  804  CGCTCTCGGAAGTTCTTCACAGGCTCTTTGGCTG-AAGTTGAGAAGTCCAATAGTCAAGT  862

Query  755  GGTAGAGGAGCAGAGTTACCTGCTTAACATTGCAGAGGTGCA-GCTGTGTCTCGCTGTGA  813
            |||||||||||||||||||||||||||||||||||||||||| ||||||||||||||||
Sbjct  863  GGTAGAGGAGCAGAGTTACCTGCTTAACATTGCAGAGGTGCAGGCTGTGTCTCGCTGTGA  922

Query  814  CTACTTCCTGGCCAAGATCAAGCAGGCAGATGTAGCACTACTGGAGGAGACAGCTGATGA  873
            ||||||||||||||||||||||||||||||||||||||||||||||||||||||||||||
Sbjct  923  CTACTTCCTGGCCAAGATCAAGCAGGCAGATGTAGCACTACTGGAGGAGACAGCTGATGA  982

Query  874  GGA  876
            |||
Sbjct  983  GGA  985
```

Clone 7: pDEST- EGFP-TRIM32- K50R/K401R/K247R

```
Query  88   ATGGCTGCAGCAGCAGCTTCTCACCTGAACCTGGATGCCCTCCGGGAAGTGCTAGAATAC  147
            |||||||||||||||||||||||||||||||||||||||||||||||||||||||||| |
Sbjct  204  ATGGCTGCAGCAGCAGCTTCTCACCTGAACCTGGATGCCCTCCGGGAAGTGCTAGAATGC  263
```

```
Query  148  CCCATCTGCATGGAGTCCTTCACAGAAGAGCAGCTGCGTCCCAAGCTTCTGCACTGTGGC  207
            ||||||||||||||||||||||||||||||||||||||||||||||||||||||||||||
Sbjct  264  CCCATCTGCATGGAGTCCTTCACAGAAGAGCAGCTGCGTCCCAAGCTTCTGCACTGTGGC  323

Query  208  CATACCATCTGCCGCCAGTGCCTGGAGCGCCTATTGGCCAGTAGCATCAATGGTGTCCGC  267
            ||||||||||||||||||||||||||   ||||||||||||||||||||||||||||||
Sbjct  324  CATACCATCTGCCGCCAGTGCCTGGAGAAGCTATTGGCCAGTAGCATCAATGGTGTCCGC  383

Query  268  TGTCCCTTTTGCAGCAAGATTACCCGCATAACCAGCTTGACCCAGCTGACAGACAATCTG  327
            ||||||||||||||||||||||||||||||||||||||||||||||||||||||||||||
Sbjct  384  TGTCCCTTTTGCAGCAAGATTACCCGCATAACCAGCTTGACCCAGCTGACAGACAATCTG  443

Query  328  ACAGTGCTAAAGATCATTGATACAGCTGGGCTCAGCGAGGCTGTGGGGCTGCTCATGTGT  387
            ||||||||||||||||||||||||||||||||||||||||||||||||||||||||||||
Sbjct  444  ACAGTGCTAAAGATCATTGATACAGCTGGGCTCAGCGAGGCTGTGGGGCTGCTCATGTGT  503

Query  388  CGGTCCTGTGGGCGGCGTCTGCCCCGGCAATTCTGCCGGAGCTGTGGTTTGGTGTTATGT  447
            ||||||||||||||||||||||||||||||||||||||||||||||||||||||||||||
Sbjct  504  CGGTCCTGTGGGCGGCGTCTGCCCCGGCAATTCTGCCGGAGCTGTGGTTTGGTGTTATGT  563

Query  448  GAGCCCTGCCGGGAGGCAGACCATCAGCCTCCTGGCCACTGTACACTCCCTGTCAAAGAA  507
            ||||||||||||||||||||||||||||||||||||||||||||||||||||||||||||
Sbjct  564  GAGCCCTGCCGGGAGGCAGACCATCAGCCTCCTGGCCACTGTACACTCCCTGTCAAAGAA  623

Query  508  GCAGCTGAGGAGCGGCGTCGGGACTTTGGAGAGAAGTTAACTCGTCTGCGGGAACTTATG  567
            ||||||||||||||||||||||||||||||||||||||||||||||||||||||||||||
Sbjct  624  GCAGCTGAGGAGCGGCGTCGGGACTTTGGAGAGAAGTTAACTCGTCTGCGGGAACTTATG  683

Query  568  GGGGAGCTGCAGCGGCGGAAGGCAGCCTTGGAAGGTGTCTCCAAGGACCTTCAGGCAAGG  627
            ||||||||||||||||||||||||||||||||||||||||||||||||||||||||||||
Sbjct  684  GGGGAGCTGCAGCGGCGGAAGGCAGCCTTGGAAGGTGTCTCCAAGGACCTTCAGGCAAGG  743

Query  628  TATAAAGCAGTTCTCCAGGAGTATGGGCATGAGGAGCGCAGGGTCCAGGATGAGCTGGCT  687
            ||||||||||||||||||||||||||||||||||||||||||||||||||||||||||||
Sbjct  744  TATAAAGCAGTTCTCCAGGAGTATGGGCATGAGGAGCGCAGGGTCCAGGATGAGCTGGCT  803

Query  688  CGCTCTCGGAAGTTCTTCACAGGCTCTTTGGCTGAAGTTGAGAAGTCCAATAGTCAAGTG  747
            ||||||||||||||||||||||||||||||||||||||||||||||||||||||||||||
```

```
Sbjct  804  CGCTCTCGGAAGTTCTTCACAGGCTCTTTGGCTGAAGTTGAGAAGTCCAATAGTCAAGTG  863

Query  748  GTAGAGGAGCAGAGTTACCTGCTTAACATTGCAGAGGTGCAGGCTGTGTCTCGCTGTGAC  807
            ||||||||||||||||||||||||||||||||||||||||||||||||||||||||||||
Sbjct  864  GTAGAGGAGCAGAGTTACCTGCTTAACATTGCAGAGGTGCAGGCTGTGTCTCGCTGTGAC  923

Query  808  TACTTCCTGGCCAAGATCCGCCAGGCAGATGTAGCACTTACT  849
            |||||||||||||||||   |||||||||||||||| |||
Sbjct  924  TACTTCCTGGCCAAGATCAAGCAGGCAGATGTAGCACT-ACT  964
```

CRISPR/Cas9 mutated cloned sequences

Clone 1: Sequence of pX458 + mouse TRIM32 CRISPR/Cas9 target T1 site (yellow)

```
AGATAATTGGAATTAATTTGACTGTAAACACAAAGATATTAGTACAAAATACGTGACGTA
GAAAGTAATAATTTCTTGGGTAGTTTGCAGTTTTAAAATTATGTTTTAAAATGGACTATC
ATATGCTTACCGTAACTTGAAAGTATTTCGATTTCTTGGCTTTATATATCTTGTGGAAAG
GACGAAACACCGRTACKAYARTWGCMCCGGTGTTTTAGAKCTARAAATARCAWGTTAAAA
TARSGCTASTCCGWTATCAWCTTGAAAAAGTGGCMCCGASTCKGYGCTTTTTTGTTTTAG
AKCTARAAATARCAWGTTAAAATARSGMTASTCCGTTTTTAGCGCGTGCSCCWWTTCTGC
ASACAARTGGCTCTAGAGGTACCCGWTACATAWCTTACGGWAAATGGCCCGCCTGGSTGA
CCGCCCAACSACCCCCGCCCATTGACSTCWATARTAACSCCAATAGGGACTTTCCWTTGA
CSTCWRTGGGTGGARTATTTACGGWAAACTGCCCACTTGGCARTACMTCRWGTGTATCAT
ATGCCAARTACSCCCCCTATTGACSTCWATGACGGWAAATGGCCCGCCTGGYATTGTGCC
CARTACRTGACCTTATGGGACTTTCCTACTTGGCARYACMTCTACRTATTASTCMTCKCT
ATTACCRTGGTCGAGGWGAGCCCCACGTTCTGCTTCWCTCTCCCYATCTCCCCCCYCTCC
CCACCCCCWATTTTGTATTTATTTATTTTWTAAWTATTTTGYGCAGCKATGGGSGCGGGG
GGGGGGGGGGG
```

Clone 2: Sequence of pX458 + mouse TRIM32 CRISPR/Cas9 target T2 site (yellow)

```
AGATAATTGGAATTAATTTGACTGTAAACACAAAGATATTAGTACAAAATACGTGACGTA
GAAAGTAATAATTTCTTGGGTAGTTTGCAGTTTTAAAATTATGTTTTAAAATGGACTATC
ATATGCTTACCGTAACTTGAAAGTATTTCGATTTCTTGGCTTTATATATCTTGTGGAAAG
GACGAAACACCGTGCYCGGGGCRACMTCAKTGGTTTTAGAGCTAGAAATAGCAAGTTAAA
ATAAGGCTAGTCCGTTATCAACTTGAAAAAGTGGCACCGAGTCGGTGCTTTTTTGTTTTA
GAGCTAGAAATAGCAAGTTAAAATAAGGCTAGTCCGTTTTTAGCGCGTGCGCCAATTCTG
CAGACAAATGGCTCTAGAGGTACCCGTTACATAACTTACGGTAAATGGCCCGCCTGGMTG
ACCGCCCAACGACCCCCGCCCATTGACGTCAATAGTAACGCCAATARGGACTTTCYATTG
ACGTCRATGGGTGGAGTATTTACGGTAAACTGCCCACTTGGCAGTACATCARGTGTATCA
TATGCCAAGTACGCCCCCTATTGACGTCRATGACGGTAAATGGCCCGCCTGGCATTGTGC
CCAGTACATGACCTTATGGGACTTTCCTACTTGGCAGTACATCTACGTATTAGTCATCGC
TATTACCATGGTCGAGGTGAGCCCCACGTTCTGCTTCACTCTCCCCATCTCCCCCCCCTC
CCCACCCCCAATTTTGTATTTATTTATTTTTTAATTATTTTGTGCARCGATGGGGGCGGG
```

GGGGGGGGGGGG

Clone 3: Sequence of pX458 + Rat TRIM32 CRISPR/Cas9 T1 target site (yellow)

CTGTTAGAGAGATAATTGGAATTAATTTGACTGTAAACACAAAGATATTAGTACAAAATA
CGTGACGTAGAAAGTAATAATTTCTTGGGTAGTTTGCAGTTTTAAAATTATGTTTTAAAA
TGGACTATCATATGCTTACCGTAACTTGAAAGTATTTCGATTTCTTGGCTTTATATATCT
TGTGGAAAGGACGAAACACC**GAAGATTTCCGCTGCATCGC**GTTTTAGAGCTAGAAATAGC
AAGTTAAAATAAGGCTAGTCCGTTATCAACTTGAAAAAGTGGCACCGAGTCGGTGCTTTT
TTGTTTTAGAGCTAGAAATAGCAAGTTAAAATAAGGCTAGTCCGTTTTTAGCGCGTGCGC
CAATTCTGCAGACAAATGGCTCTAGAGGTACCCGTTACATAACTTACGGTAAATGGCCCG
CCTGGCTGACCGCCCAACGACCCCCGCCCATTGACGTCAATAGTAACGCCAATAGGGACT
TTCCATTGACGTCAATGGGTGGAGTATTTACGGTAAACTGCCCACTTGGCAGTACATCAA
GTGTATCATATGCCAAGTACGCCCCCTATTGACGTCAATGACGGTAAATGGCCCGCCTGG
CATTGTGCCCAGTACATGACCTTATGGGACTTTCCTACTTGGCAGTACATCTACGTATTA
GTCATCGCTATTACCATGGTCGAGGTGAGCCCCACGTTCTGCTTCACTCTCCCCATCTCC
CCCCCCTCCCCACCCCCAATTTTGTATTTATTTATTTTTTAATTATTTTGTGCAGCGATG
GGGGCGGGGGGGGGGGGGGGG